AD-A092 028 AIR FORCE AERO PROPULSION LAB WRIGHT-PATTERSON AFB OH F/G 20/4
DETERMINATION OF FLOW DIRECTION WITH PRESSURE PROBES.(U)
JUL 79 G D HUFFMAN, D C RABE, D N BARLOW
UNCLASSIFIED AFAPL-TR-79-2077 NL

1 OF 1
AD
A092028

END
DATE
FILMED
1 81
DTIC

AFAPL-TR-79-2077

AD A092028

DETERMINATION OF FLOW DIRECTION WITH PRESSURE PROBES

G.D. HUFFMAN
Purdue University
West Lafayett, Indiana 47907

D.C. RABE
N.D. POTI
U.S. Air Force Aero Propulsion Laboratory
Wright-Patterson Air Force Base, Ohio 45433

D.N. BARLOW
U.S. Air Force Academy
Colorado Springs, Colorado 80840

SEPTEMBER 1980

TECHNICAL REPORT AFAPL-TR-79-2077

Final Report for Period 1 June 1978 - 1 July 1979

AERO PROPULSION LABORATORY
AIR FORCE WRIGHT AERONAUTICAL LABORATORIES
AIR FORCE SYSTEMS COMMAND
WRIGHT-PATTERSON AIR FORCE BASE, OHIO 45433

NOTICE

When Government drawings, specifications, or other data are used for any purpose other than in connection with a definitely related Government procurement operation, the United States Government thereby incurs no responsibility nor any obligation whatsoever; and the fact that the government may have formulated, furnished, or in any way supplied the said drawings, specifications, or other data, is not to be regarded by implication or otherwise as in any manner licensing the holder or any other person or corporation, or conveying any rights or permission to manufacture use, or sell any patented invention that may in any way be related thereto.

This report has been reviewed by the Office of Public Affairs (ASD/PA) and is releasable to the National Technical Information Service (NTIS). At NTIS, it will be available to the general public, including foreign nations.

This technical report has been reviewed and is approved for publication.

Douglas C. Rabe

DOUGLAS C. RABE
Aerospace Engineer
Compressor Test Group
Technology Branch

Francis R. Ostdiek

DR. FRANCIS R. OSTDIEK
Chief, Compressor Test Group
Technology Branch

FOR THE COMMANDER

H I Bush

H. I. BUSH
Deputy Director
Turbine Engine Division
Aero Propulsion Laboratory

"If your address has changed, if you wish to be removed from our mailing list, or if the addressee is no longer employed by your organization please notify AFWAL/POTX *W-PAFB, OH 45433 to help us maintain a current mailing list".*

Copies of this report should not be returned unless return is required by security considerations, contractual obligations, or notice on a specific document.

SECURITY CLASSIFICATION OF THIS PAGE (When Data Entered)

REPORT DOCUMENTATION PAGE		READ INSTRUCTIONS BEFORE COMPLETING FORM
1. REPORT NUMBER AFAPL-TR-79-2077	2. GOVT ACCESSION NO. AD-A092028	3. RECIPIENT'S CATALOG NUMBER
4. TITLE (and Subtitle) DETERMINATION OF FLOW DIRECTION WITH PRESSURE PROBES		5. TYPE OF REPORT & PERIOD COVERED Final Report, Jun 78 - 1 Jul 79
		6. PERFORMING ORG. REPORT NUMBER
7. AUTHOR(s) G. David Huffman, Purdue University D. Rabe N. Poti D. N. Barlow, AF Academy		8. CONTRACT OR GRANT NUMBER(s) AFOSR Grant IPA-808-78-01010
9. PERFORMING ORGANIZATION NAME AND ADDRESS AF Aero Propulsion Laboratory FJ Seiler Research Laboratory AF Academy		10. PROGRAM ELEMENT, PROJECT, TASK AREA & WORK UNIT NUMBERS Program Element - 646100 Project-3066, Task-306617 Work Unit - 30661740
11. CONTROLLING OFFICE NAME AND ADDRESS Air Force Aero Propulsion Laboratory Air Force Wright Aeronautical Laboratories Wright-Patterson Air Force Base, Ohio 45433		12. REPORT DATE July 1979 13. NUMBER OF PAGES 85
14. MONITORING AGENCY NAME & ADDRESS (if different from Controlling Office)		15. SECURITY CLASS. (of this report) UNCLASSIFIED 15a. DECLASSIFICATION DOWNGRADING SCHEDULE

16. DISTRIBUTION STATEMENT (of this Report)

Approved for public release; distribution unlimited.

17. DISTRIBUTION STATEMENT (of the abstract entered in Block 20, if different from Report)

18. SUPPLEMENTARY NOTES

19. KEY WORDS (Continue on reverse side if necessary and identify by block number)

Cone Probes
Pressure Probes
Flow Direction Measurement
Slender Body Theory

20. ABSTRACT (Continue on reverse side if necessary and identify by block number)

This report documents the results of a theoretical and experimental study of flow direction probes for use in turbomachines. The theoretical analyses employ slender body theory with the resulting expressions converted into angular and averaged pressure coefficients. These are in turn used to quantify the effects of probe geometry on probe sensitivity. Furthermore, the analytic expressions are employed to predict the impact of probe alignment on the angular and averaged pressure coefficients.

DD FORM 1 JAN 73 1473 EDITION OF 1 NOV 65 IS OBSOLETE

SECURITY CLASSIFICATION OF THIS PAGE (When Data Entered)

20. Abstract

In addition to the analytic studies, an experimental evaluation of a typical flow direction probe is also presented. Measurements are carried out over a series of Mach numbers and angle of attack and sideslip angles. Angular, averaged and total pressure coefficients are determined from the measured pressures for Mach numbers of from 0.05 to 0.80 and angles of attack from -20° to 20° and sideslip angles from 0° to 20°.

The theoretical results are compared to two sets of experimental data. The first consists of measurements made using a large cone model and the second is made up of the data taken in the current study. The qualitative trends with Mach number and flow angles are the same in both cases and are well reproduced by the theory. Quantitatively the data taken on the large cone agrees well with the theory while the data from the miniature flow-direction probe tends to differ from the analytic predictions. The divergence may be due to shape and pressure tap anomalies introduced in the manufacturing process.

TABLE OF CONTENTS

LIST OF ILLUSTRATIONS

LIST OF TABLES

LIST OF SYMBOLS

Symbol	Definition	Units
c	Speed of sound	m/sec
C_p	Pressure coefficient	
ΔC_p	Difference of pressure coefficient	
$<C_p>$	Averaged pressure coefficient	
d	Diameter	m or mm
f	Body geometry function	
g	Source distribution per unit length for lateral flow	m^2/sec
M	Mach number	
p	Pressure	n/m^2
$<p>$	Average pressure	n/m^2
q	Source distribution per unit length for axisymmetric flow	m^2/sec
r,θ,z	Cylindrical coordinates	m, Degrees
R	Body radius	m
Re	Reynolds number	
S	Body cross-sectional area	m^2
t	Time	sec
v	Perturbation velocity	m/sec
V	Velocity	m/sec
x,y,z	Cartesian coordinates	m
α	Angle of attack	Degrees
β	Cross-flow angle	Degrees
δ	$\sqrt{1-M}$	
δ_c	Probe half angle	Degrees
θ_j	Angle of decrease of jet potential cone	Degrees
ρ	Density	kg/m^3
ϕ	Perturbation potential	m^2/sec
Φ	Potential function	m^2/sec

LIST OF SUBSCRIPTS

Subscript	Definition
t	Total
∞	Free-stream conditions
o	Reference state
1	Probe center port
2,3,4,5	Probe side ports

LIST OF SUPERSCRIPTS

Superscript	Definition
n	Nozzle
p	Probe
r,θ,z	Cylindrical coordinates
x,y,z	Cartesian coordinates
1	Axisymmetric flow past a body of revolution
2	Lateral flow past a body of revolution

SECTION I

INTRODUCTION

Turbomachine flow fields are three-dimensional with a variation in flow direction, flow velocity, temperature and pressure occurring in both the radial and circumferential directions. The temperatures, pressures and turbulence levels encountered necessitate both simple and structurally sound probes and/or sensors. The harsh turbomachine environment makes multi-ported, pressure probes particularly attractive for measurement of flow direction.

Pressure probes usually consist of aerodynamic shapes with a symmetrical arrangement of sensing holes. A number of different geometries have been investigated and some typical cases are reviewed in references 1 through 15. A more general treatment of probes is given in references 16 and 17.

Pressure probes are normally employed in either the stationary or nulling mode. In the nulling or equal pressure mode, the probe is oriented such that each of the side ports, see Figure 1 for instance, reads the same pressure. The probe position is noted and the flow direction determined. In the stationary mode, the probe is fixed and the top-to-bottom and side-to-side pressure differences are noted. Calibration functions are then used to find α and β. The static and total pressures can also be determined in a similar manner.

Both methods offer advantages and disadvantages. The nulling technique tends to be the most accurate. The probe can be designed for maximum sensitivity at small angles. It offers the disadvantage, however, of considerable mechanical complexity particularly in three-dimensional flow fields. The stationary probe method, while mechanically superior to the nulling approach, tends to be less accurate, especially at large flow angles. Despite the accuracy of the nulling technique, this technique is considered inappropriate for turbomachine measurements because of its related mechanical complexity. Consequently, only stationary probes are considered in this work.

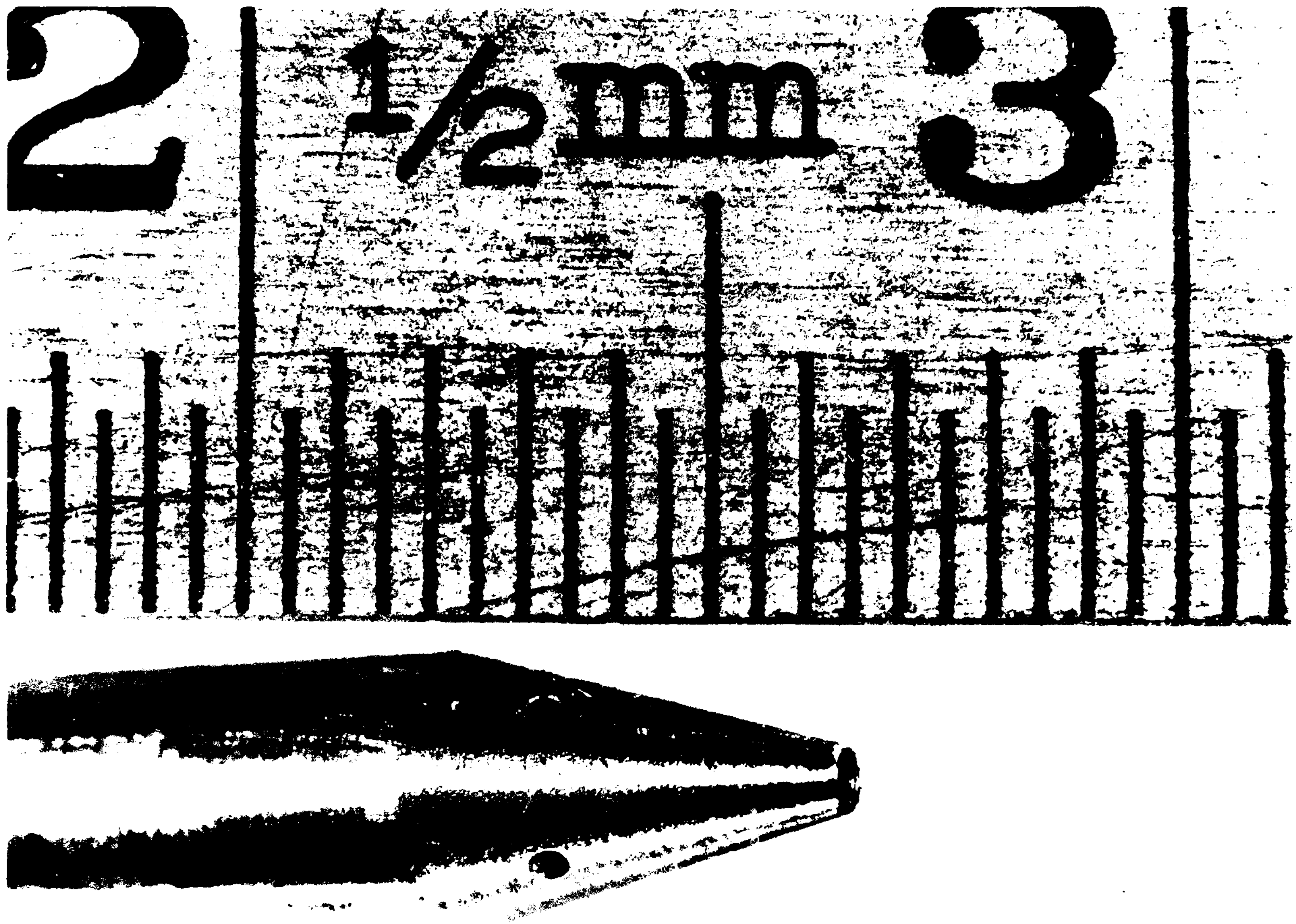

Figure 1. Typical Flow Direction Probe

Since the probes are to be used without rotation, the sensitivity to flow angularity is extremely important. While values of this parameter are available for a number of calibrated probes, this data is only of limited value in synthesizing a probe geometry yielding a desired angular sensitivity. Therefore, a general analytic model has been developed using slender body theory and this is discussed in Section 2.

In order to verify the analysis as well as calibrate a series of probes for use in an upcoming compressor test, the angular, static and total pressure sensitivities for a five-ported, conical probe have been determined experimentally. These tests are discussed in Sections 3 and 4. The results of the measurements are compared with the mathematical model of Section 2 in Section 5.

In addition to the probe sensitivity which is largely dictated by aerodynamic considerations, alignment and manufacturing defects also influence the accuracy with which flow angles and static and total pressures can be determined. Effects of this nature are discussed in Section 6. Some optimum probe geometries are also postulated.

SECTION II

A MATHEMATICAL MODEL OF PROBE AERODYNAMIC BEHAVIOR

2.1 Objectives

The objective of an aerodynamic probe - in the present context - is to determine the magnitude and direction of the velocity vector. This translates into a measurement of pressures which - by means of calibration functions - are then converted into flow angles and total and static pressures. The flow field parameters should be accurately measured with the probe, itself, creating a minimal flow disturbance. The probe must also be structurally sound - the last two requirements are somewhat at variance.

A typical flow direction probe having an "aerodynamic shape" can be thought of as a slender body, i.e., the body radius is much less than the body length. The use of slender body theory in the analysis of aerodynamic probes, thus, immediately comes to mind. There are, however, shortcomings associated with this approach. The major one being that the rate of change of body radius with respect to body length must also be small. This feature precludes stagnation points in a slender body approach.

Of course, a complete description of the flow field around an aerodynamic probe can be generated by numerically solving the three-dimensional potential flow equations, see, for instance, references 18 and 19. While this approach is more accurate than slender body theory, it does not lend itself to synthesis or probe shapes. Furthermore, analytic calibration relations are not obtained and considerable insight into the physical processes is lost. Consequently, slender body analysis will be employed in the ensuing analysis.

2.2 Basic Formulation of Slender Body Theory

A slender body of revolution in a cross-flow is shown in Figure 2. The body itself can be described in terms of axial, z, and radial, r, coordinates with

$$r = R(z) \tag{1}$$

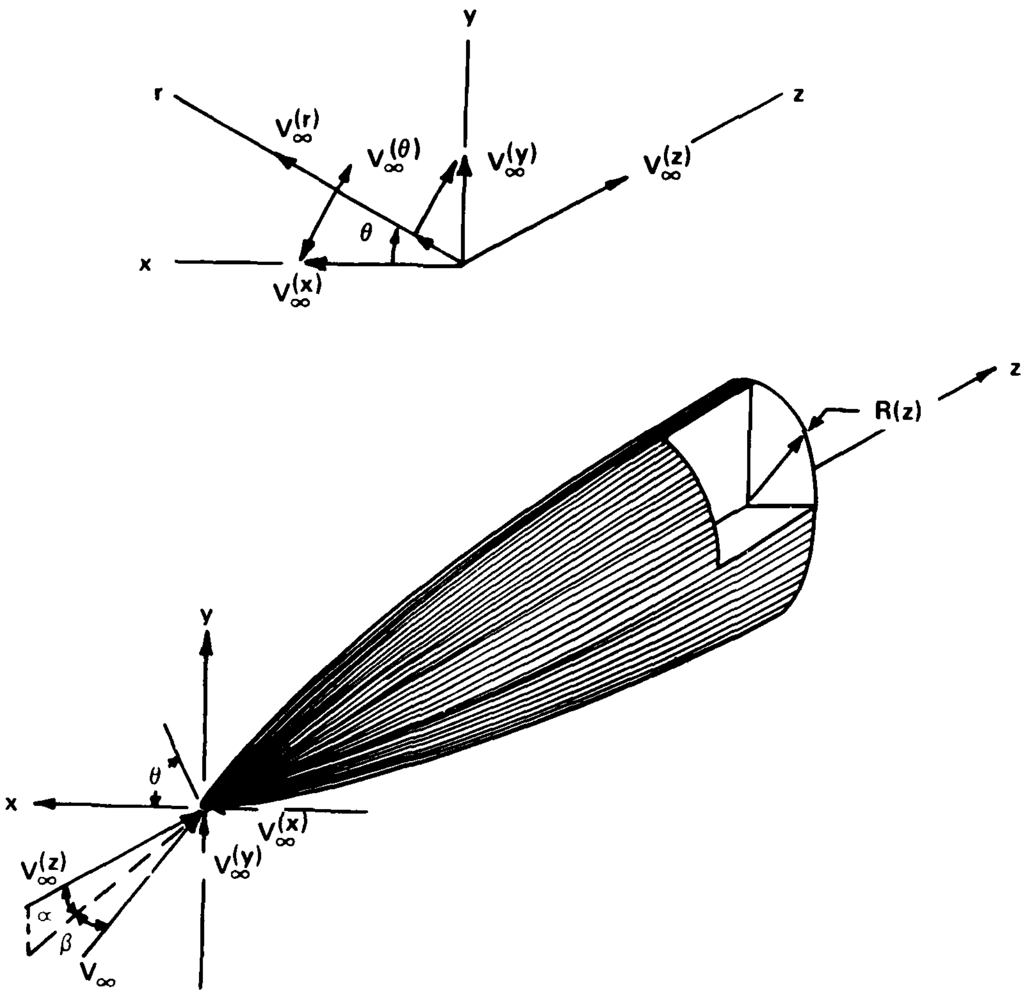

Figure 2. Slender Body of Revolution in a Cross-Flow

Following Shapiro, reference 20, the differential equation for the velocity potential, Φ, can be written as

$$\left(1 - \frac{\Phi_r^{\,2}}{c^2}\right)\Phi_{rr} + \left(1 - \frac{\Phi_\theta^{\,2}}{r^2c^2}\right)\frac{\Phi_{\theta\theta}}{r^2} + \left(1 - \frac{\Phi_z^{\,2}}{c^2}\right)\Phi_{zz} - 2\,\frac{\Phi_z\Phi_r}{c^2}\,\Phi_{zr}$$

$$- 2\,\frac{\Phi_r\Phi_\theta}{r^2c^2}\,\Phi_{r\theta} - 2\,\frac{\Phi_\theta\Phi_z}{r^2c^2}\,\Phi_{\theta r} + \frac{\Phi_r}{r}\left(1 + \frac{\Phi_\theta^{\,2}}{r^2c^2}\right) = 0 \qquad (2)$$

where

$$c^2 = c_o^{\,2} - \frac{k-1}{2}\left(\Phi_r^{\,2} + \frac{\Phi_\theta^{\,2}}{r^2} + \Phi_z^{\,2}\right) \qquad (3)$$

and

$$V^{(r)} = \Phi_r, \quad V^{(\theta)} = \frac{1}{r}\,\Phi_\theta, \quad V^{(z)} = \Phi_z \qquad (4)$$

The subscripts r, θ and z denote partial differentiation, i.e.,

$$\Phi_r = \frac{\partial\Phi}{\partial r}, \text{ etc.}$$

Equation (2) can be rewritten in terms of a perturbation velocity potential, ϕ, by expressing the potential Φ as the sum of the perturbation due to the body and the potential due to the external flow, V_∞. It then follows that

$$\Phi_r = V_\infty^{(r)} + v^{(r)} \quad \Phi_\theta = r\left(V_\infty^{(\theta)} + v^{(\theta)}\right) \quad \Phi_z = V_\infty^{(z)} + v^{(z)} \qquad (5)$$

with the perturbation potentials defined as

$$\phi_r = v^{(r)} \quad \phi_\theta = rv^{(\theta)} \quad \phi_z = v^{(z)} \qquad (6)$$

If it is now assumed that the perturbation velocities are much smaller than the free-stream conditions, i.e.,

$$\frac{v^{(r)}}{V_\infty}, \quad \frac{v^{(\theta)}}{V_\infty}, \quad \frac{v^{(z)}}{V_\infty} << 1$$

then

$$\phi_{rr} + \frac{1}{r}\,\phi_r + \frac{1}{r^2}\,\phi_{\theta\theta} + (1-M_\infty{}^2)\,\phi_{zz} = 0 \qquad (7)$$

following Liepman and Roshko, reference 21. Note that $M_\infty = V_\infty/c_\infty$.

The boundary conditions on the body surface can be written as

$$\text{grad } \Phi \cdot \text{grad } F = 0 \text{ on } F(r,\theta,z)$$

when $F(r,\theta,z) = r - R(z)$. With grad $\Phi = \vec{V}_\infty$ + grad $\phi = \vec{V}_\infty + \vec{v}$, then equation (8) becomes

$$(\vec{V}_\infty + \vec{v}) \cdot \text{grad } F = 0 \quad \text{on } F(r,\theta,z) = 0$$

and

$$\left[V_\infty{}^{(r)} + v^{(r)}\right] \frac{\partial F}{\partial r} + \left[V_\infty{}^{(z)} + v^{(z)}\right] \frac{\partial F}{\partial z} = 0 \quad \text{on } F(r,\theta,z) = 0 \qquad (8)$$

The outer boundary condition is simply

$$v^{(r)},\ v^{(\theta)},\ v^{(z)} \to 0 \quad r \to \infty \qquad (9)$$

Equations (7), (8) and (9) comprise the basic relations for the perturbation flow around a slender body. The solution of equation (7) subject to the boundary conditions of equations (8) and (9) is discussed in the following section.

2.3 Solution of the Partial Differential Equations

The system of equations of Section 2.2 is generally solved by using superposition after subdividing the flow field into two elements - the first being the axisymmetric flow past the body of revolution and the second being the transverse and/or lateral flow past the same body. These conditions can be expressed mathematically as

$$\left.\begin{array}{ll}\phi_{rr}^{(1)} + \dfrac{\phi_r^{(1)}}{r} + (1-M_\infty^2)\,\phi_{zz}^{(1)} = 0 & \\ \phi_r^{(1)} = v^{(r)} = V_\infty^{(z)} \dfrac{dR}{dz} & F(r,\theta,z) = 0 \\ v^{(r)},\ v^{(z)} \to 0 \qquad r \to \infty & \end{array}\right\} \begin{array}{l}\text{Axisymmetric Flow}\\ \text{Past a Body}\\ \text{of Revolution}\end{array} \tag{10}$$

and

$$\left.\begin{array}{ll}\phi_{rr}^{(2)} + \dfrac{\phi_r^{(2)}}{r} + \dfrac{\phi_{\theta\theta}^{(2)}}{r^2} + \phi_{zz}^{(2)} = 0 & \\ v^{(r)} = -V_\infty^{(r)} & F(r,\theta,z) = 0 \\ v^{(r)},\ v^{(\theta)},\ v^{(z)} \to 0 \qquad r \to \infty & \end{array}\right\} \begin{array}{l}\text{Lateral Flow}\\ \text{Past a Body}\\ \text{of Revolution}\end{array} \tag{11}$$

with $\phi = \phi^{(1)} + \phi^{(2)}$.

Equation (10) can be written in terms of a source distribution, $q(z)$, per unit length along the z axis following Sears, reference 22. This yields the integral equation

$$\phi^{(1)} = -\frac{1}{4\pi}\int_o^\ell q(\xi)\,\frac{d\xi}{\sqrt{(z-\xi)^2 + \delta^2 r^2}} \tag{12}$$

where $\delta = \sqrt{1-M_\infty^2}$. The velocity components $v^{(r)}$ and $v^{(z)}$ are then given by

$$v^{(z)} = \phi_z^{(1)} = \frac{1}{4\pi\delta}\int_o^\ell \frac{(z-\xi)q(\xi)d\xi}{[(z-\xi)\ \ + \delta^2 r^2]^{3/2}} \tag{13}$$

and

$$v^{(r)} = \frac{\delta r}{4\pi}\int_o^\ell \frac{q(\xi)d\xi}{[(z-\xi)^2 + \delta^2 r^2]^{3/2}}$$

At this point the source distribution function $q(\xi)$ is unspecified. In essence, an arbitrary specification of q produces an arbitrary body R(z). Presumably, $q(\xi)$ could be systematically evaluated until the boundary conditions of equation (10) were satisfied. This is obviously unsatisfactory and an approximate technique yielding a direct solution was developed by Laitone, references 23 and 24. He presumed that $q(\xi)$ could be written as

$$q(\xi) = q(z+\delta r\eta) = \sum_{n=0}^{\infty} \frac{(\delta r\eta)^n}{n!} q^{(n)}(z)$$

It thus follows that

$$\phi_z^{(1)} = -\frac{1}{4\pi\delta} \sum_{n=0}^{\infty} \frac{(\delta r)^{n-1}}{n!} f^{(n)}(z) \int_{-z/\delta r}^{(\ell-z)/\delta r} \frac{\eta^{n+1} d\eta}{(\eta^2+1)^{3/2}}$$

$$\phi_r^{(1)} = \frac{1}{4\pi\delta} \sum_{n=0}^{\infty} \frac{(\delta r)^{n-1}}{n!} f^{(n)}(z) \int_{-z/\delta r}^{(\ell-z)/\delta r} \frac{\eta^{n} d\eta}{(\eta^2+1)^{3/2}} \tag{14}$$

The integrals in equation (14) can be evaluated on a term-by-term basis and

$$\phi_z^{(1)} = -\frac{1}{4\pi\delta} \left\{ \frac{q(z)}{z} \left[\frac{1}{\sqrt{z^2+\delta^2 r^2}} - \frac{1}{\sqrt{(\ell-z)^2+\delta^2 r^2}} \right] - \right.$$

$$q'(z) \left[\frac{z}{\sqrt{z^2+\delta^2+r^2}} + \frac{\ell-z}{\sqrt{(\ell-z)^2+\delta^2 r^2}} + \ln \left(\frac{-z+\sqrt{z^2+\delta^2 r^2}}{\ell-z+\sqrt{(\ell-z)^2+\delta^2 r^2}} \right) \right] +$$

$$\left. \tfrac{1}{2} q''(z) \left[\frac{z^2}{\sqrt{z^2+\delta^2 r^2}} - \frac{(\ell-z)^2}{\sqrt{(\ell-z)^2+\delta^2 r^2}} + 2\sqrt{(\ell-z)^2+\delta^2 r^2} - 2\sqrt{z^2+\delta^2 r^2} \right] + \ldots \right\}$$

$$\phi_r^{(1)} = \frac{1}{4\pi} \left\{ \frac{2q(z)}{\delta r} \right\} \tag{15}$$

for terms of order less than δr. $q(z)$ can now be related to the body coordinates through the boundary condition on the body and

$$\phi_r^{(1)} = \frac{1}{4\pi} \left\{ \frac{2q(z)}{\delta R} \right\} + V_\infty^{(z)} R'$$

where R' denotes dR/dz, etc. It thus follows that

$$q(z) = 2\pi\delta V_\infty^{(z)} RR' = \delta V_\infty^{(z)} S' \tag{16}$$

where S denotes the body cross-sectional area, πR^2. With $q(z)$ related to the body cross-sectional area, the velocities, i.e., $\phi_z^{(1)}$ and $\phi_r^{(1)}$, are completely defined.

The lateral flow past the body can be determined in a similar manner by noting that if $\phi^{(1)}(r,z)$ is a solution of equation (10) then both $\sin\theta\phi_r^{(1)}$ and $\cos\theta\phi_r^{(1)}$ are solutions of equation (11). Using term by term integration and applying the boundary condition on the body yields

$$\begin{aligned}
\phi_r^{(2)} &= \frac{V_\infty^{(x)}\cos\Theta + V_\infty^{(y)}\sin\theta}{\pi} \left\{ -\frac{S}{r^2} \right\} \\
\phi_\theta^{(2)} &= \frac{V_\infty^{(y)}\cos\theta - V_\infty^{(x)}\sin\theta}{\pi} \left\{ \frac{S}{r} \right\} \\
\phi_z^{(2)} &= \frac{V_\infty^{(x)}\cos\theta + V_\infty^{(y)}\sin\theta}{\pi} \left\{ \frac{S'}{r} \right\}
\end{aligned} \tag{17}$$

2.4 The Velocity Components and Pressure Coefficient

Equations (15), (16) and (17) can be combined to yield the perturbation velocities and

$$\begin{aligned}
v^{(r)} &= \tfrac{1}{2} V_\infty^{(z)} \frac{(R^2)'}{r} - (V_\infty^{(x)}\cos\theta + V_\infty^{(y)}\sin\theta)\left(\frac{R}{r}\right)^2 \\
v^{(\theta)} &= (V_\infty^{(y)}\cos\theta - V_\infty^{(x)}\sin\theta)\frac{R^2}{r^2} \\
v^{(z)} &= \tfrac{1}{2} V_\infty^{(z)} f + (V_\infty^{(x)}\cos\theta + V_\infty^{(y)}\sin\theta)\frac{(R^2)'}{r}
\end{aligned} \tag{18}$$

where $V_\infty^{(x)}$, $V_\infty^{(y)}$ and $V_\infty^{(z)}$ can be related to V_∞ through the angles α and β.

The pressure coefficient is the major concern in probe analysis and this parameter can be related to the velocities by means of

$$p = p_\infty + \tfrac{1}{2}\rho V_\infty^2 \left[1 - \frac{V^2}{V_\infty^2}\right] \tag{19}$$

In terms of the perturbation velocities $\vec{v}$, the above relation becomes

$$p = p_\infty - \tfrac{1}{2}\rho V_\infty^2 \left[2\,\frac{\vec{V}_\infty \cdot \vec{v}}{V_\infty^2} + \frac{v^2}{V_\infty^2}\right]$$

where $\vec{v}$ is evaluated on the body surface. The pressure coefficient, C_p is defined as

$$C_p = \frac{p-p_\infty}{\tfrac{1}{2}\rho V_\infty^2} = -\,2\,\frac{\vec{V}_\infty \cdot \vec{v}}{V_\infty^2} - \frac{v^2}{V_\infty^2} \tag{20}$$

Following Karamcheti, reference 25, v^2 can be approximated as $[v^{(r)}]^2 + [v^{(\theta)}]^2$ and the pressure coefficient becomes

$$\begin{aligned} C_p V_\infty^2 = {} & [V_\infty^{(z)}]^2[-f-(R')^2] + [V_\infty^{(x)}]^2[1-4\sin^2\theta] + [V_\infty^{(y)}]^2[1-4\cos^2\theta] + \\ & V_\infty^{(z)}V_\infty^{(x)}\,[-4R'\cos\theta] + V_\infty^{(z)}V_\infty^{(y)}[-4R'\sin\theta] + \\ & V_\infty^{(x)}V_\infty^{(y)}\,[8\sin\theta\cos\theta] \end{aligned} \tag{21}$$

and the body surface function f is

$$\begin{aligned} f = {} & -\tfrac{1}{2}\,(R^2)'\left\{\frac{1}{\sqrt{z^2+\delta^2r^2}} - \frac{1}{\sqrt{(\ell-z)^2+\delta^2r^2}}\right\} + \\ & \tfrac{1}{2}\,(R^2)''\left\{\frac{\ell-z}{\sqrt{(\ell-z)^2+\delta^2r^2}} + \frac{z}{\sqrt{z^2+\delta^2r^2}} + \ell n\left[\frac{-z+\sqrt{z^2+\delta^2r^2}}{\ell-z+\sqrt{(\ell-z)^2+\delta^2r^2}}\right]\right\} - \\ & \tfrac{1}{4}\,(R^2)'''\left\{\frac{z^2}{\sqrt{z^2+\delta^2r^2}} - \frac{(\ell-z)^2}{\sqrt{(\ell-z)^2+\delta^2r^2}} + 2\sqrt{(\ell-z)^2+\delta^2r^2} - 2\sqrt{z^2+\delta^2r^2}\right\} + \ldots \end{aligned} \tag{22}$$

Equation (21) can be rewritten in terms of the angles α and β by noting that

$$V_\infty^{(x)} = V_\infty \sin \beta$$
$$V_\infty^{(y)} = V_\infty \sin \alpha \cos \beta \tag{23}$$
$$V_\infty^{(z)} = V_\infty \cos \alpha \cos \beta$$

and, thus,

$$C_p = \cos^2\alpha\cos^2\beta[-f-(R')^2] + \sin^2\beta[1-4\sin^2\theta] + \sin^2\alpha\cos^2\beta[1-4\cos^2\theta] +$$
$$\cos\alpha\sin2\beta[-2R'\cos\theta] + \sin2\alpha\cos^2\beta[-2R'\sin\theta] +$$
$$\sin2\alpha\cos\beta[4\sin\theta\cos\theta] \tag{24}$$

where f and R' are evaluated on the body surface, i.e., $r = R(z)$.

2.5 Angular and Static Pressure Sensitivity

The flow angularity is normally determined by differencing the measured pressures between the side and top and bottom parts, see Figure 1 for *instance*. Since these pressure ports are at the same z and R locations, the pressure difference is generated by subtracting C_p values at different θ locations and

$$\Delta C_p = -4\sin^2\beta(\sin^2\theta_2-\sin^2\theta_1) - 4\sin^2\alpha\cos^2\beta(\cos^2\theta_2-\cos^2\theta_1) -$$
$$2R'\cos\alpha\sin2\beta(\cos\theta_2-\cos\theta_1) - 2R'\sin2\alpha\cos^2\beta(\sin\theta_2-\sin\theta_1) +$$
$$4\sin2\alpha\cos\beta(\sin\theta_2\cos\theta_2-\sin\theta_1\cos\theta_1) \tag{25}$$

The sensitivity to changes in flow angle is defined as $\partial\Delta C_p/\partial\alpha$ or $\partial\Delta C_p/\partial\beta$. The former can be written as

$$\frac{\partial \Delta C_p}{\partial \alpha} = -4\sin 2\alpha \cos^2\beta(\cos^2\theta_2 - \cos^2\theta_1) + 2R'\sin\alpha \sin 2\beta(\cos\theta_2 - \cos\theta_1) -$$

$$4R'\cos 2\alpha \cos^2\beta(\sin\theta_2 - \sin\theta_1) +$$

$$8\cos 2\alpha \cos\beta(\sin\theta_2\cos\theta_2 - \sin\theta_1\cos\theta_1) \qquad (26)$$

This expression can be considerably simplified by choosing θ_1 and θ_2 as 90^o and 270^o respectively. Equation (26) then becomes

$$\frac{\partial \Delta C_p}{\partial \alpha} = 8R'\cos 2\alpha \cos^2\beta \qquad (27)$$

Note that the sensitivity to flow direction in one plane depends to some extent on the flow angle in the other direction.

$\partial \Delta C_p / \partial \beta$ can be determined in a similar manner with θ_1 and θ_2 taking the values of 0 and 180. This yields

$$\frac{\partial \Delta C_p}{\partial \beta} = 8R'\cos\alpha \cos 2\beta \qquad (28)$$

Note that the two expressions, i.e., $\partial \Delta C_p / \partial \alpha$ and $\partial \Delta C_p / \partial \beta$, are not symmetric in terms of α and β even though equation (21) is symmetric in terms of $V_\infty^{(x)}$, $V_\infty^{(y)}$ and $V_\infty^{(z)}$. This is due to the definition of α and β. α is referenced to x, y and z while β is referenced to a vector rotated through the angle α. If both α and β are referenced to the x, y and z axes, then equations (27) and (28) - although somewhat more complex - are symmetric with regard to flow angle.

Equation (27) is plotted in Figure 3. It is quite apparent from both the mathematical relation and the figure that the probe sensitivity - regardless of shape - depends on α and β. A 10% reduction in sensitivity occurs for α and β of 10^o. Note that $\partial \Delta C_p / \partial \alpha$ is the same for both positive and negative values of α and β.

The averaged pressure coefficient can be used to determine the actual flow field static pressure, i.e., p_∞. C_p is evaluated at a number of theta values, normally 0^o, 90^o, 180^o and 270^o, the results summed and divided by the number of points. Mathematically, this becomes

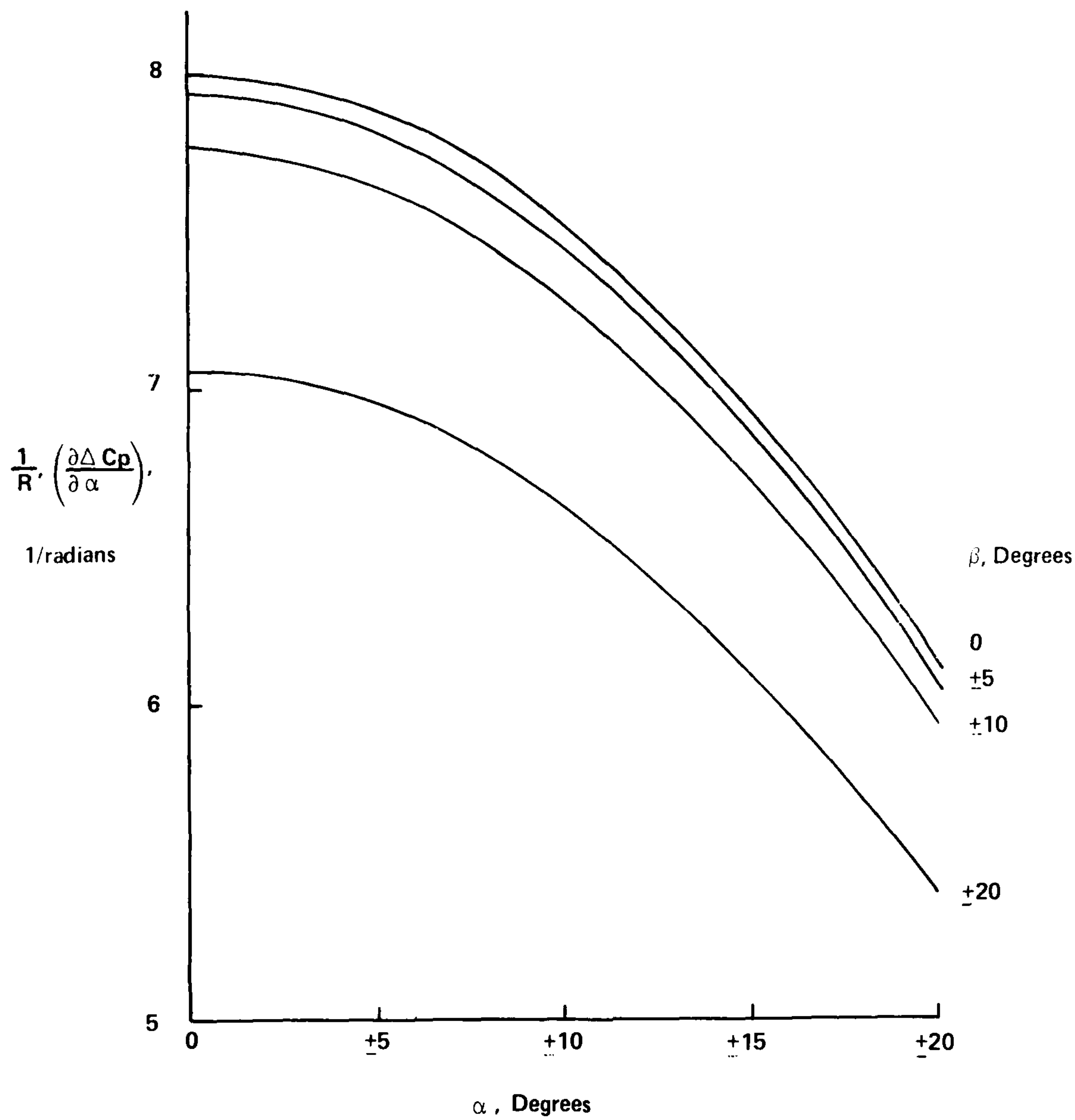

Figure 3. Probe Angular Sensitivity as a Function of α and β

$$<C_p> = \cos^2\alpha\cos^2\beta[-f-(R')^2] + \sin^2\beta\left(1-\sum_{i=2}^{5}\sin^2\theta_i\right) +$$

$$\sin^2\alpha\cos^2\beta\left(1-\sum_{i=2}^{5}\cos^2\theta_i\right) - \tfrac{1}{2}R'\cos\alpha\sin2\beta\sum_{i=2}^{5}\cos\theta_i -$$

$$\tfrac{1}{2}R'\sin2\alpha\cos^2\beta\sum_{i=2}^{5}\sin\theta_i + \sin2\alpha\cos\beta\sum_{i=2}^{5}\sin\theta_i\cos\theta_i \qquad (29)$$

When θ_i is chosen as 0^o, 90^o, 180^o and 270^o, the above relation becomes

$$<C_p> = \cos^2\alpha\cos^2\beta[-f-(R')^2] - \sin^2\beta - \sin^2\alpha\cos^2\beta \qquad (30)$$

which is approximately parabolic with regard to α and β. Equation (30) also has the same value for both positive and negative α and β's.

The analysis is restricted to small perturbation velocities and, thus, a total pressure coefficient cannot be directly derived. A quasi-total pressure can be formulated by integrating the pressure over the body surface area and resolving this force into x, y and z components. An axial pressure can be generated by dividing the z component by the probe cross-sectional area. This has the form of a total pressure but is less in value since the flow is never stagnated - except at z = 0 where the body cross-sectional area is also zero. The functional form of this relation is

$$C_{p_z} = \frac{p_z-p_\infty}{q_\infty} = \frac{\cos^2\alpha\cos^2\beta}{R_\ell^{\,2}}\int_0^\ell (R^2)'[-f-(R')^2]dz - \sin^2\beta - \sin^2\alpha\cos^2\beta \qquad (31)$$

where ℓ denotes the length of the body in the z-direction over which the integration is to be performed. The coefficient again decreases in an approximately parabolic manner with α and β.

The analytical relationships of this section are compared to measured probe characteristics in Section 4. The experimental data in conjunction with the theoretical results is used to demonstrate the general characteristics of probes in Section 6.

SECTION III

EXPERIMENTAL PROGRAM

3.1 Introduction

While the relationships of Section 2 are valuable for characterization of probe behavior, they are not capable of replacing individual probe calibrations. This is due to the limitations of the derivation itself, i.e., inviscid flow and slender body assumptions, as well as the manufacturing irregularities in the probe, i.e., asymmetric construction, misalignment of pressure ports, static ports not normal to probe surface, etc. Regardless of the accuracy of the theoretical derivations, the latter effects may necessitate individual probe calibrations - particularly for small probes. In the present context, the data generated in the calibration can be used to assess the reliability of the mathematical model as well as furnish the angular and Mach number characteristics of the probe which will, in turn, be used in the experimental study of compressor performance, reference 26. The details of the probe calibration are discussed in the following sections.

3.2 Experimental Apparatus

The probe employed in the calibration process consisted [illegible] truncated cone with four side pressure taps nominally normal [illegible] surface. The maximum conic diameter is 3.175mm (0.1250 in.) [illegible] or total pressure port having an internal diameter of 0.[illegible] and the side ports having internal diameters of 0.457mm (0.018 [illegible] photograph and a dimensioned sketch of the probe are shown in Figure [illegible].

The probe was calibrated using a DISA 55D90 calibration system, reference 27. This system consists of a pressure controller, stagnation chamber and nozzle asembly and a three-axis probe positioning system. The system elements are shown in Figures 5 and 6.

The flow and/or pressure controller utilizes a three-stage pressure regulator producing an extremely stable flow which is supplied to the stagnation chamber in the nozzle assembly. The stagnation chamber contains a honeycomb flow straightner and four turbulence damping screens. This generates a very low turbulence level flow field. The unit is fitted with

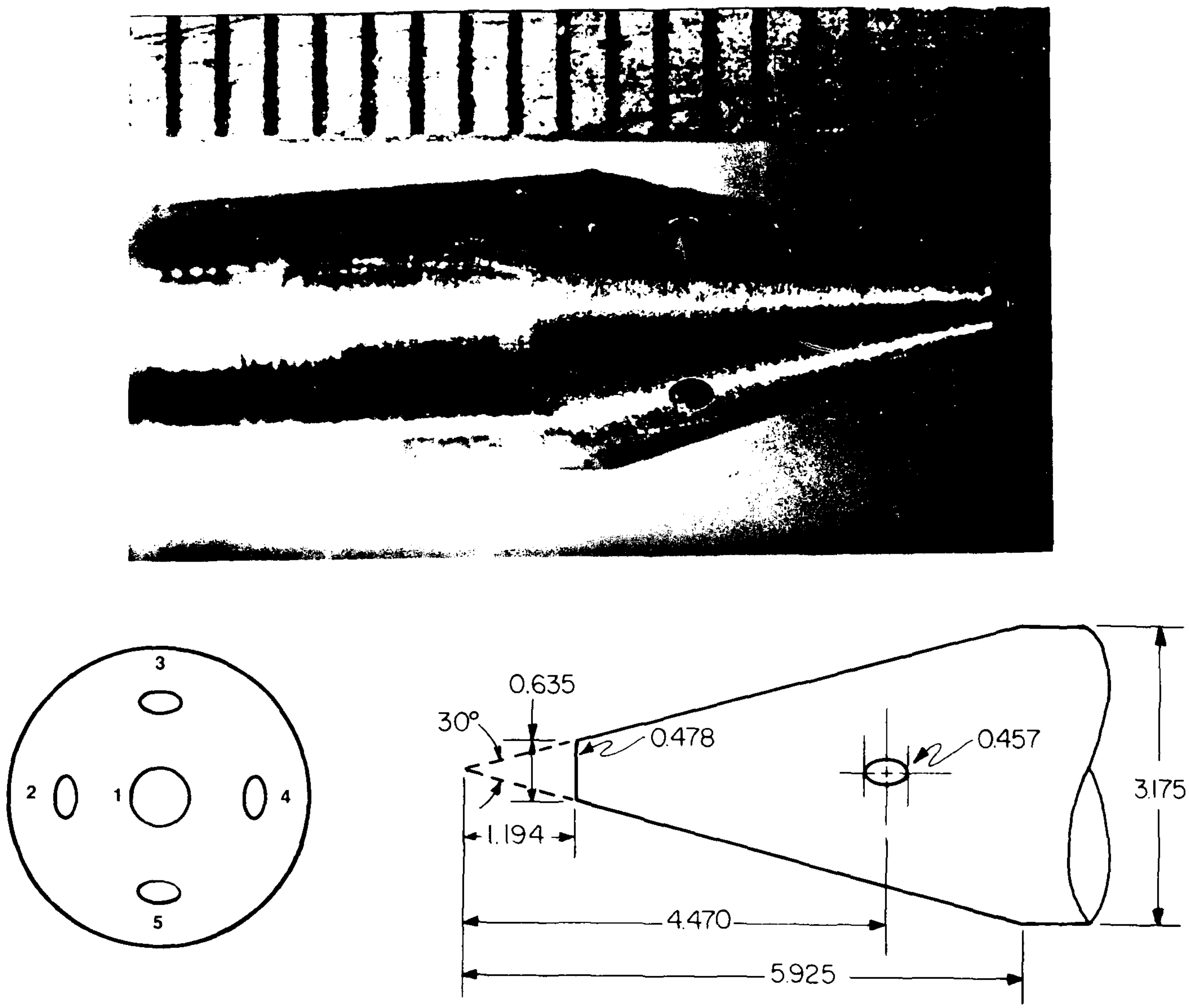

Figure 4. 30° Included Angle, Truncated Conical Probe (all dimensions in mm)

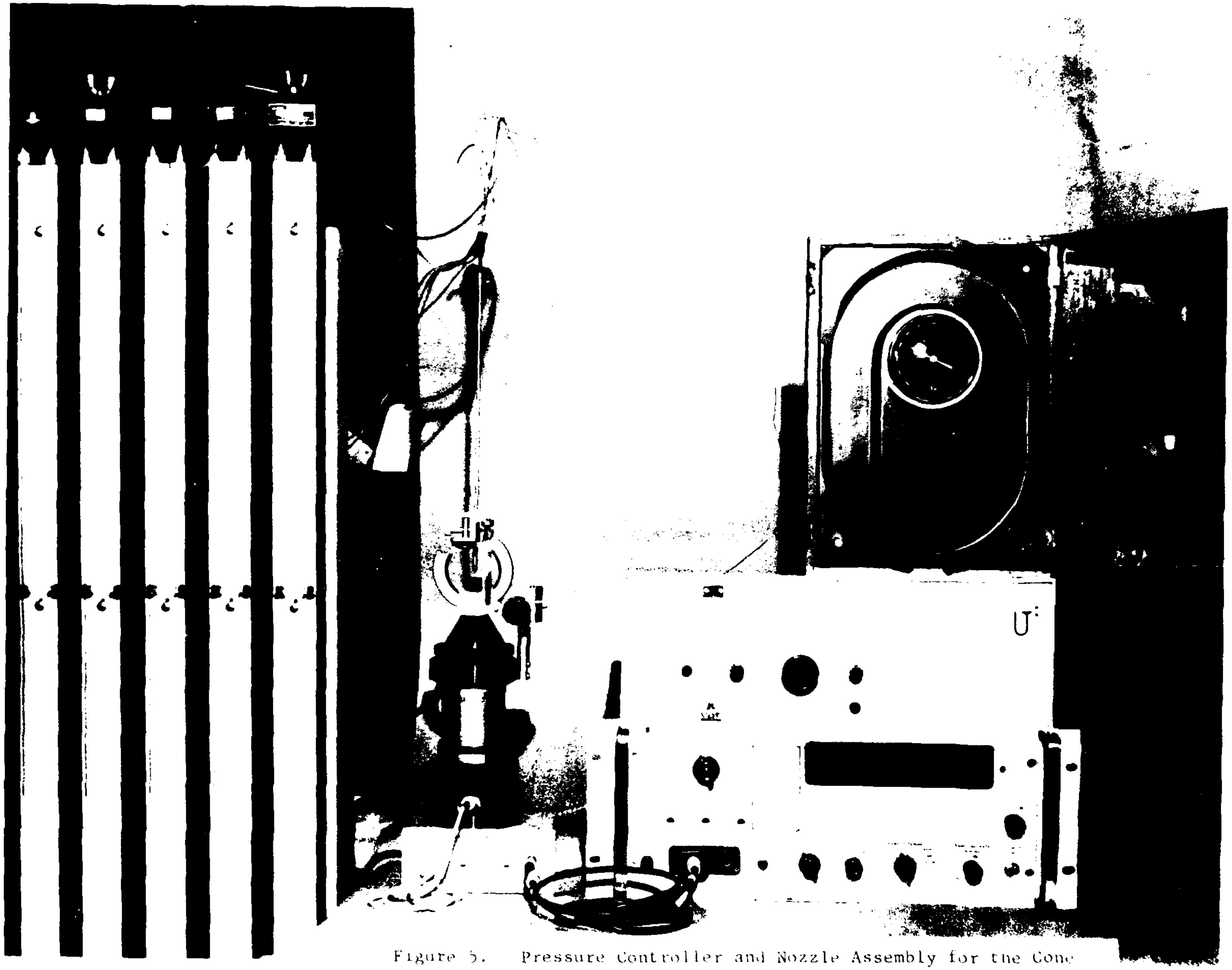

Figure 5. Pressure Controller and Nozzle Assembly for the Cone Probe Calibration

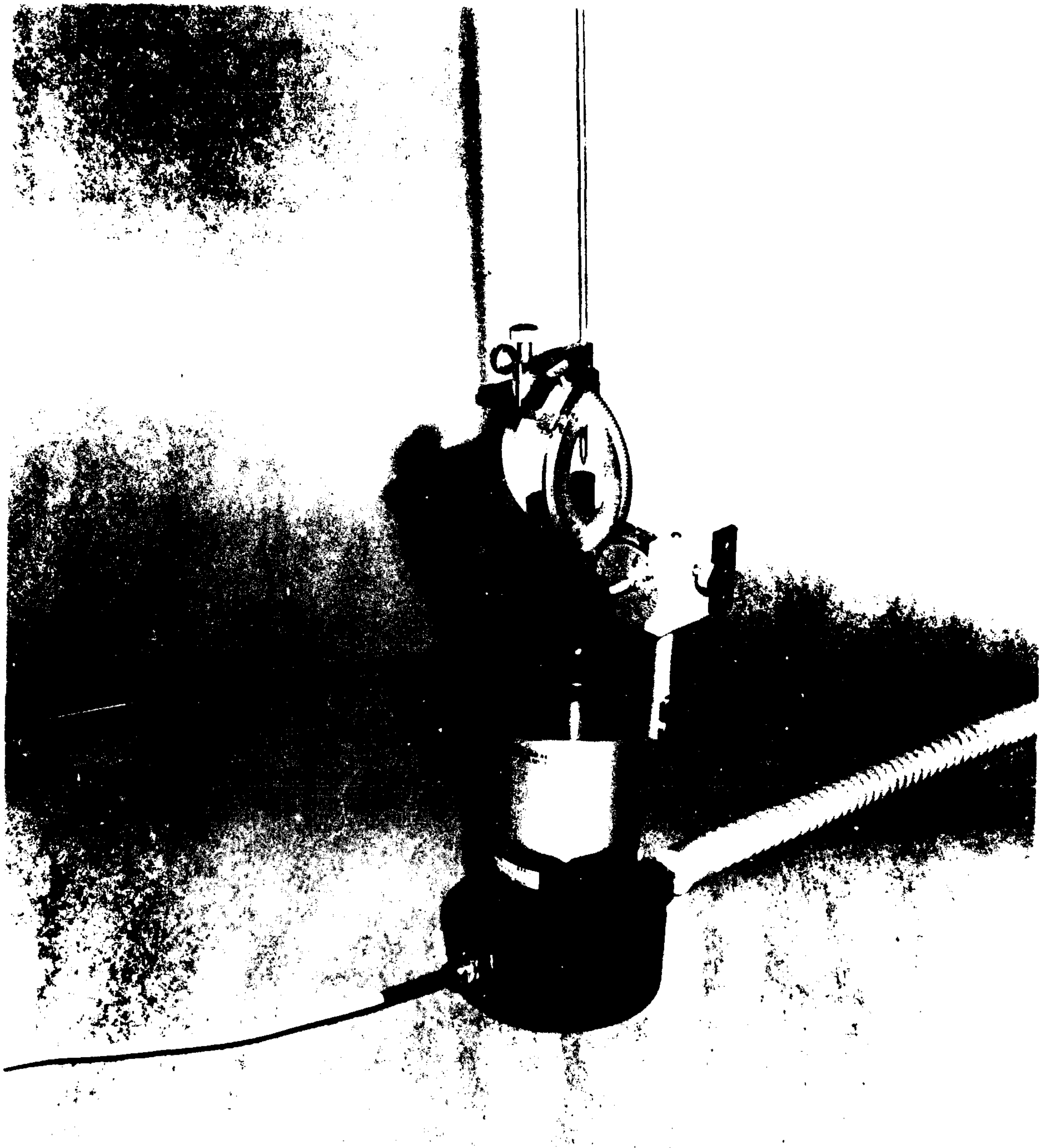

Figure 6. Stagnation Chamber, Nozzle and Probe Positioning Assembly

four interchangeable converging nozzles. The velocity can be varied from 0.5 m/sec (1.6 ft/sec) to sonic conditions by interchanging nozzles and varying the stagnation chamber pressure levels. The pressure controller is nominally supplied with air at an absolute pressure of 144.8 x 10^8 kgr/m^2 (100 lb_f/in^2).

The nozzle chosen for the experimentation has a discharge area of $60mm^2$ (0.093 in^2). Probe blockage corrections - discussed in Section 3.4 - indicated that this nozzle could be used for all Mach numbers investigated. The fairly large mass flow rates at the higher Mach numbers exceeded the capacity of the DISA pressure controller and it was replaced with two series installed, control valves for the high Mach number tests. The flow remained stable but controllability was sacrificed.

The probe is mounted in the potential core of the free jet discharged from the nozzle. The probe positioning mechanism is mounted on a vertical column which is permanently fixed to the main nozzle unit. The nozzles can be interchanged without removing the probe. The probe can be rotated in both the angie-of-attach, α , and side-slip, β , planes - α can be measured to an accuracy of $\pm$ 0.1° while the β resolution is limited to $\pm$ 0.5°. The probe can also be positioned both axially and in roll. All four of these positioning freedoms are shown in Figure 6. The probe tip is nominally located one nozzle radius downstream of the nozzle exit plane. The size of the probe relative to the nozzle limits α and β to

$$\begin{aligned} -20^\circ &\leq \alpha \leq 20^\circ \\ 0 &\leq \beta \leq 20^\circ \end{aligned} \qquad (32)$$

3.3 Measurement Methods

The primary objective of the calibration was to determine the angular, $\Delta C_{p\alpha}$ and $\Delta C_{p\beta}$, averaged, $<C_p>$, and total, $C_{p\tau}$, pressure coefficients. These are easily generated from the measured probe pressures and the nozzle total and static pressures. Since the parameters are all - more or less - Mach number and Reynolds number dependent, the gas temperature and relative humidity must also be measured.

The angular coefficients are defined as

$$\Delta C_{p_\alpha} = \frac{p_2 - p_4}{p_t - p_\infty} \tag{33}$$

$$\Delta C_{p_\beta} = \frac{p_3 - p_5}{p_t - p_\infty} \tag{34}$$

which correspond to the definitions of Section 2. The averaged pressure coefficient can be defined as

$$< C_p > = \frac{<p> - p_\infty}{p_t - p_\infty} \tag{35}$$

where $<p> = \frac{1}{4}(p_2+p_3+p_4+p_5)$. The total pressure coefficient follows the definition in equation (31) and

$$C_{p_t} = \frac{p_1 - p_\infty}{p_t - p_\infty} \tag{36}$$

Alternate formulations are certainly possible, i.e., replace $p_t - p_\infty$ with $p_1 - p_\infty$ in equations (33), (34) and (35) and redefine C_{p_t} as $(p_t - p_1)/p_1 - <p>)$, but the above most closely follow the theory and should exhibit more nearly universal behavior.

In any event, all coefficients represent pressure differences and one is tempted to measure these directly. Direct measurement of the differences is, however, complicated by the requirement to average the side port pressures. When all the necessary pneumatic connections are formulated, this task becomes formidable. Furthermore, the frequency response - which is already of order of minutes due to the small tube diameters - is further degraded as a result of the tubing, connectors and fittings required in the differencing and averaging processes. Note also that the pneumatic connections are designed for a specific series of coefficients. This considerably limits the computation of different forms of coefficients in the data reduction process.

As a result of these considerations, the pressures p_1, p_2, p_3, p_4, p_5, and p_t were measured independently using a bank of inclined water manometers. The manometers could be read to 1.270mm (0.05 in) of water in the vertical position. With the manometer bank inclined at 10°, the

maximum pressure resolution then becomes 0.221mm (0.009 in) of water. At a Mach number of 0.2, the maximum angular resolution - as determined from pressure measurements - is approximately 0.02° for a 30° conical probe. This is well in excess of the angular measurement accuracy of 0.1° and, thus, the pressure measurement accuracy as afforded by the inclined water manometers is sufficient. In terms of pressure differences, the angular probe sensitivity scales with the dynamic head and, thus, pressure measurement resolution can be increased with increasing Mach numbers while maintaining the same pressure based, angular resolution. In the test program, the manometer inclination was increased at the higher Mach numbers which reduced the pressure measurement resolution but maintained the angular resolution at its low Mach number value.

The gas total temperature was measured in the nozzle unit stagnation chamber prior to the flow conditioning devices with a bimetallic element. Air temperatures nominally varied from 20 to 30°C. The relative humidity of the supply air remained below 5% as measured by an Environmental Tektronics Corporation Psychor-dial Model CP-147 psychrometer.

As previously noted, the probe can be rotated along its longitudinal axis. It is essential that the probe side ports be aligned with the α and β axes respectively. This alignment was done by rotating the probe until the p_3-p_5 pressure differential was symmetric throughout the usable range. This proved to be a time consuming process because the probe was extremely sensitive to even the slightest rotation and the manometer response was very slow, i.e., approximately five minutes were required for the manometers to come to equilibrium.

3.4 Aerodynamic Considerations

The use of a free jet in the calibration process presumes that the jet velocity in the vicinity of the probe is uniform and equal to the value of the nozzle exit plane. Two major factors can influence the above assumptions. First, the presence of the probe in the jet creates "blockage" which causes the jet to spread and can result in a reduction of velocity. In a closed wind tunnel, probe and/or model blockage results in velocity increases. Secondly, the jet potential core decreases with downstream distance yielding a spatially non-uniform flow field.

If the free jet is assumed to be similar to an open jet wind tunnel, then probe blockage effects can be computed using the wind tunnel techniques. Following the methods of reference 28, a velocity decrease, i.e., $\Delta V_\infty/V_\infty$, of approximately 1.7% will occur for Mach number of 0.2 increasing to 3.1% at Mach numbers of 0.6. The results are based on a jet nozzle diameter of 8.740mm (0.344 in) and a probe diameter of 3.175mm (0.125 in). The blockage increases rapidly with reduction in nozzle size reaching a value of 12.2% for a nozzle diameter of 5.528mm (0.218 in) at $M_\infty = 0.6$. In general, the blockage obtained with the larger nozzle, $d_n = 8.740$mm, is satisfactory; smaller nozzles, however, should not be used.

The decrease in jet potential core width can result in an apparent spatially non-uniform flowfield if the probe is not positioned within the potential core - a potential problem at large values of α and β. The jet potential core decreases at the angle θ_j which is approximately 6-7°, reference 29. This value implies a potential core having a diameter of about 77% of the nozzle diameter d_n downstream of the nozzle. Data from reference 30 indicates a potential core diameter of about 0.85 d_n at the same axial location. Consequently, 6-7° may slightly overestimate the core decrease but should yield conservative results. The probe in the aligned and maximum displacement positions is shown in Figure 7. It is well within the jet potential core even in the latter case.

The nozzle of diameter 8.740mm (0.344 in) coupled with the probe of diameter 3.175mm (0.125 in) yield acceptably low blockage values at α and β values of up to 20° Furthermore, the probe tip and side ports remain within the potential jet core at the same angles.

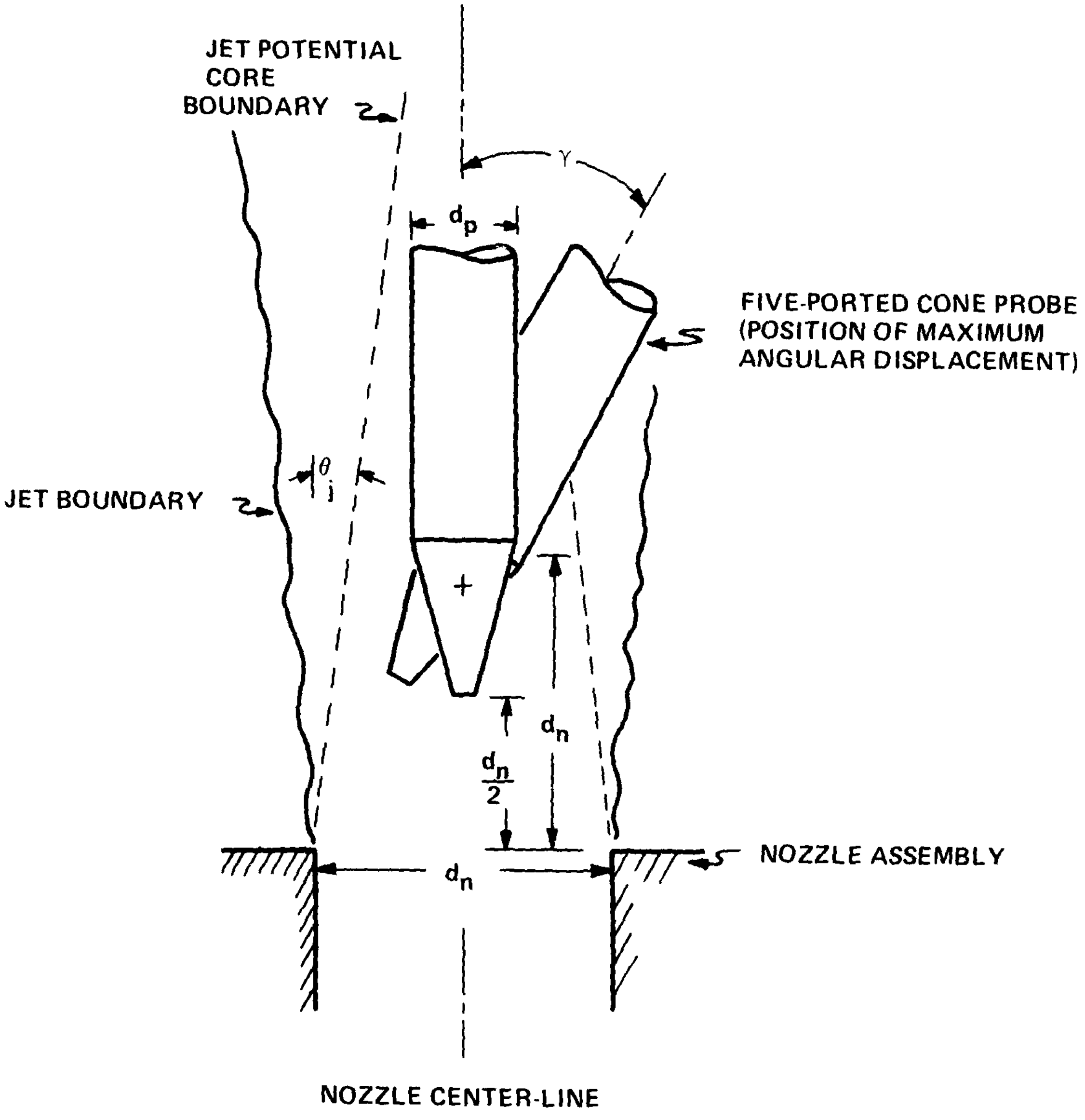

Figure 7. Schematic Diagram of the Calibration Jet and the Five-ported, Conical Probe

SECTION IV

EXPERIMENTAL RESULTS

4.1 Introduction

The experimental data was acquired using the apparatus and measurement techniques described in the previous section. Probe calibration data was taken at three Mach numbers and 91 angular positions per Mach number, i.e., β = 0, 2.5, 5.0, 7.5, 10, 15, and 20, and α = -20, -15, -10, -7.5, -5.0, -2.5. 0, 2.5, 5.0, 7.5, 10, 15, 20 for each β value; M_∞ = 0.2, 0.4 0.6. In addition, $\langle C_p \rangle$ was evaluated at 16 Mach numbers ranging from 0.05 to 0.60. Data reduction and plotting was automated using the AF Academy computer system. The data reduction techniques and the data itself are discussed in the following sections.

4.2 Data Reduction Methods

The angular, total and static pressure coefficients were computed as defined in Section 3.3. The velocity, Mach number and Reynolds numbers were computed using the algorithms of reference 26. Since the nozzle assembly discharges to atmospheric pressure, the Reynolds number and Mach number are uniquely related with Reynolds numbers of 10505, 23896, and 37853 based on probe diameter, corresponding to Mach numbers of 0.2, 0.4 and 0.6.

The probe Reynolds numbers encountered in the compressor tests will range from 29700 to 61052. This exceeds the calibration values at the equivalent Mach number; however, the probe boundary layers are undoubtedly turbulent in either case and, thus, the difference in Reynolds numbers should not influence the calibration functions.

4.3 Experimental Data

The experimental results are presented in Tables 1, 2, 3 and 4 and Figures 8 through 19. Table 1 and Figures 8 through 11 summarize the data for a Mach number of approximately 0.2, with Table 2 and Figures 12 through 15 corresponding to $M_o \simeq 0.4$, and Table 3 and Figures 16 through 19 dealing with data of $M_\infty \simeq 0.6$. Table 4 and Figure 20 contains the results of the fixed position, i.e., $\alpha = \beta = 0$, variable Mach number runs, i.e., $0.05 \leq M_\infty \leq 0.6$.

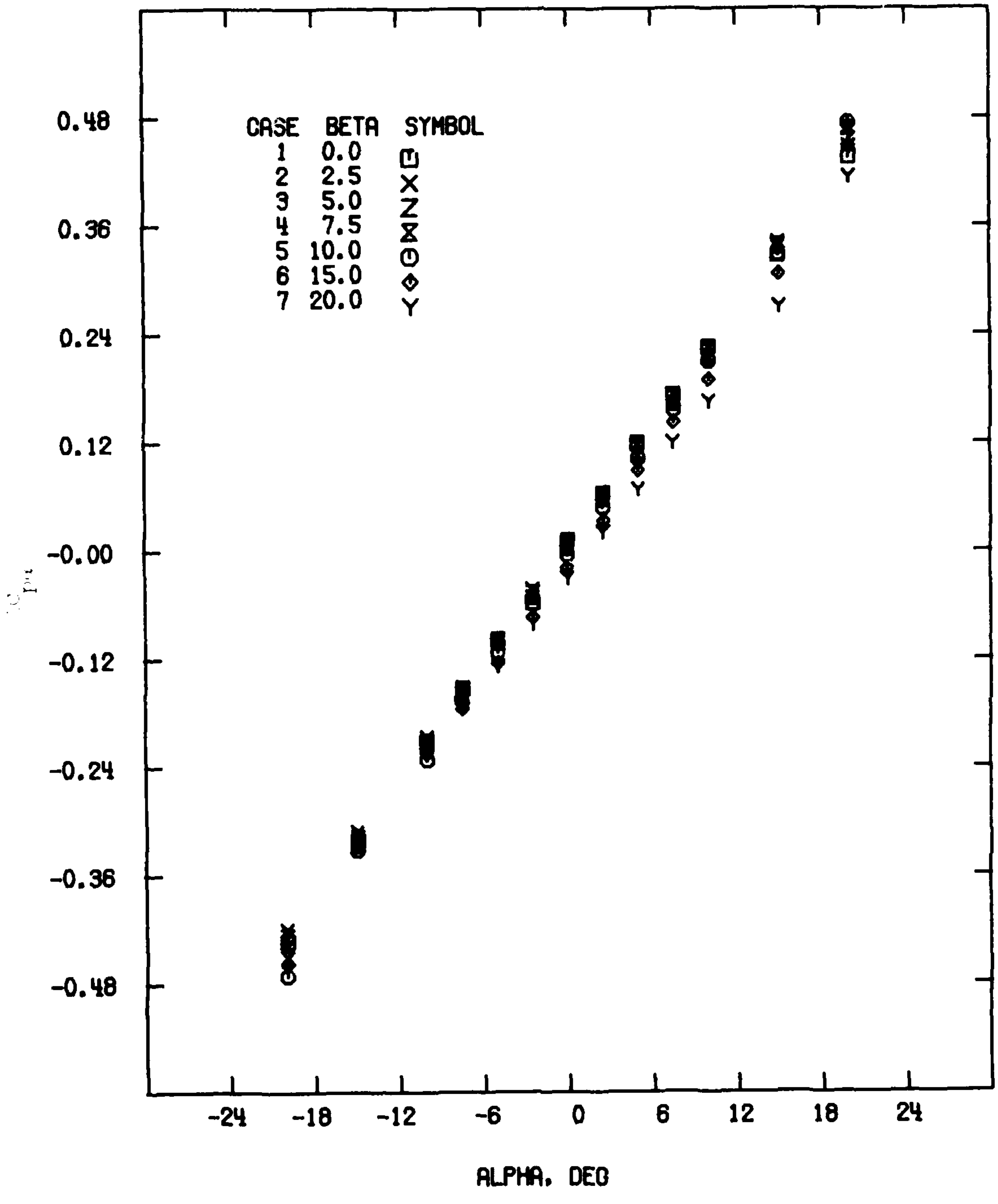

Figure 8. ΔC_{p_α} versus α and β for the Five-ported, Conical Probe, $M_\infty \simeq 0.2$

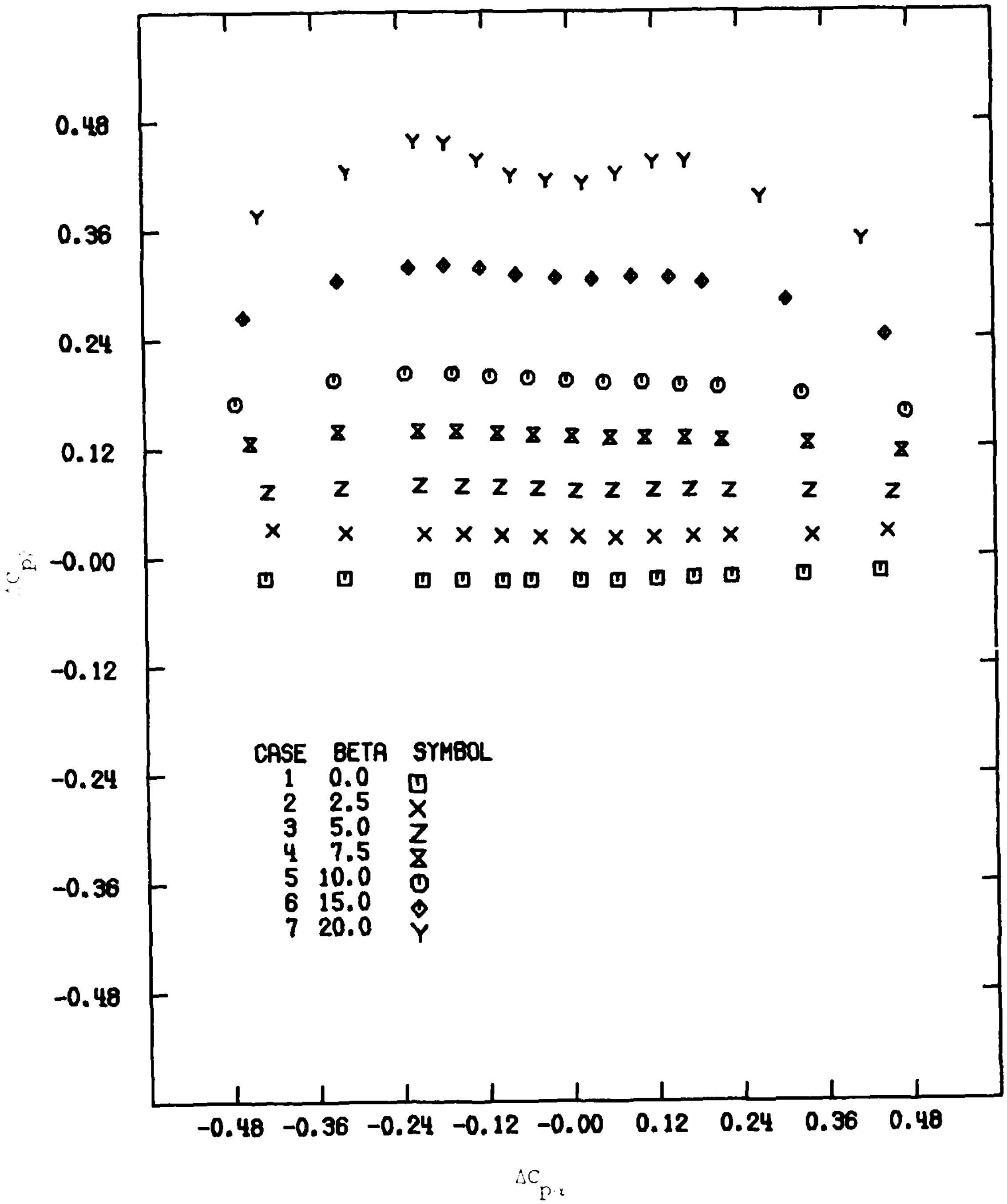

Figure 9. ΔC_{p_α} versus ΔC_{p_β} for the Five-ported, Conical Probe $M_\infty \simeq 0.2$

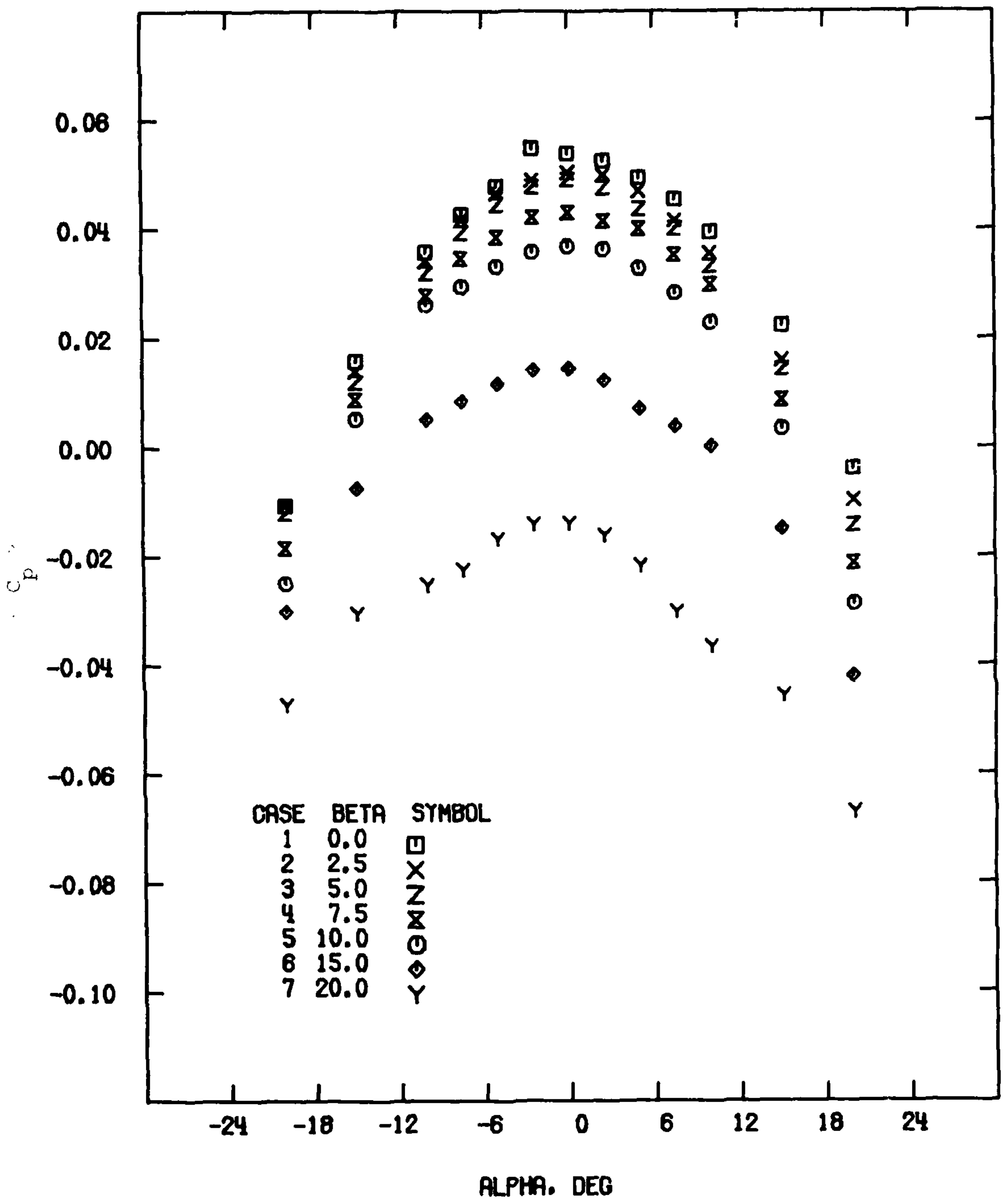

Figure 10. $\langle C_p \rangle$ versus α and β for the Five-ported, Conical Probe, $M_\infty \simeq 0.2$

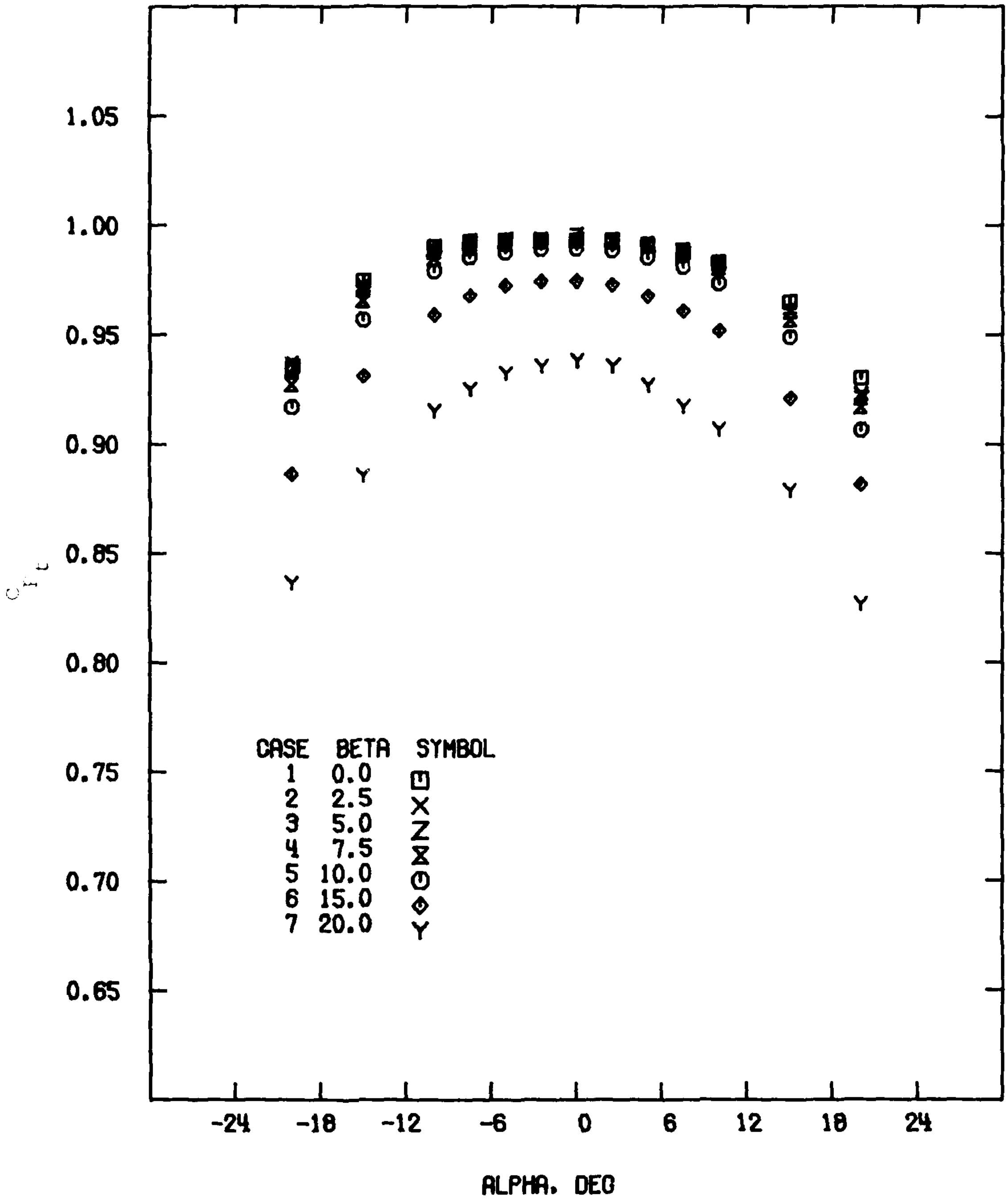

Figure 11. C_{p_t} versus α and β for the Five-ported, Conical Probe, $M_\infty \approx 0.2$

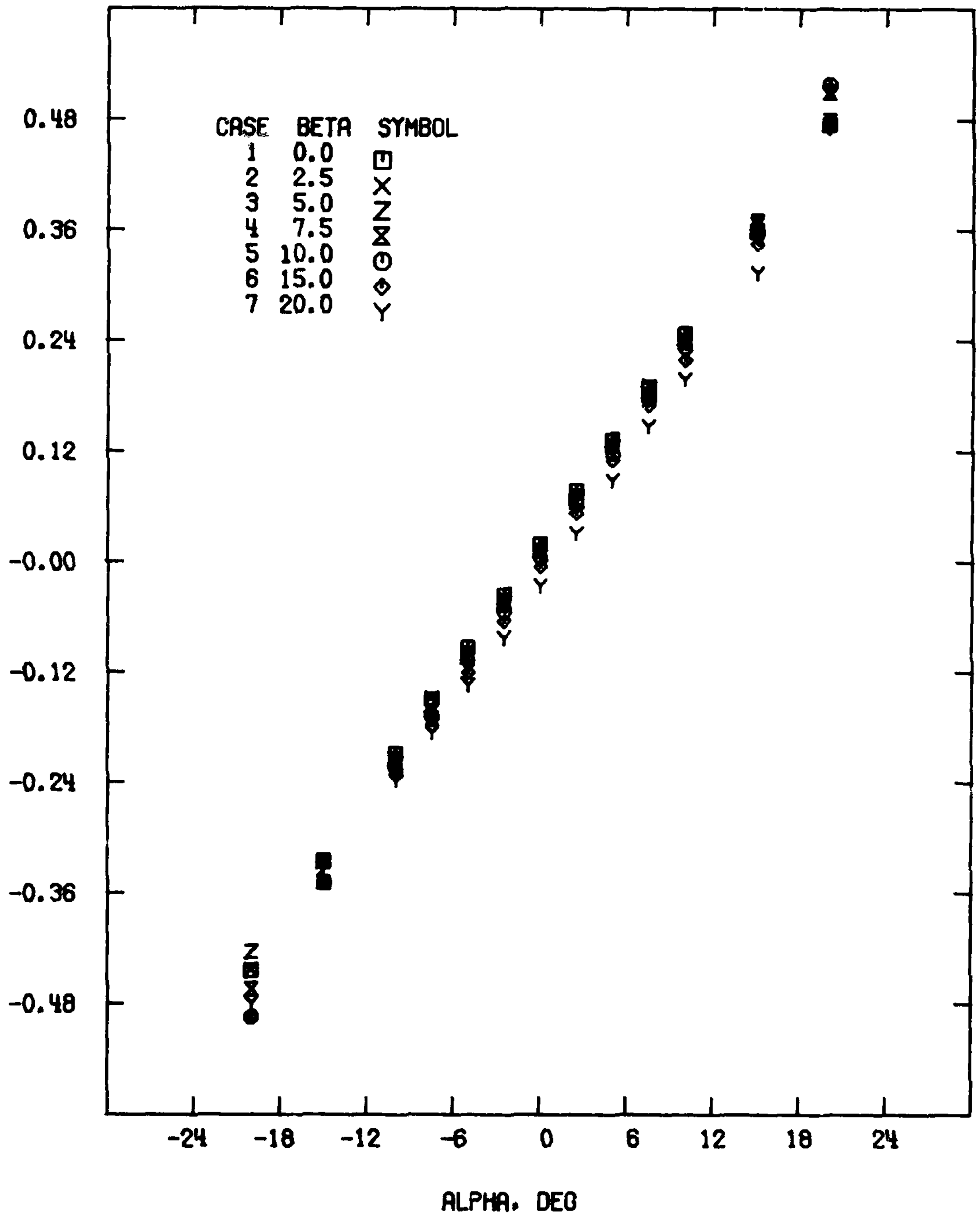

Figure 12. ΔC_{p_α} versus α and β for the Five-ported, Conical Probe, $M_\infty \simeq 0.4$

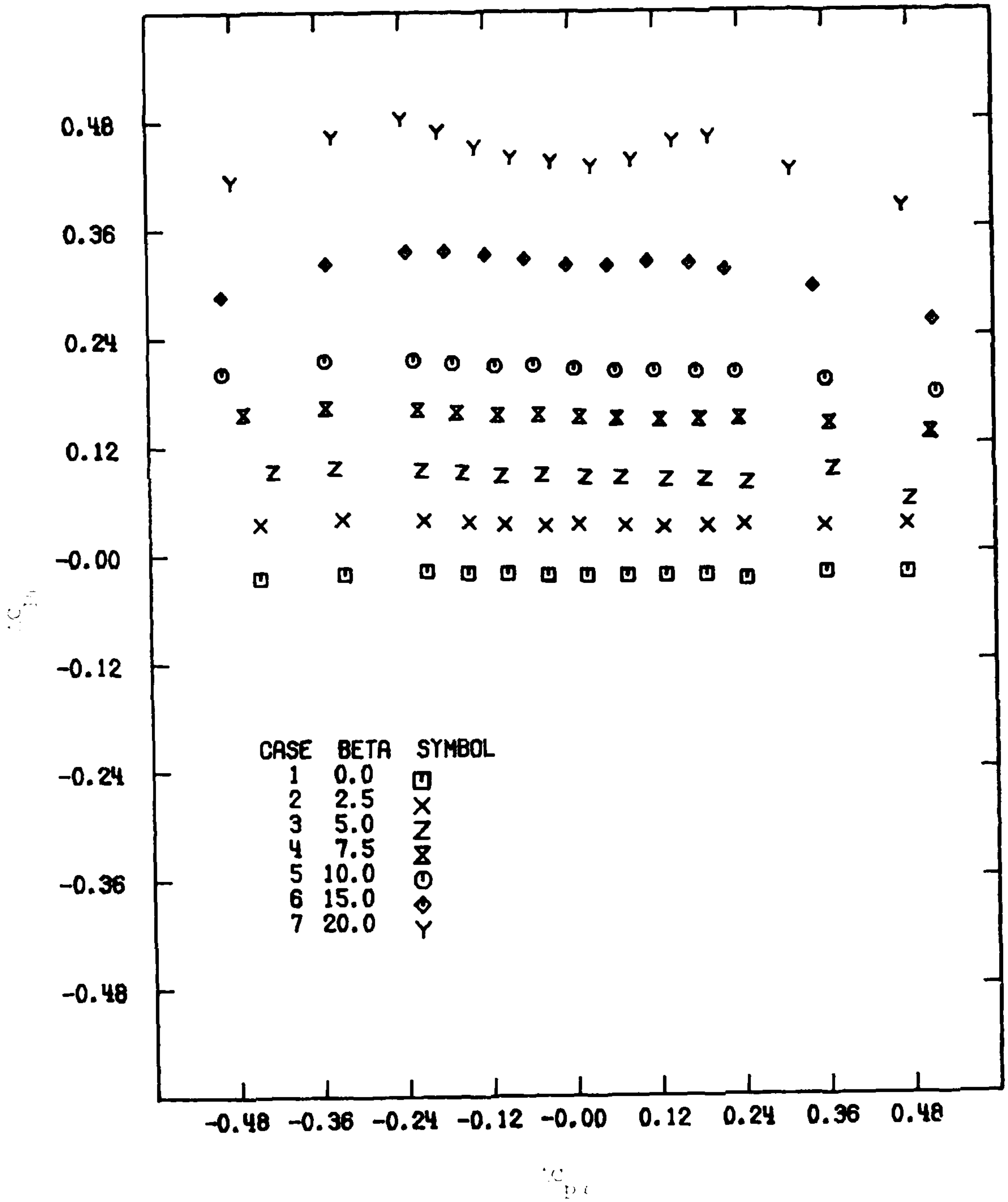

Figure 13. ΔC_{p_α} versus ΔC_{p_β} for the Five-ported, Conical Probe, $M_\infty \approx 0.4$

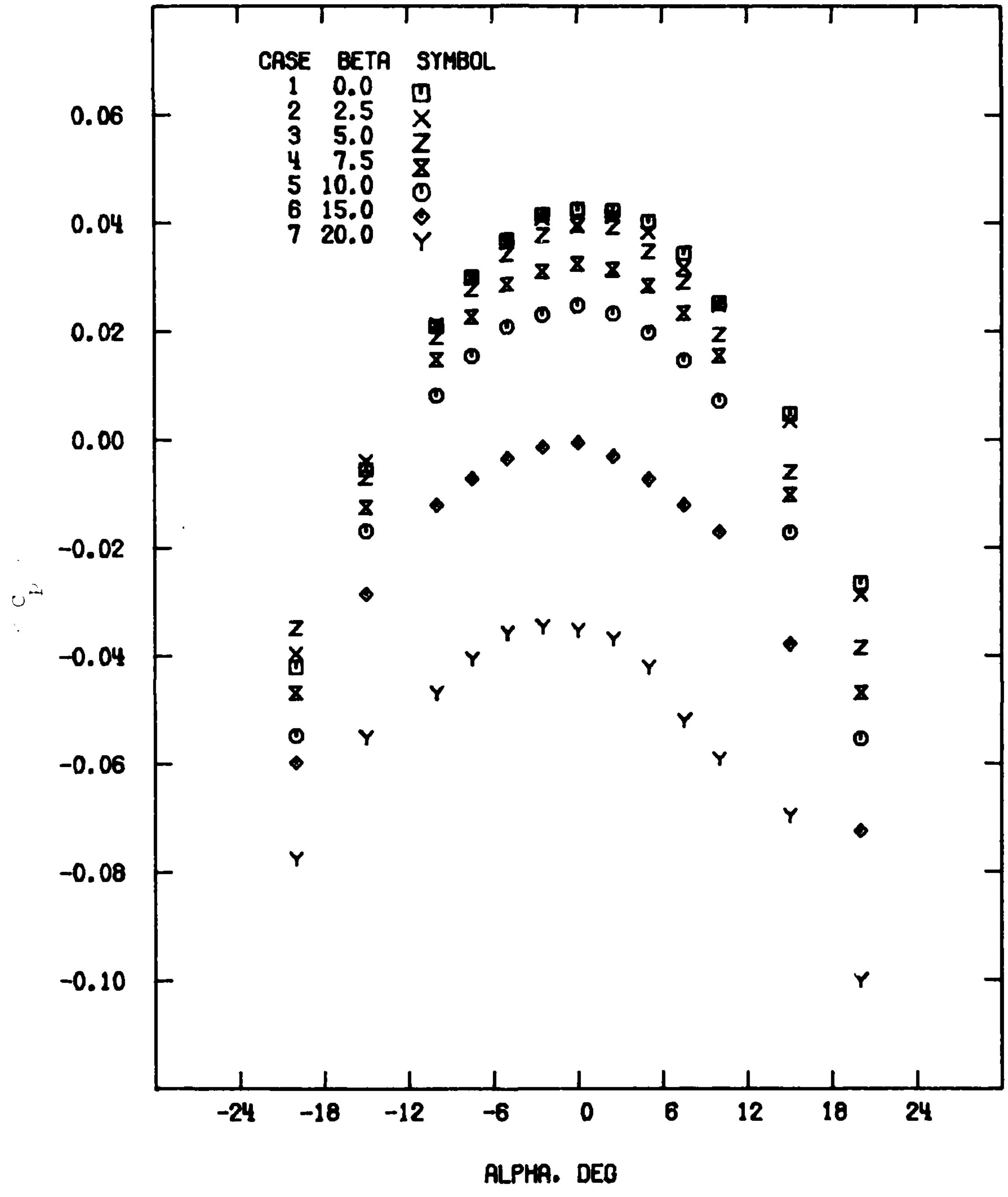

Figure 14. $\langle C_p \rangle$ versus α and β for the Five-ported, Conical Probe, $M_\infty \simeq 0.4$

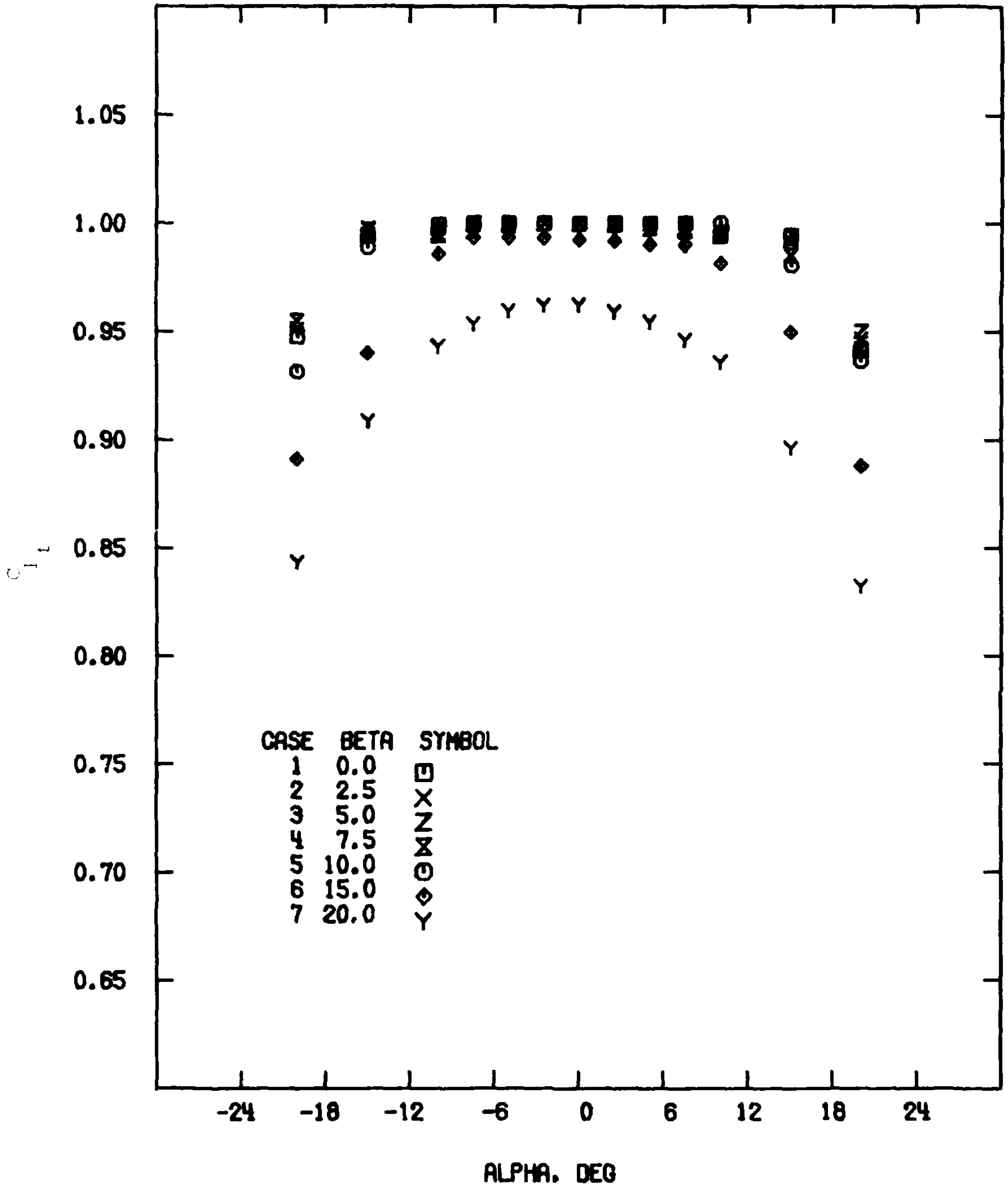

Figure 15. C_{p_t} versus α and β for the Five-ported, Conical Probe, $M_\infty \approx 0.4$

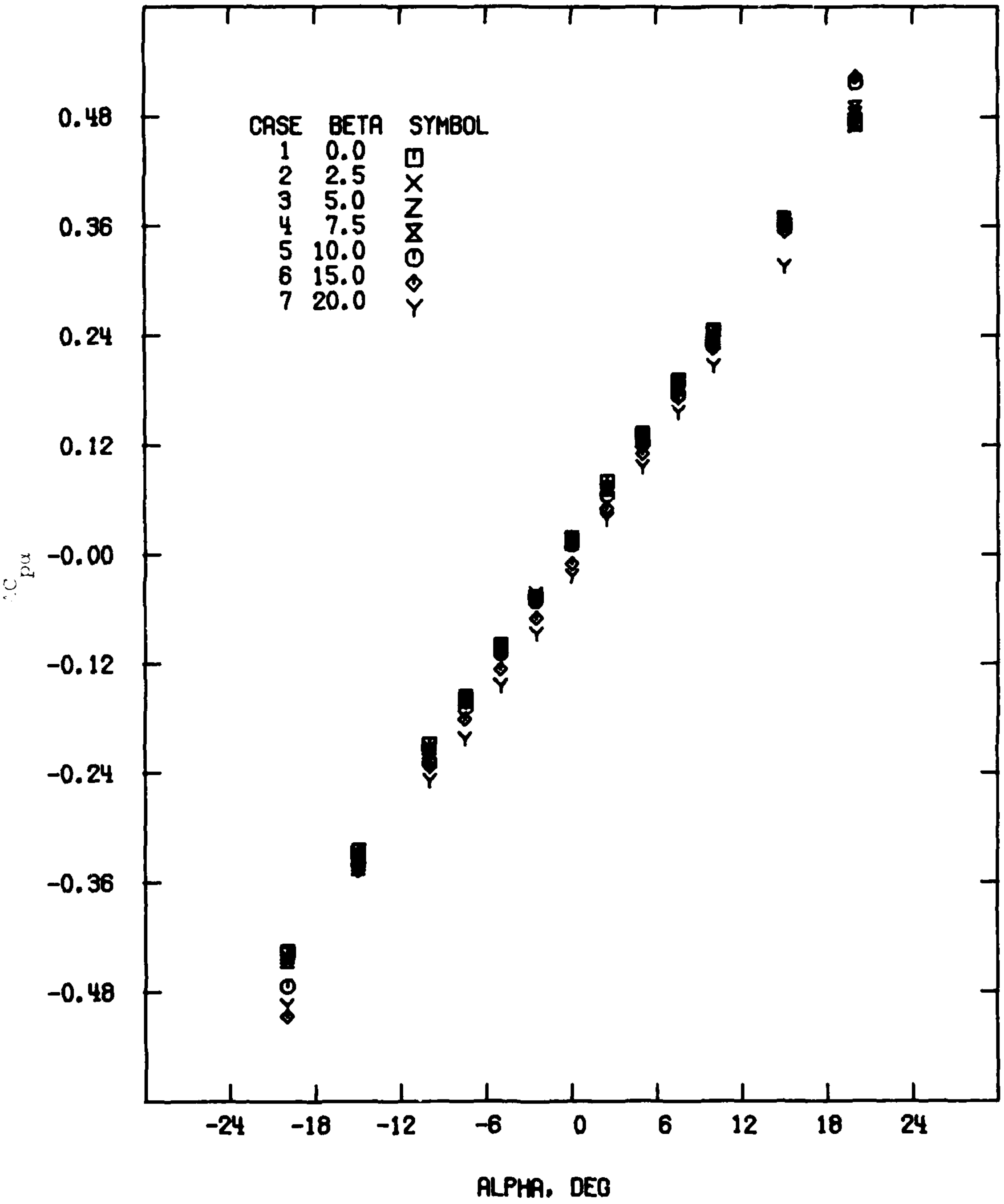

Figure 16. ΔC_{p_α} versus α and β for the Five-ported, Conical Probe, $M_\infty \simeq 0.6$

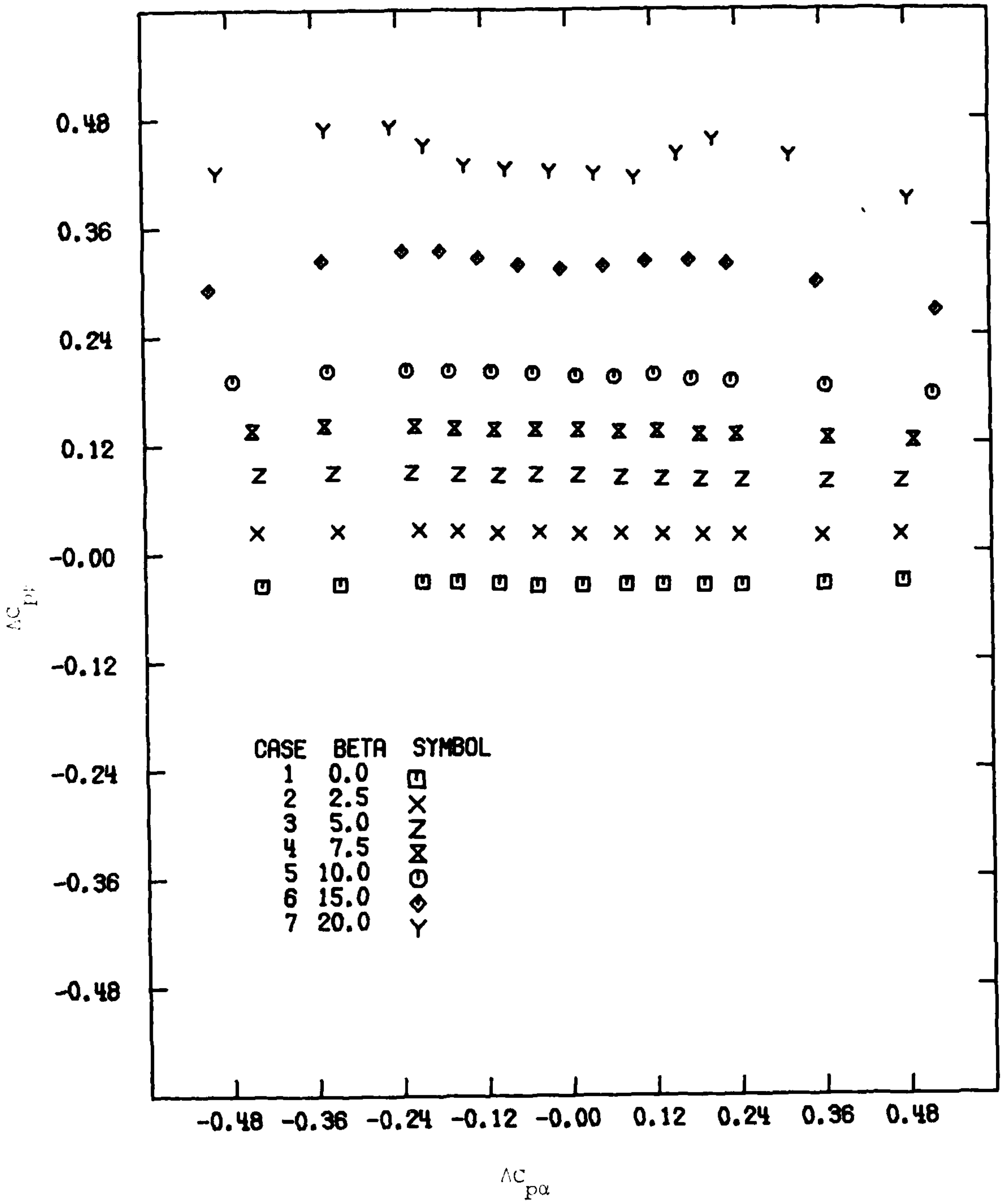

Figure 17. ΔC_{p_α} versus ΔC_{p_β} for the Five-ported, Conical Probe, $M_\infty \cong 0.6$

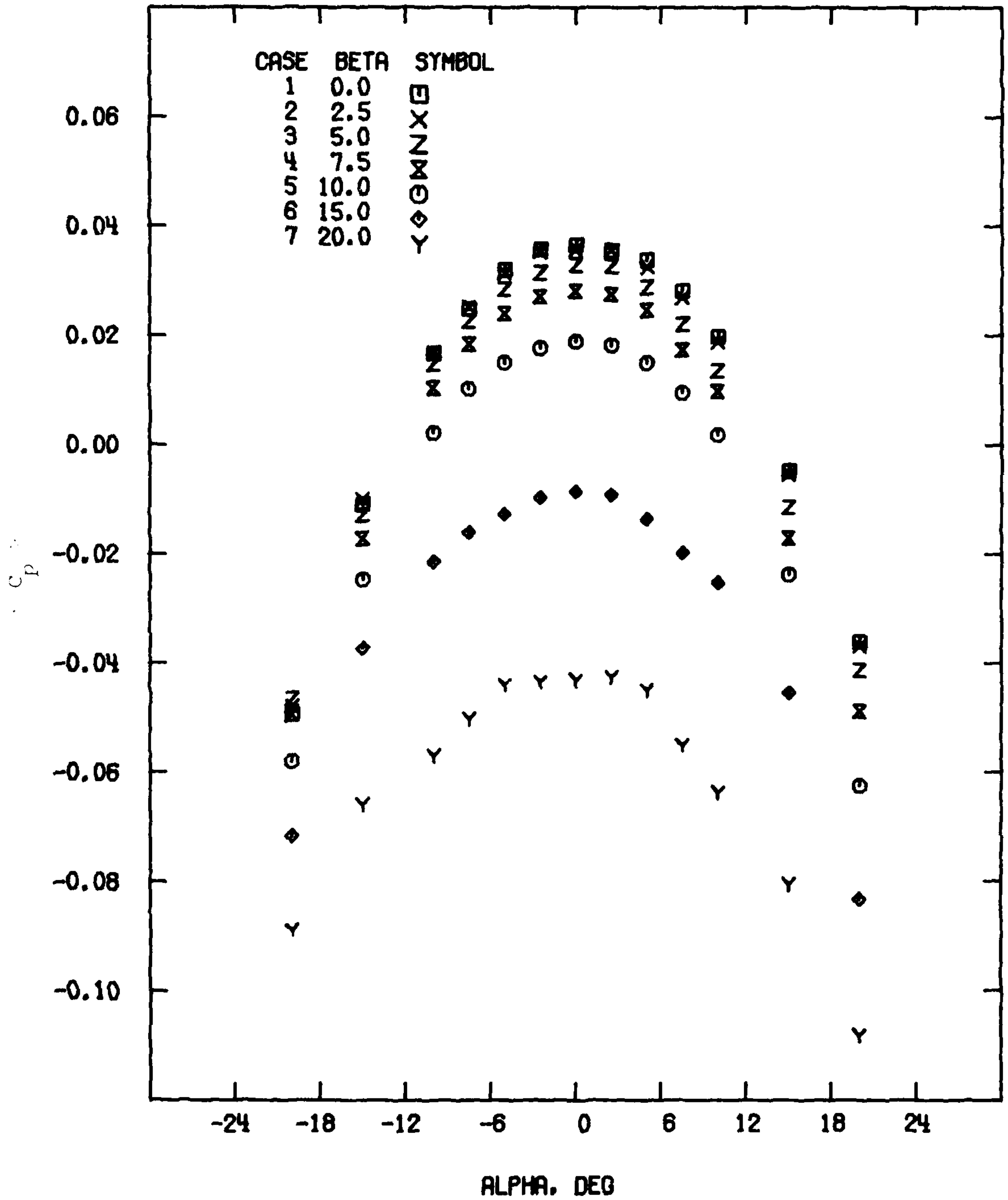

Figure 18. $\langle C_p \rangle$ versus α and β for the Five-ported, Conical Probe, $M_\infty \simeq 0.6$

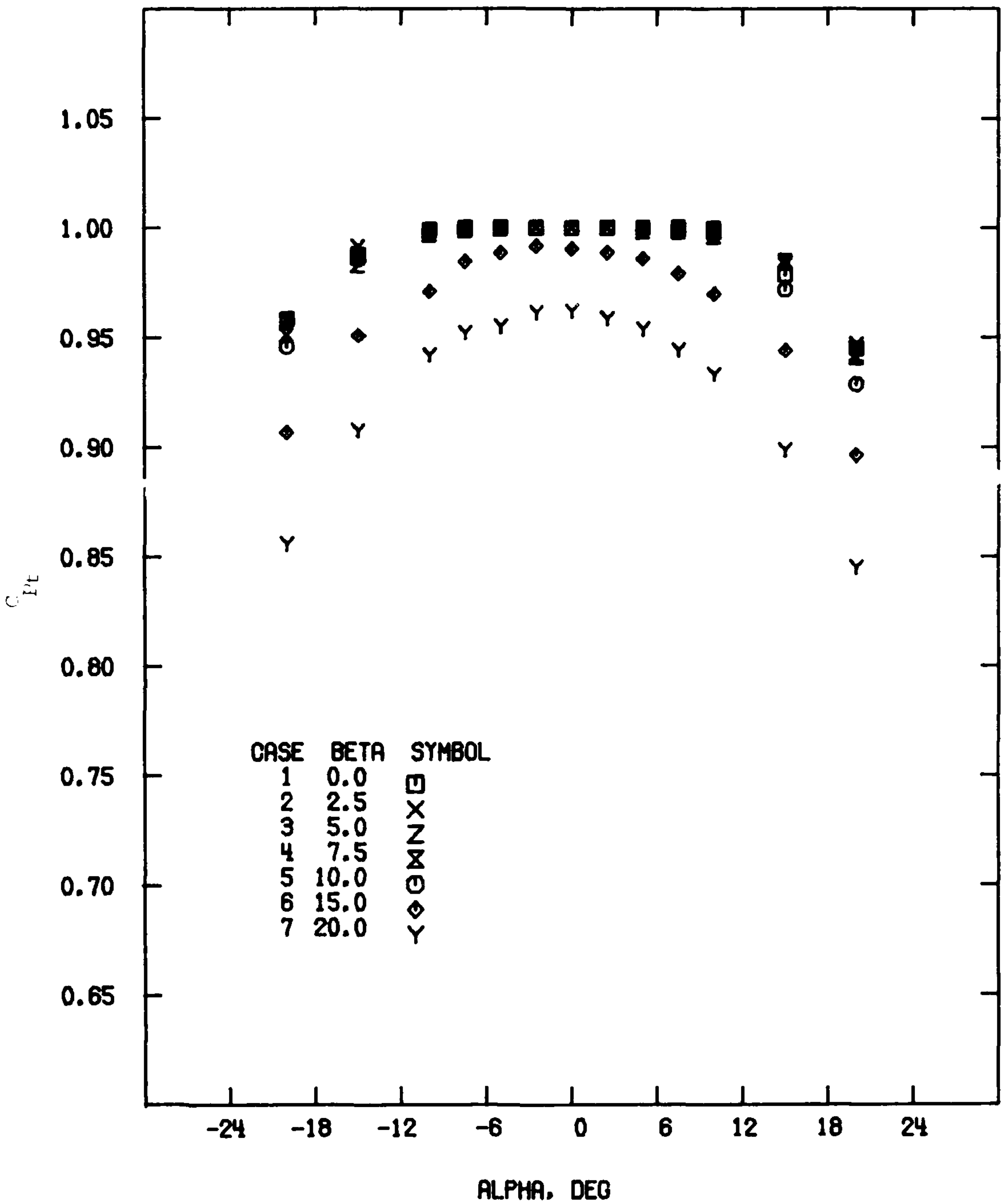

Figure 19. C_{P_t} versus α and β for the Five-ported, Conical Probe, $M_\infty = 0.6$

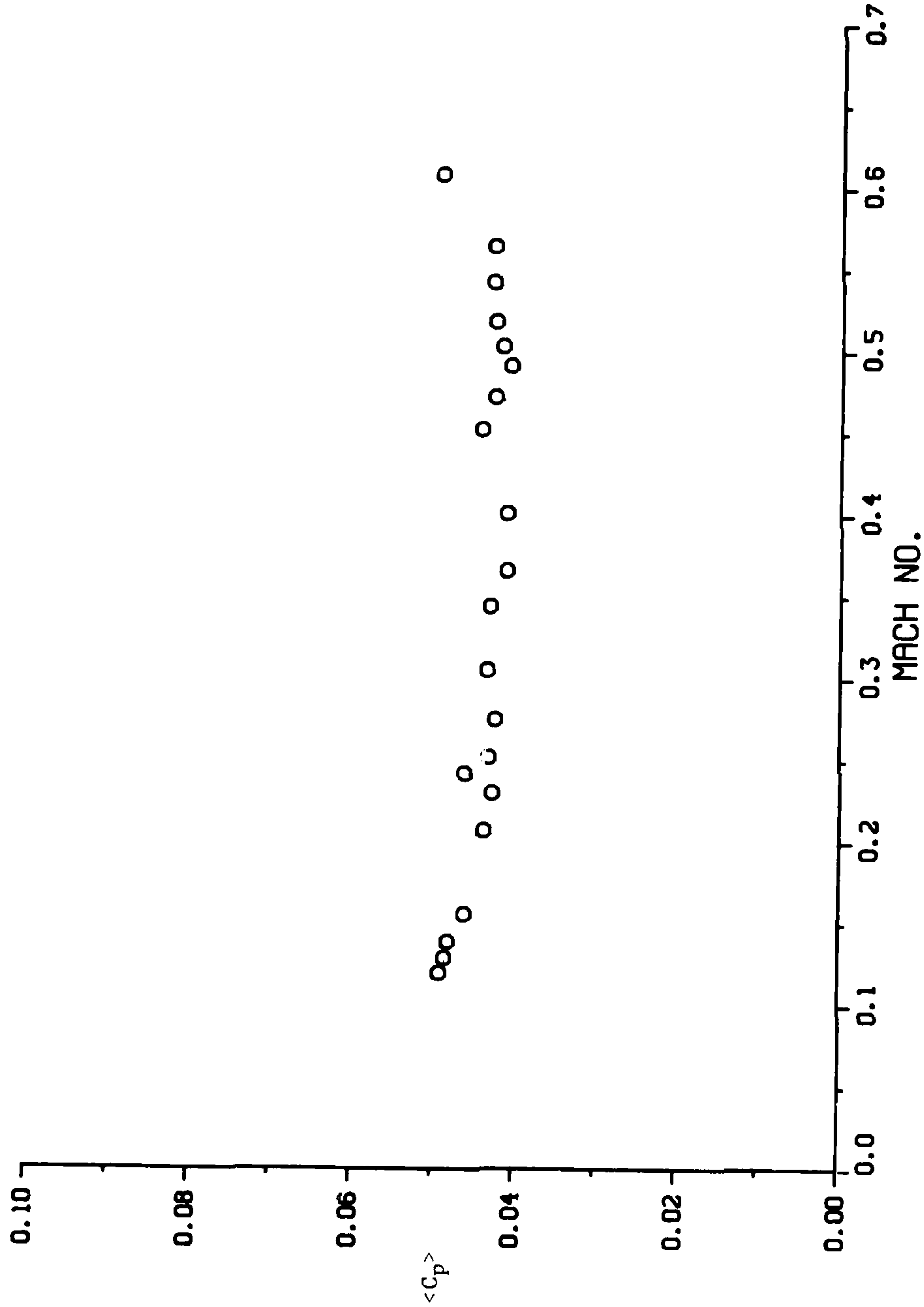

FIGURE 20. $\langle C_p \rangle$ VERSUS M_∞ FOR THE FIVE-PORTED, CONICAL PROBE, $\alpha=\beta=0$

The parameters of Section 2, ΔC_{p_α}, ΔC_{p_β}, $\langle C_p \rangle$ and C_{p_t}, are plotted in the three groups of figures. Figures 8, 12 and 16 depict the variation of ΔC_{p_α} with α, β and Mach number. Figures 9, 13 and 17 consist of cross-plots of ΔC_{p_α} versus ΔC_{p_β}. $\langle C_p \rangle$ is plotted in Figures 10, 14 and 18 for the three Mach numbers with C_{p_t} plotted in Figures 11, 15 and 19. Figure 20 shows the variability of $\langle C_p \rangle$ with Mach number.

The probe performance generally confirms to the analytic relations of Section 2. From Figure 3, it can be concluded that ΔC_{p_α} and/or ΔC_{p_β} should vary linearily with α and for β over small angular ranges becoming non-linear as the angles increase. This trend is shown in Figures 8, 9, 12, 13, 16 and 17. The decrease in angular response is particularly evident in Figures 9, 13 and 17 at the higher values of α and β, i.e., ΔC_{p_β} tends to increase at a lesser rate as α and β exeed about 10°.

$\langle C_p \rangle$ and C_{p_t} both vary predominately with α^2 and β^2 as shown in equations (30) and (31), i.e.,

$$\begin{aligned} \langle C_p \rangle &\approx (1-\alpha^2-\beta^2)[-f-(R')^2]-\beta^2-\alpha^2 \\ C_{p_z} &\approx \frac{(1-\alpha^2-\beta^2)}{R_\ell^{\,2}} \int_o^\ell (R^2)'[-f-(R')^2]dz-\beta^2-\alpha^2 \end{aligned} \tag{37}$$

where higher order terms have been neglected.

According to the slender body analysis of Section 2, only the function f is Mach number dependent and, thus, ΔC_{p_α} and ΔC_{p_β} should be independent of Mach number while $\langle C_p \rangle$ and C_{p_z} are functions of Mach number. This result is more--or less--confirmed experimentally. The angularity coefficients are much less Mach number dependent than the averaged static pressure or total pressure coefficients. This can be seen by comparing Figures 8 through 11 with Figures 12 through 15 or Figures 16 through 19.

The Mach number dependence of $\langle C_p \rangle$ is not particularly pronounced in the subsonic flow regions. Figure 20 and Table 4 show only a modest variation in this parameter as the Mach number is increased from 0.12 to 0.61.

4.4 Summary of Experimental Results

The angularity coefficients, i.e., flow direction coefficients, and static and total pressure coefficients behave, functionally, in a manner

consistent with equations (25), (30) and (31). ΔC_{p_α} and ΔC_{p_β} vary linearly with α and β for small and moderate angles while $\langle C_p \rangle$ and C_{p_t} varying with α^2 and β^2. Both ΔC_{p_α} and ΔC_{p_β} are independent of Mach number while $\langle C_p \rangle$ and C_{p_t} are Mach number dependent. The data scatter is well within acceptable bounds for angles up to 10° and increases somewhat at the larger angles. The behavior at the larger angles may be due to flow separation on the probe itself or flow blockage effects as discussed in Section 3.4.

SECTION V

COMPARISON OF THEORETICAL AND EXPERIMENTAL RESULTS

5.1 Averaged Pressure Coefficient

The subsonic, transonic and supersonic flow field about a cone has been measured by many investigators. Some typical experimental results, reference 29, are compared with equation (30) in Figure 21. Note that the conditions correspond to an angle of attack and side-slip angle of 0°. The mathematical model of Section 2 is limited to subsonic Mach numbers, i.e., the Mach number must be less than 1 on all points of the conic surface. This corresponds to a freestream Mach number, M_{∞}, of approximately 0.9 and, thus, the experimental theoretical comparison has been limited to this value. The analytic predictions correspond closely to the measured values over about 75-80% of the cone length. The calculated $\langle C_p \rangle$ values are less than the measured points over the latter portions of the cone, $0.75 \leq z/\ell \leq 1.00$, with the deviation increasing as the Mach numbers approach one.

The cone of reference 29 has an included angle of 6.983°, a length of 139.7mm (5.50 in) and a maximum diameter of 34.214mm (1.347 in). The model is sufficiently large so that the static pressure ports can be assumed to be normal to the cone surface. The tests were carried out in two separate wind tunnels, i.e., NASA Ames 2 by 2 foot and 14 by 14 foot transonic wind tunnels, and both sets of data agree to within the accuracy of the measurements. As a consequence, there is every reason to believe that the data is accurate. The disparity between the measured and calculated results over the aft-portion of the cone must then be due to a failure of the theory itself.

The calculated pressure coefficients for the cone probe of Section 4 are shown in Figures 22, 23 and 24. Figure 22 depicts the variation of the averaged pressure coefficient as a function of position, z/ℓ, and Mach number. The section diagram shows the location of the static ports and the point of cone truncation. Figure 23 is a plot of $\langle C_p \rangle$ as a function of Mach number while Figure 24 shows $\langle C_p \rangle$ as a function of α and β.

While the general trends of the data are reproduced by the analysis of Section 2, the overall levels are considerably less than the measured values. As noted in previous paragraphs, the mathematical model tends to

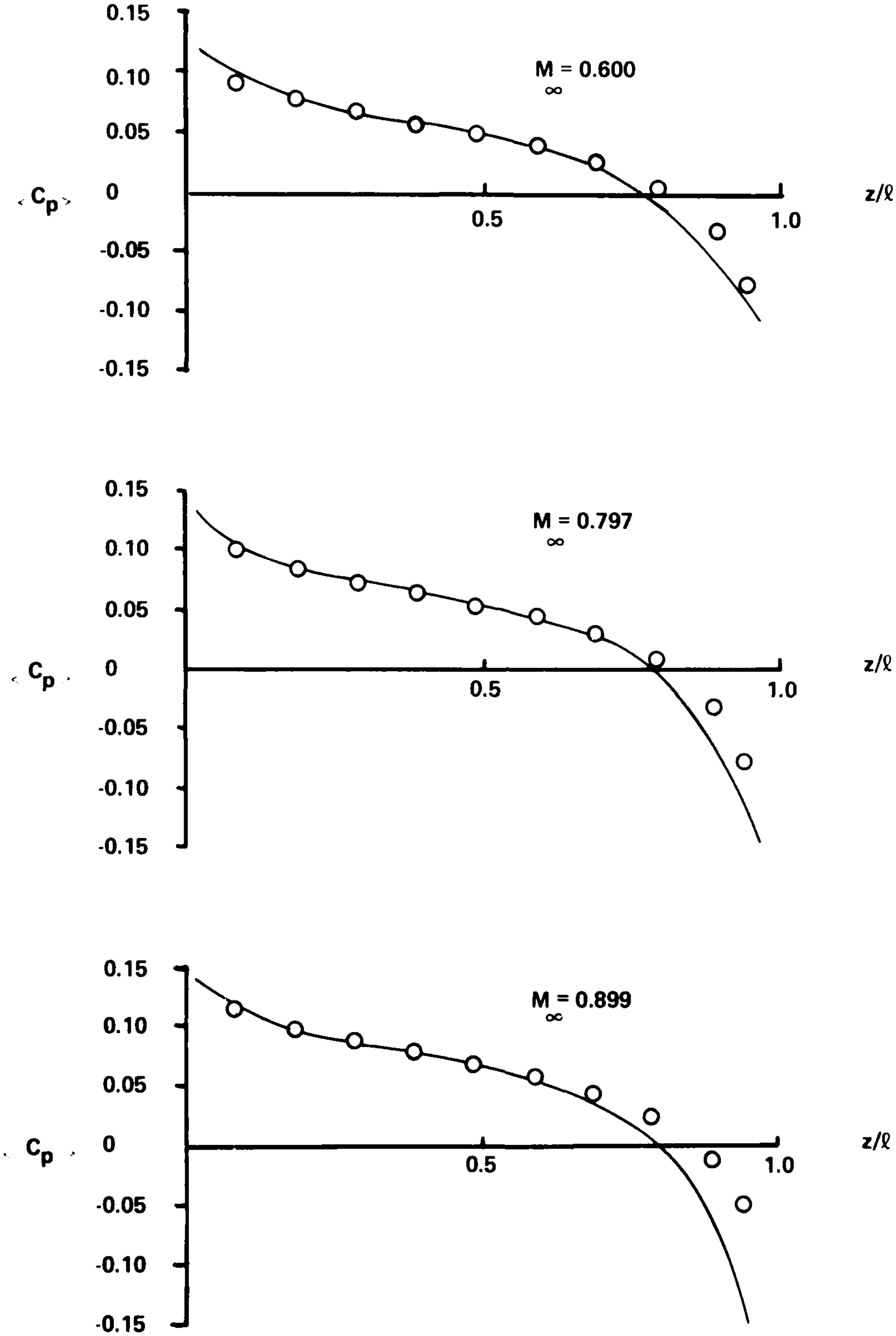

Figure 21. Comparison of Measured and Calculated Averaged Pressure Coefficients for a 7° Conic Section

Figure 22. Calculated Average Pressure Coefficient for a 30° Conic Section as a Function of Position and Mach Number

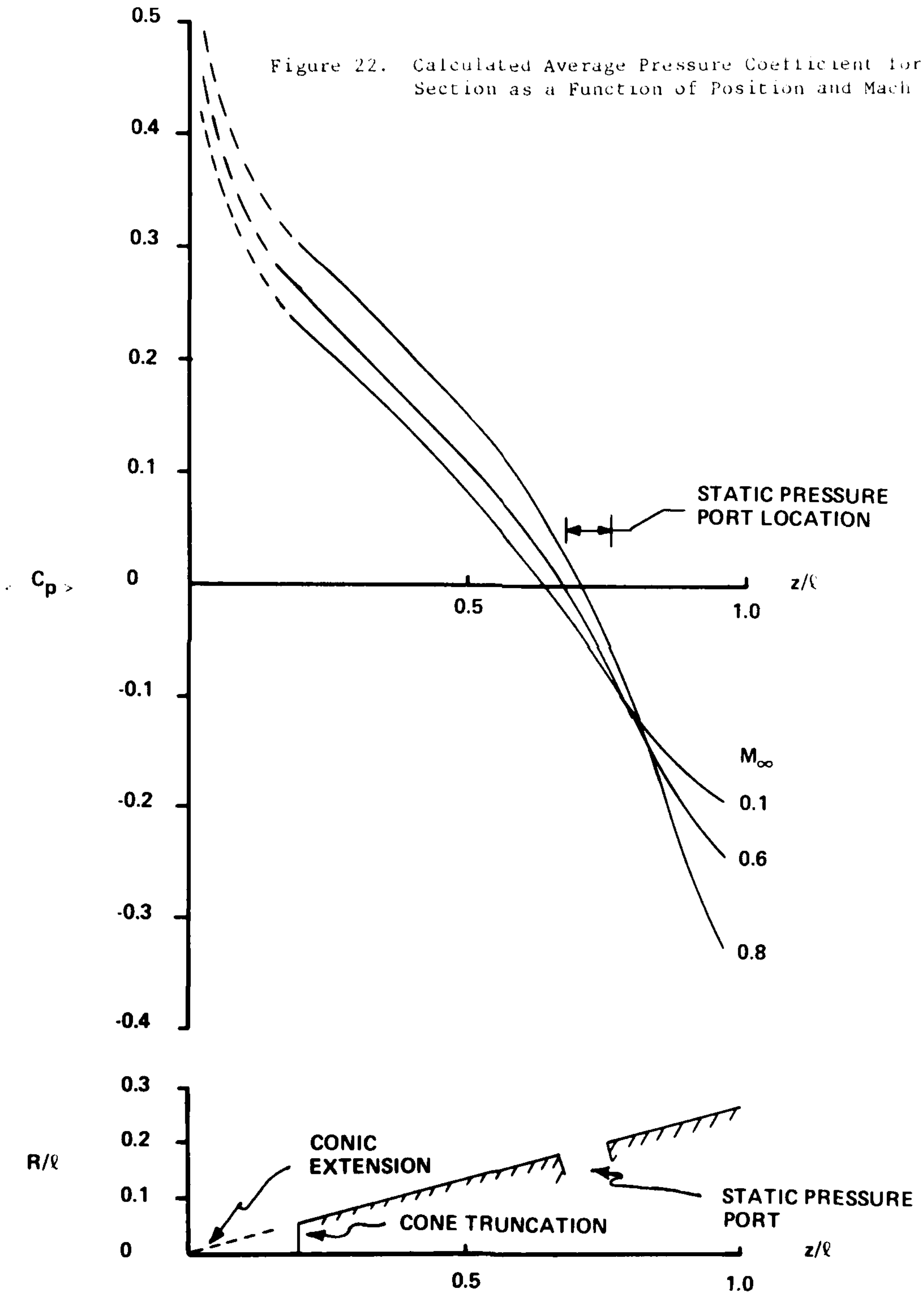

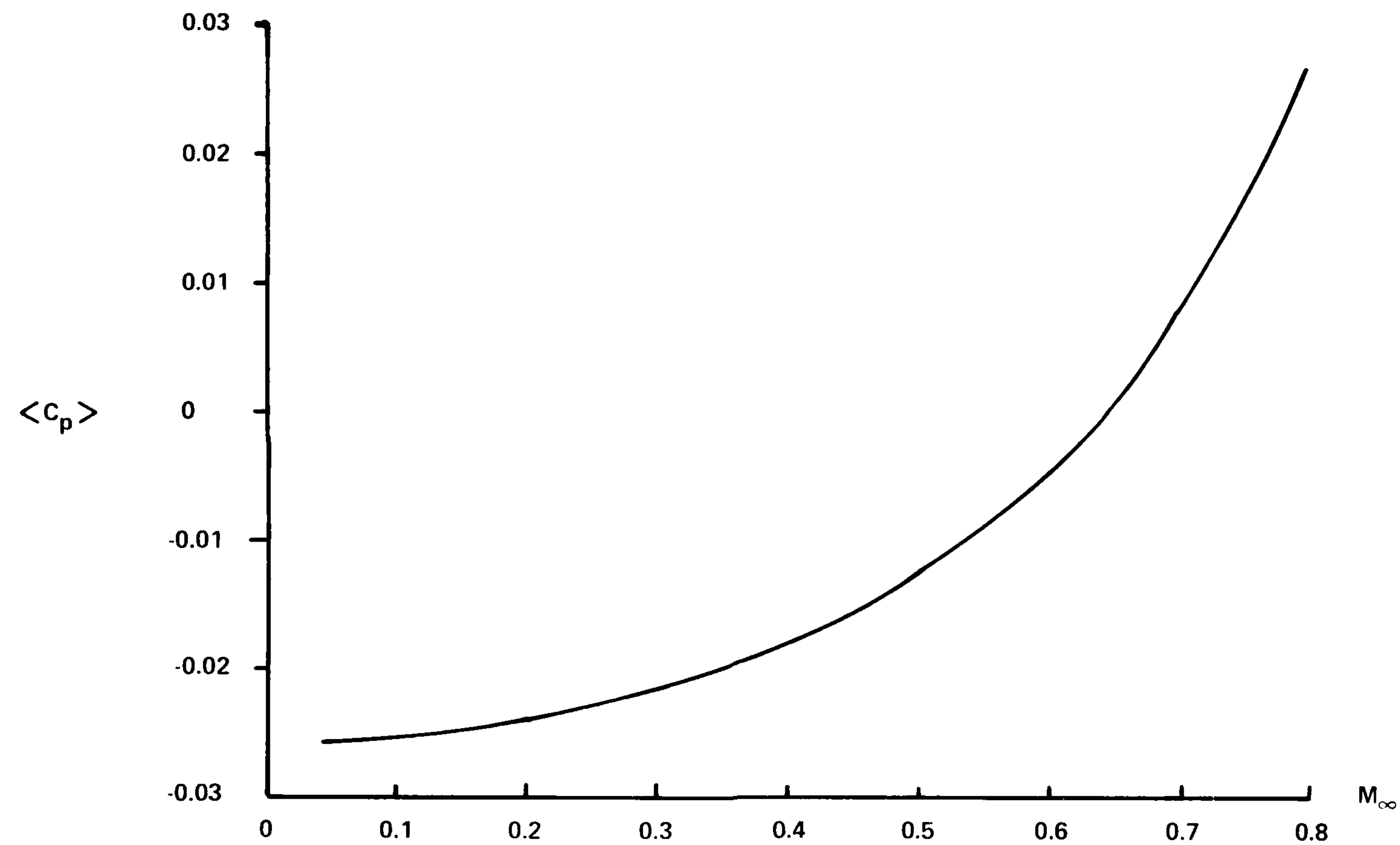

Figure 23. Calculated Cone Probe Pressure Distribution as a Function of Mach Number, $\alpha = \beta = 0$ and $z/\ell = 0.68$

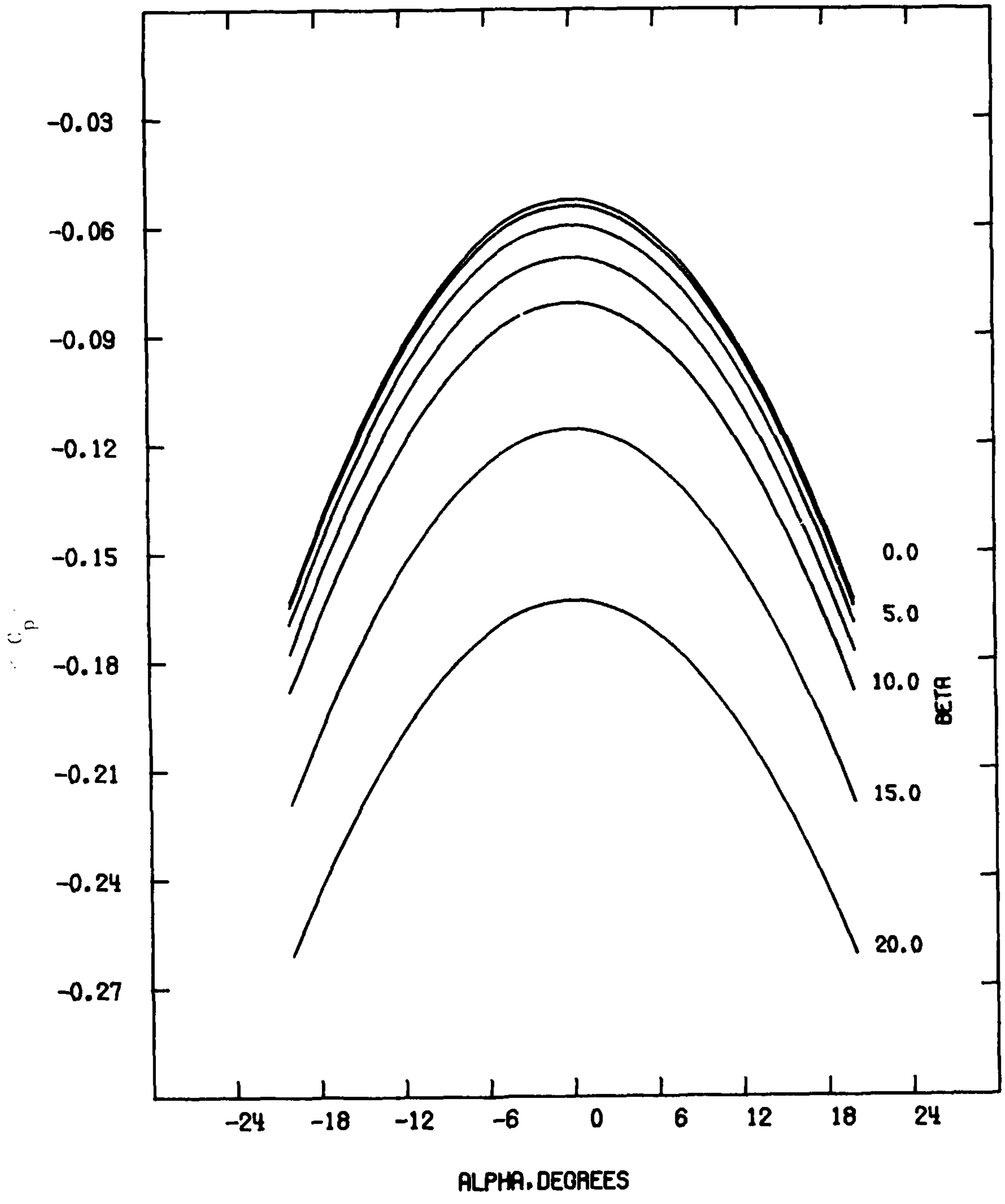

Figure 24. Averaged Pressure Coefficient for a 30° Cone Probe, $M_\infty = 0.20$ and $z/\ell = 0.68$

underestimate the C_p values on the latter portion of the cone. Other potential sources of error are static pressure hole diameter and depth, references 30 and 31, hole geometry, reference 32, hole not normal to cone surface and turbulence level, reference 33. It was initially believed that the truncation of the cone might alter the measured static pressures. The low and variable Mach number tests of Section 4 were, however, repeated for a sharp-nosed cone with little or no change in the measured pressure coefficients. As a consequence, it was concluded that cone truncation - of the magnitude shown in Figure 22 - does not influence the static pressure measurements.

The magnitude of corrections for pressure tube geometry are of the order of the difference between the calculated and measured values if the static holes are slightly rounded, i.e., a correction of approximately 0.5-1% of the dynamic head for a corner radius of 0.114mm (0.005 in). This effect, coupled with the underestimate of Figure 21, are probably the main cause of the discrepancy between the calculated and measured values, e.g., Figures 20 and 23 and Figures 10 and 24.

The difference between the calculated and measured results again points out the need to calibrate individual probes, particularly the extremely small sensors used in turbine engine tests. It is unlikely that probes of the type and size discussed in Section 4 can be manufactured without some anamolous behavior.

5.2 Angular Pressure Coefficients

The angular pressure coefficient data of Section 4, $\Delta C_{p\alpha}$ and $\Delta C_{p\beta}$, can be compared to the theoretical results of Section 2, equation (25). Equation (25) infers that $\Delta C_{p\alpha}$ is proportional to the local surface gradient, dR/dz, the sin 2α and $\cos^2\beta$. As a consequence, $\Delta C_{p\alpha}$ is approximately linear with α for small angles of attach, is independent of Mach number and is only slightly dependent on β for small β values. Calculated values for $\Delta C_{p\alpha}$ and $\Delta C_{p\beta}$ as a function of α and β are shown in Figure 25. These results are in general comparable to Figures 9, 13 and 17, although the magnitude of pressure coefficients is overestimated by the theory. This may be due to the error sources noted in Section 5.1. Rounding of the

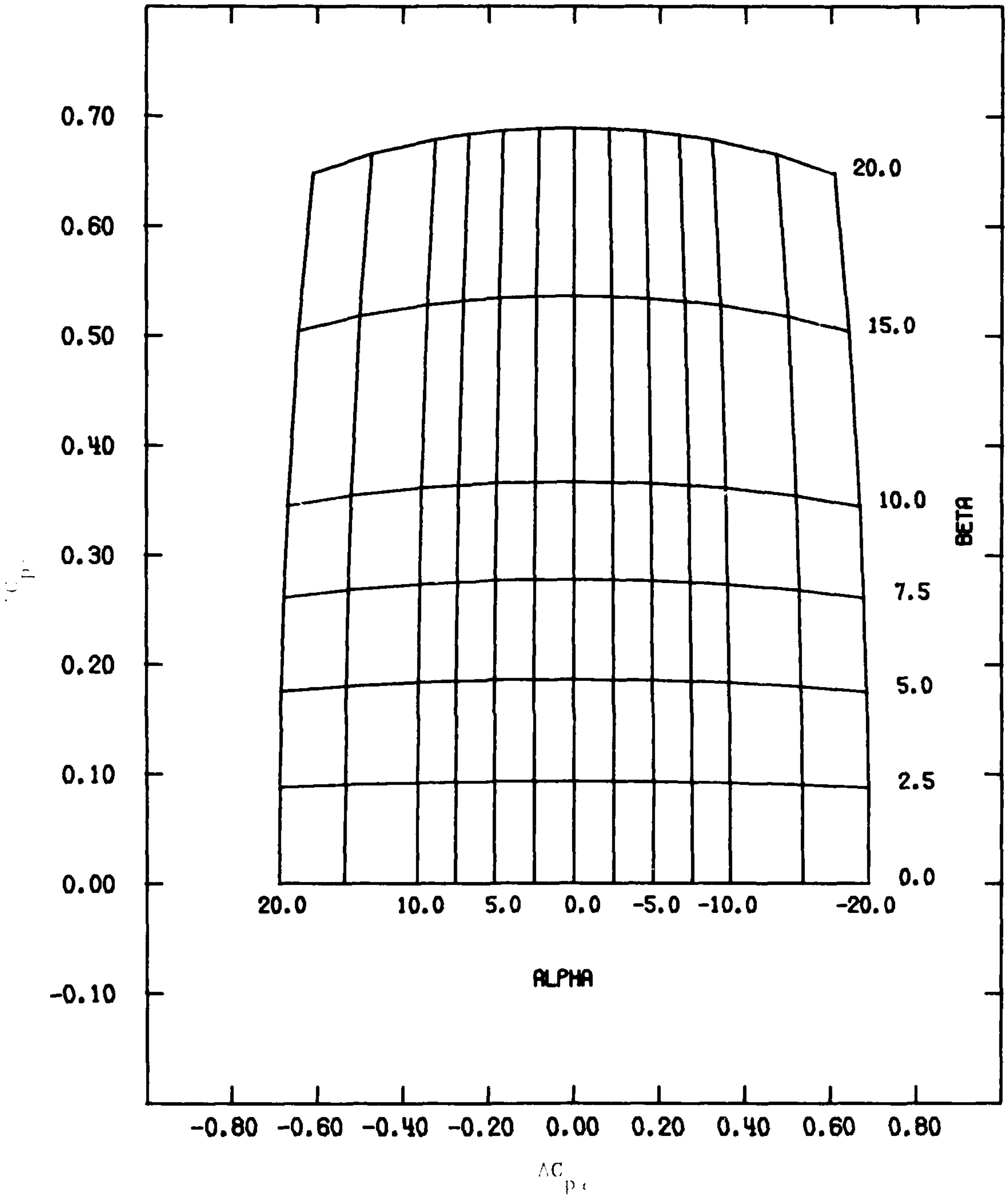

Figure 25. Angular Pressure Coefficients for a 30° Cone Probe, M_∞ = 0.20 and z/ℓ = 0.68

pressure ports coupled with a slight misalignment of the ports, i.e., not normal to the local cone surface, may also contribute to the slightly overestimated values.

The experimental values are reasonably independent of Mach number as predicted with only slight variations over the Mach number range $0.2 \leq M_\infty \leq 0.6$. The angular functional relationships of equation (25) characterize the data up to β values of 15^o. Beyond this point, the curves assume a double-lobed appearance which is probably due to flow separation.

5.3 Calibration Functions

The theoretically derived averaged pressure coefficient agrees well with experimental measurements carried out on large cones. The agreement - in an absolute sense - is, however, much poorer on the smaller cone probe. The functional variation with α and β is correctly predicted by the theory but again the magnitude of change is slightly overestimated by the equations of Section 2.

The angular pressure coefficients of Section 2 exceed the measured values with the dependence of ΔC_{p_α} and ΔC_{p_β} on α, β and M_∞ correctly represented by the theory. Since the functional relationships are correctly predicted by the slender body theory, the equations of Section 2 can be used as a framework for a series of empirical calibration relations. These will take the form

$$\begin{aligned} \langle C_p \rangle &= f_1(M_\infty)\cos^2\alpha\cos^2\beta - C_1\sin^2\beta - C_2\sin^2\alpha\cos^2\beta \\ \Delta C_{p_\alpha} &= C_3\sin 2\alpha\cos^2\beta \\ \Delta C_{p_\beta} &= C_4\cos\alpha\sin 2\beta \\ C_{p_t} &= f_2(M_\infty)\cos^2\alpha\cos^2\beta - C_5\sin^2\beta - C_6\sin^2\alpha\cos^2\beta \end{aligned} \tag{38}$$

where $f_1(M_\infty)$ and $f_2(M_\infty)$ are functions of Mach number and C_1, C_2, C_3, C_4, C_5 and C_6 are constants. All of these parameters will depend on the body geometry.

Note that the functions of Section 2 are valid in a comparative sense, i.e., the effects of Mach number and body geometry on the pressure coeffi-

cients can be compared for a series of probes. This implies that the theoretical relationships can be used in the preliminary design of pressure probes while the final configuration must be calibrated.

SECTION VI

GENERAL CHARACTERISTICS OF PRESSURE PROBES

6.1 Introduction

The theoretical relationships of Section 2, while not capable of replacing individual probe calibrations, are suitable for evaluating sensor geometry and Mach number effects. Furthermore, effects of probe alignment on averaged and angular pressure coefficients can also be determined. These effects will be discussed in the ensuing sections.

6.2 Influence of Body Geometry and Mach Number on the Pressure Coefficients

As was noted in Section 5, the angular pressure coefficient is primarily a function of body geometry and flow angle and is independent of Mach number, i.e.,

$$\Delta C_{p_\alpha} = 4R'\sin 2\alpha \cos^2\beta \tag{39}$$

Consequently, the sensitivity to flow angles is directly proportional to R' or dR/dz. For example, the angular sensitivity, $\partial\Delta C_p/\partial\alpha$, of a 40° included angle cone is 2.06 times greater than that for a 20° cone. It would then seem desirable to choose a large cone angle in an effort to improve angular sensitivity.

Since the probe is also to be used to measure total and static pressure, the effect of increasing cone included angle on these parameters must also be investigated. Calculations for a 20° and 40° cone have been carried out using equation (30) and these results are shown in Figures 26 and 27. These figures depict the variation of $\langle C_p \rangle$ with position, z/ℓ, and Mach number. As can be seen, $\langle C_p \rangle$ increases with increasing conic angle as does the sensitivity to Mach number, i.e., at a given z/ℓ location $\partial\langle C_p \rangle/\partial M_\infty$ increases with increasing cone angle. The latter infers greater Mach number dependence for the static and total pressure coefficients - an undesirable characteristic.

While increasing the cone angle increases the angular sensitivity, it also increases the Mach number sensitivity. Hence, a trade-off between

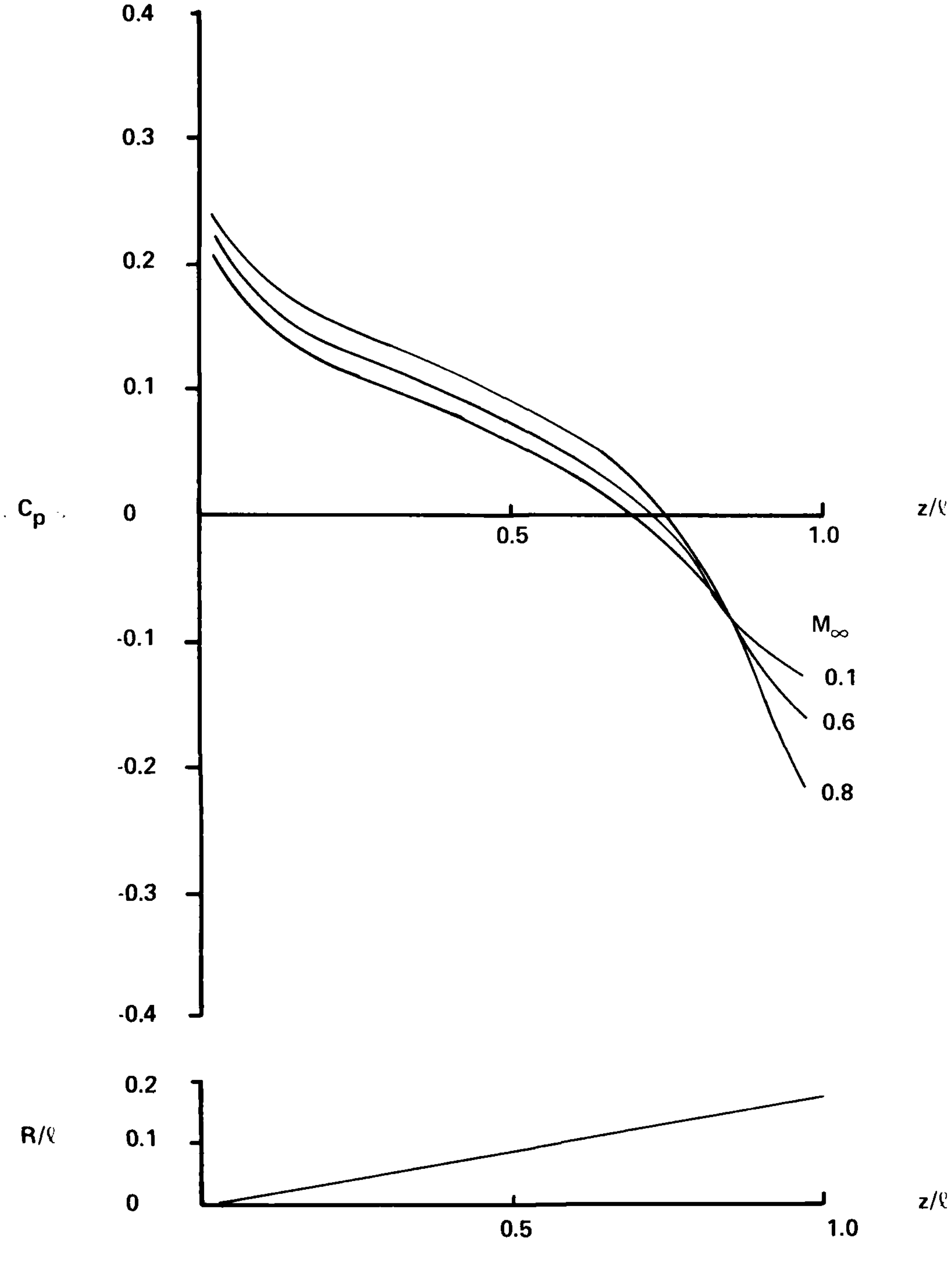

Figure 26. Calculated Averaged Pressure Coefficient for a 20^{o} Conic Section as a Function of Position and Mach Number

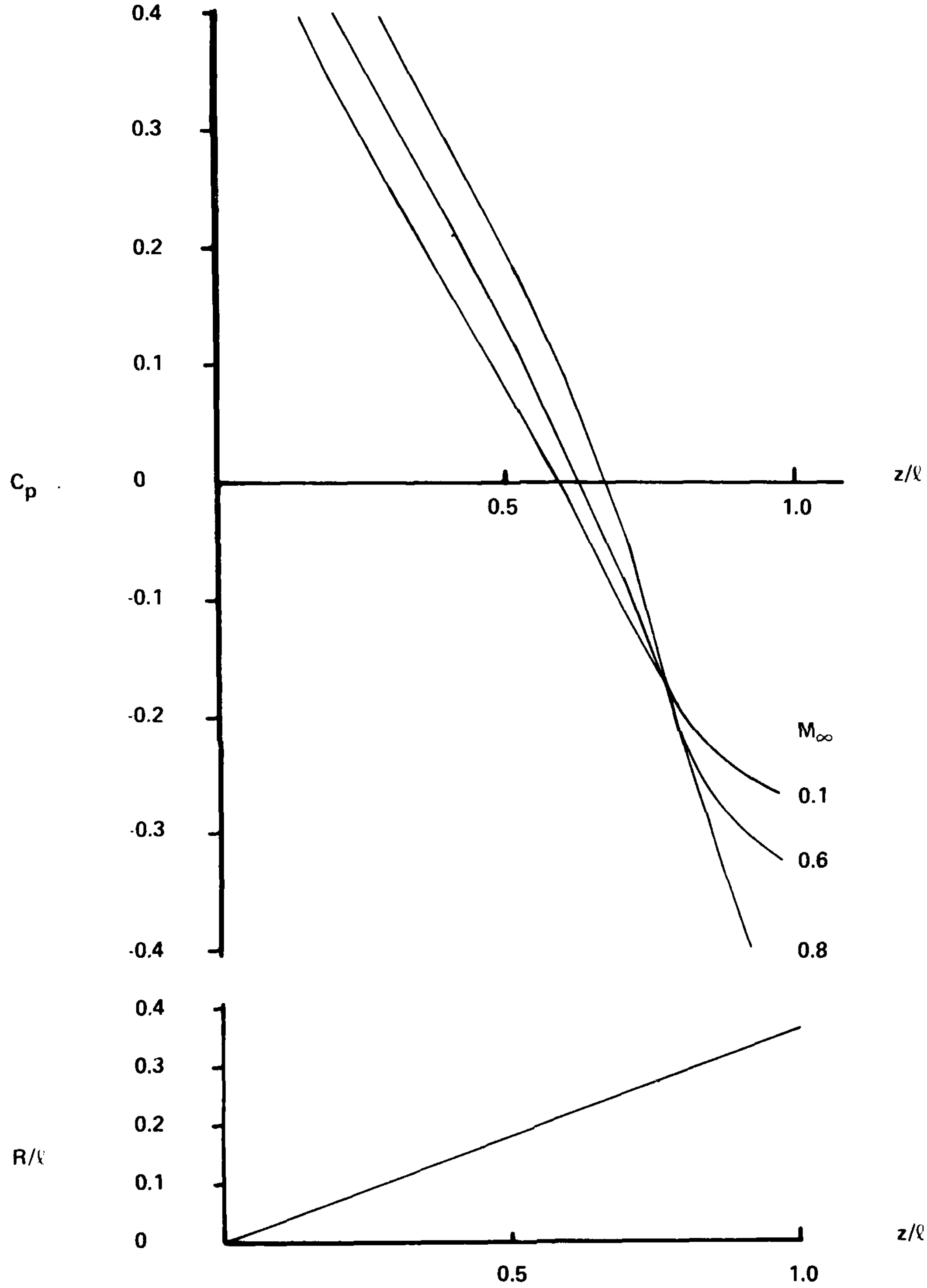

Figure 27. Calculated Averaged Pressure Coefficient for a 40^o Conic Section as a Function of Position and Mach Number

angular and Mach number sensitivity must be made and the cone geometry selected for a given application, i.e., flow angle and Mach number range.

While flow direction probes are normally formed from either cones or hemispheres, other shapes may be used. Figures 28 and 29 show the variation of $<C_p>$ with z/ℓ and M_∞ for two bodies having

$$\frac{R}{\ell} = \sqrt{\frac{z}{\ell}} \tan \delta_c \tag{40}$$

so that dR/dz is equal to 1/2 the value for a cone of included angle $2\delta_c$ at $z = \ell$. $<C_p>$ tends to be much less sensitive to Mach number than the conic sections of Figures 22 and 26. At the same time, the angular sensitivity, dR/dz, is also reduced unless the static pressure ports are located well forward on the body, i.e., $z/\ell \sim 0.2$. While this geometry appears to be superior to the cones, it might offer manufacturing difficulties since the static ports must be located in a region of fairly small radius. If a relatively large diameter probe can be used, this may pose no problem. Again, the sensor geometry must be chosen for a specific application in order to satisfy the trade-off between measurement accuracy and manufacturing difficulties.

6.3 Effect of Probe and/or Side Port Alignment on the Pressure Coefficients

The influence of probe and/or side port alignment on the angular and averaged pressure coefficients can be ascertained from equations (25) and (29). The port locations denoted by θ_i can be rotated relative to the design locations of 0^o, 90^o, 180^o and 270^o and the resulting coefficients computed.

Probe misalignments are of two types. The first consists of a manufacturing defect where one port is angularly or axially displaced relative to the other three static taps. A case of this type is plotted in Figures 30 and 31 for a 30^o cone probe with one port displaced 2.5^o, i.e., $\theta_i = 2.5^o$, 90^o, 180^o and 270^o. This results in a skewing of ΔC_{p_α} and ΔC_{p_β} with $<C_p>$ also displaced. The nonlinearity in the differential pressure coefficients is quite obvious at the higher α and β values.

The second misalignment consists of a rotation of the probe body itself relative to a fixed or predetermined coordinate system. This could occur

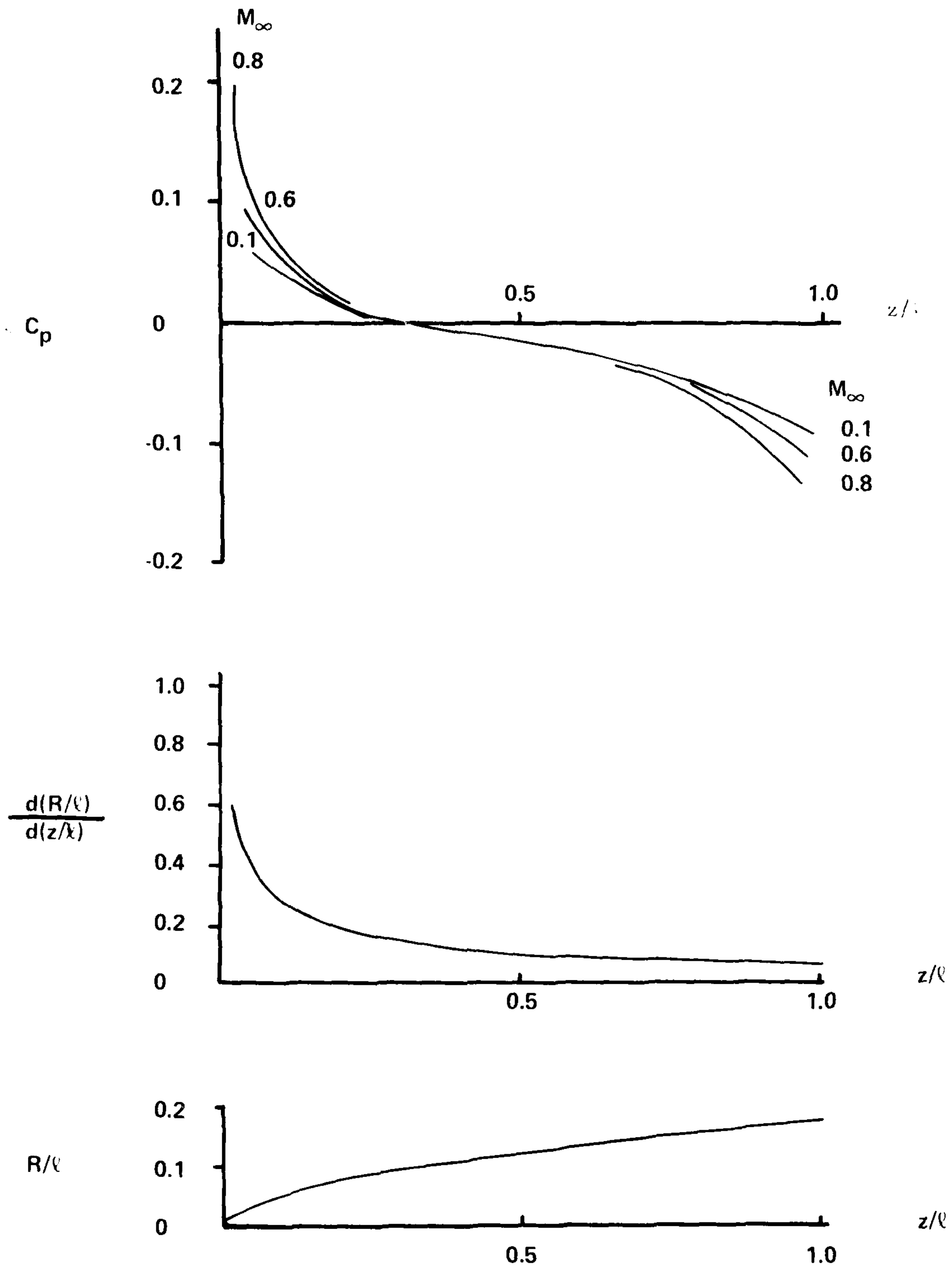

Figure 28. Calculated Averaged Pressure Coefficient for a 20° Rounded Cone as a Function of Position and Mach Number

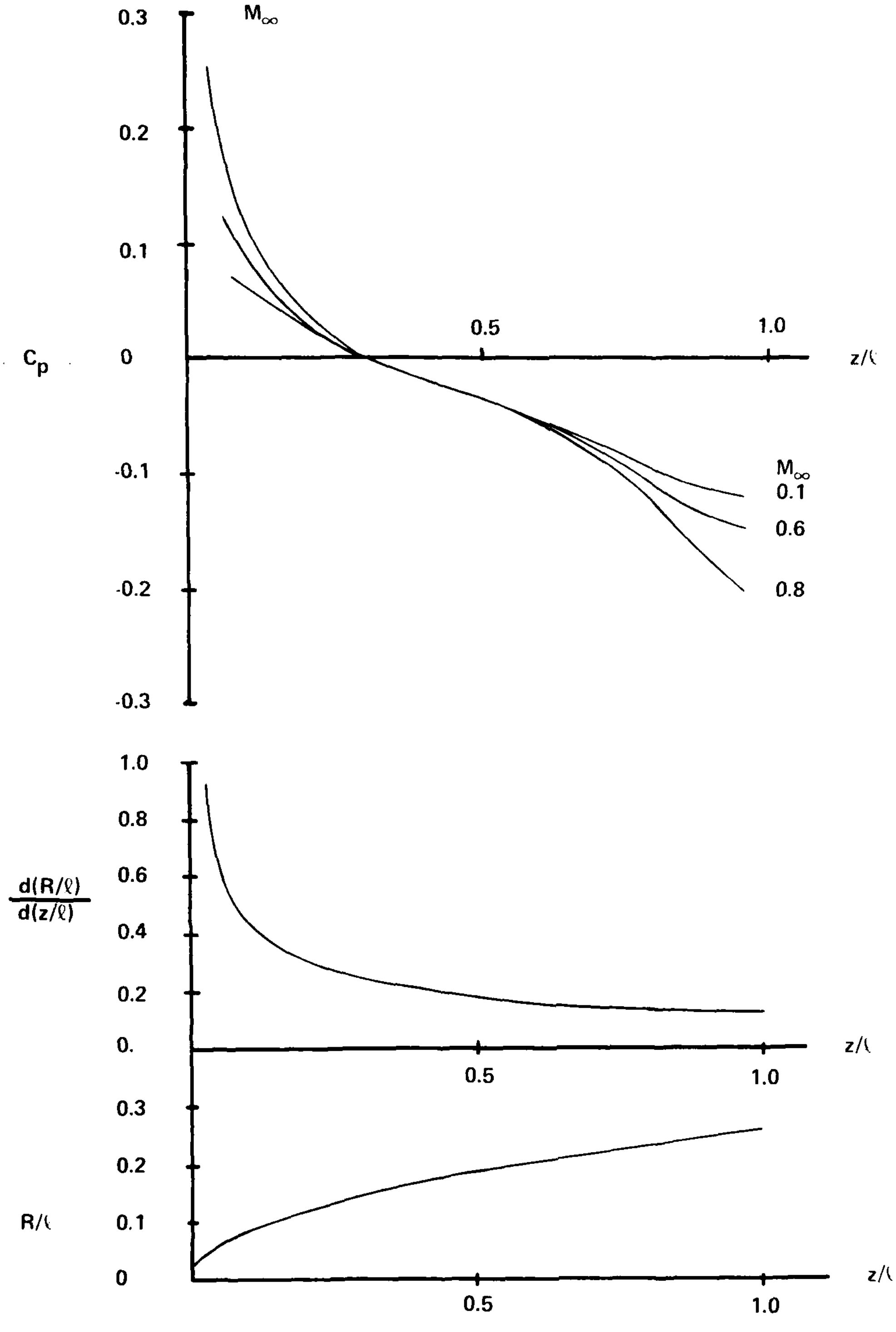

Figure 29. Calculated Averaged Pressure Coefficient for a 30° Rounded Cone as a Function of Position and Mach Number

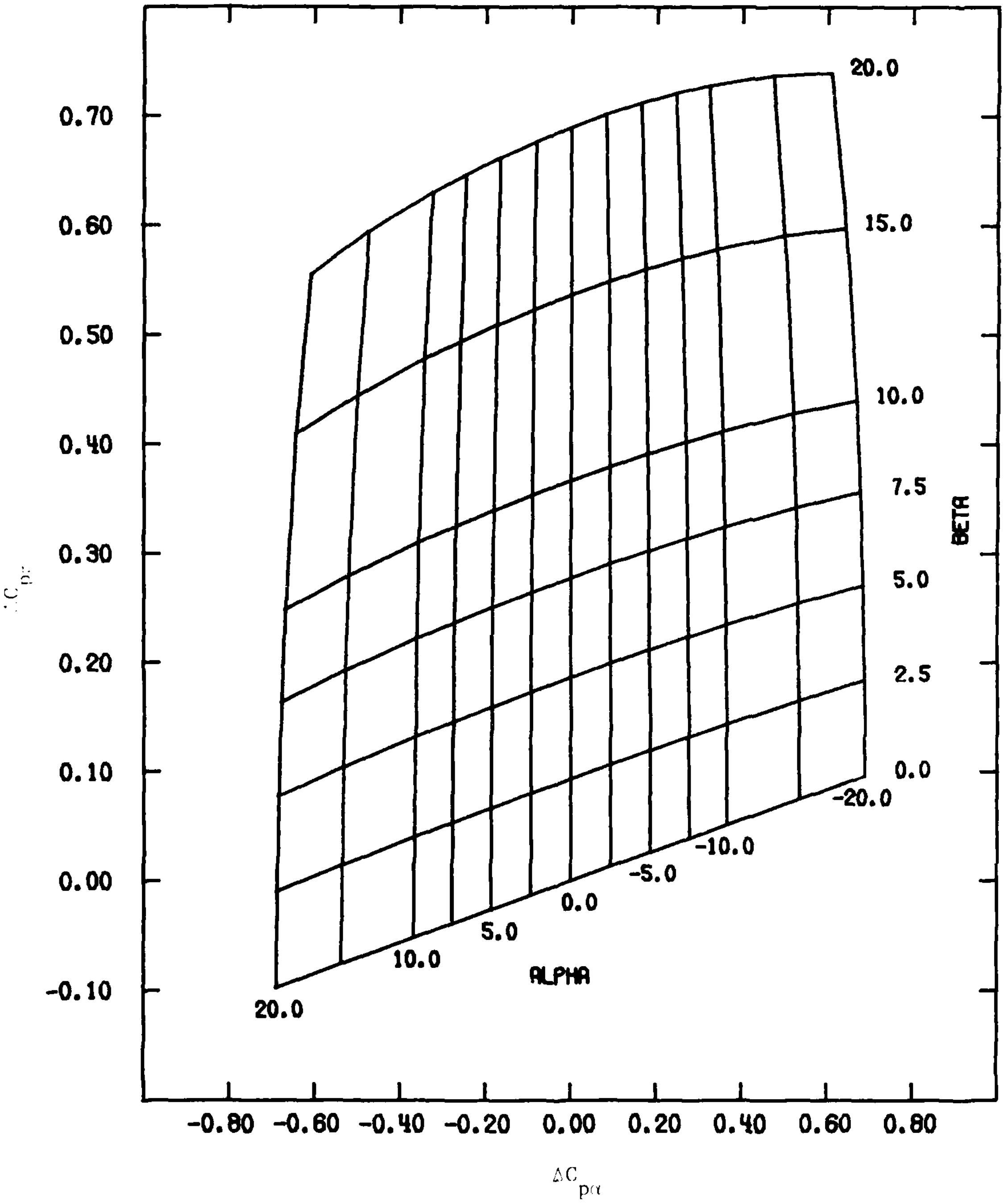

Figure 30. Angular Pressure Coefficients for a 30^o Cone Probe. Side Ports Located at θ_i = 2.5^o, 90^o, 180^o and 270^o. z/ℓ = 0.68 and M_∞ = 0.2

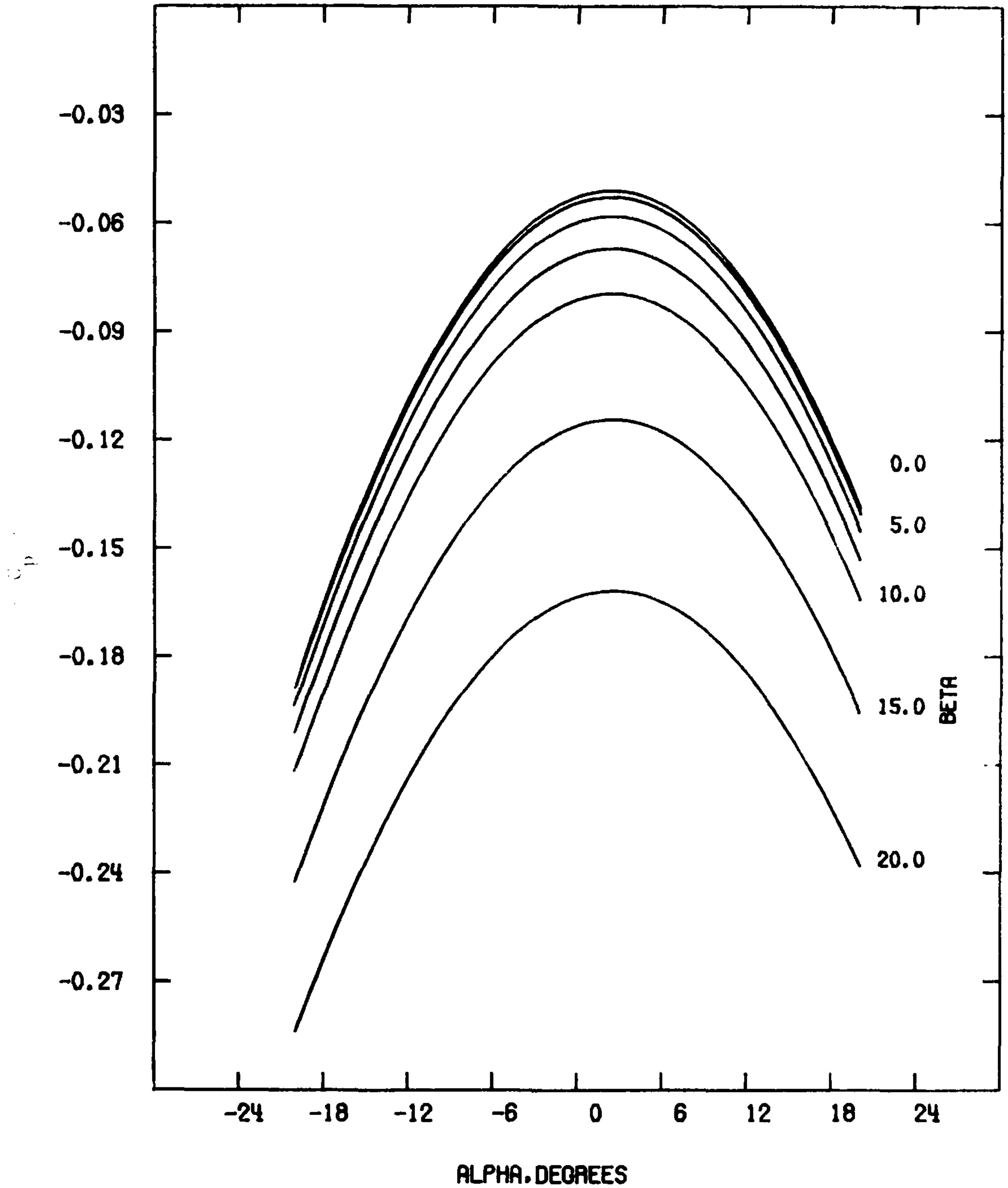

Figure 31. Averaged Pressure Coefficients for a 30° Cone Probe. Side Ports Located at θ_i = 2.5°, 90°, 180° and 270°. z/ℓ = 0.68 and M_∞ = 0.2

in a turbomachine application during installation of the sensor. In this case, all θ values are displaced by the same amount. The angular and averaged coefficients are plotted in Figures 32 and 33 for a port displacement of 2.5^{o}. Note that ΔC_{p_α} and ΔC_{p_β} are strongly influenced by the rotation, but $\langle C_p \rangle$ is unchanged.

The independence of $\langle C_p \rangle$ with regard to probe rotations can be employed to isolate probe manufacturing defects in the calibration process. If ΔC_{p_α} and ΔC_{p_β} are skewed but $\langle C_p \rangle$ is symmetric with α and/or β, then the probe is merely misaligned. If, however, both ΔC_{p_α} - ΔC_{p_β} and $\langle C_p \rangle$ are skewed, then the probe ports are not normal to one another.

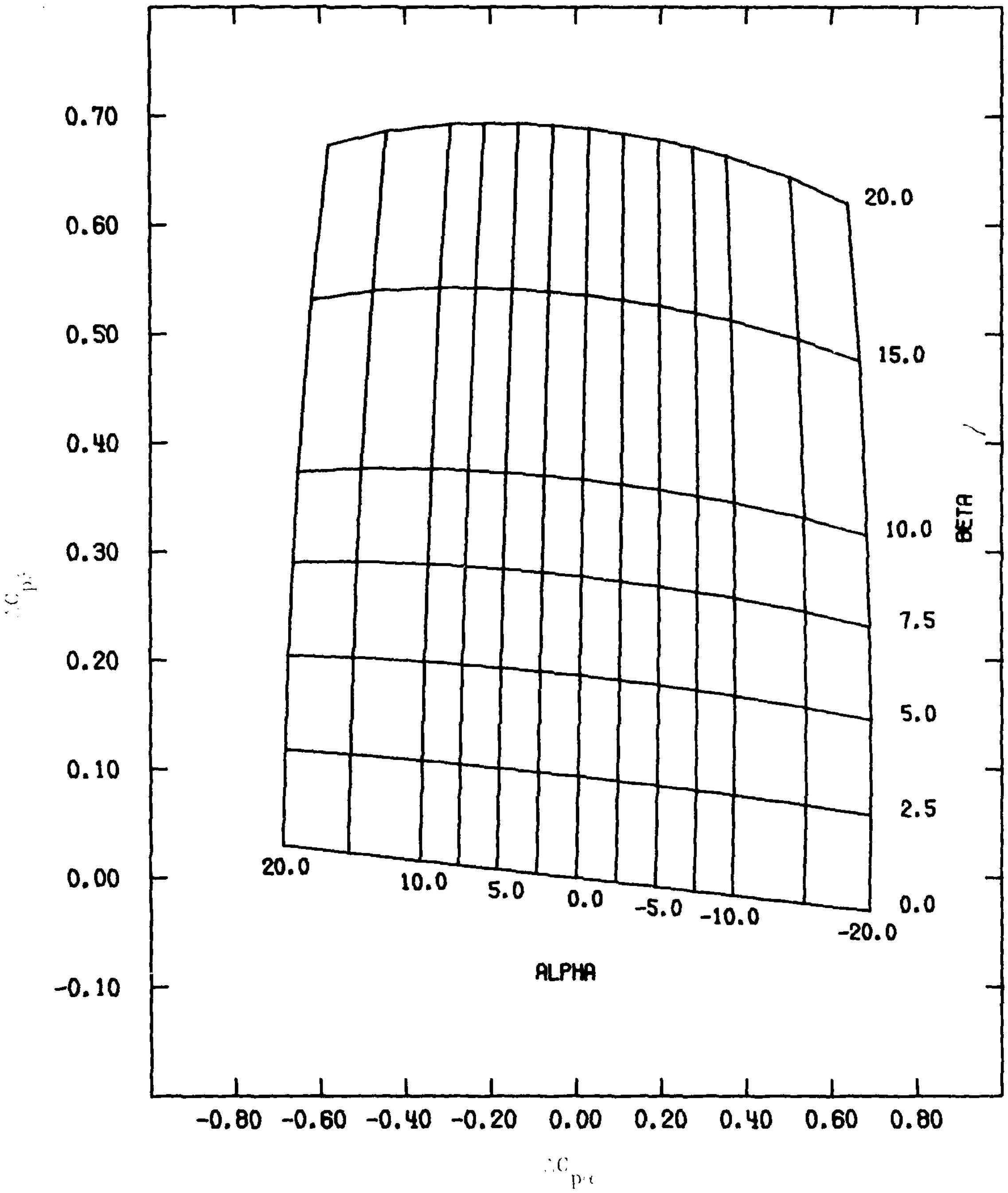

Figure 32. Angular Pressure Coefficients for a 30° Cone Probe. Side Ports Located at θ_i = 2.5°, 92.5°, 182.5° and 272.5°. z/ℓ = 0.68 and M_∞ = 0.2

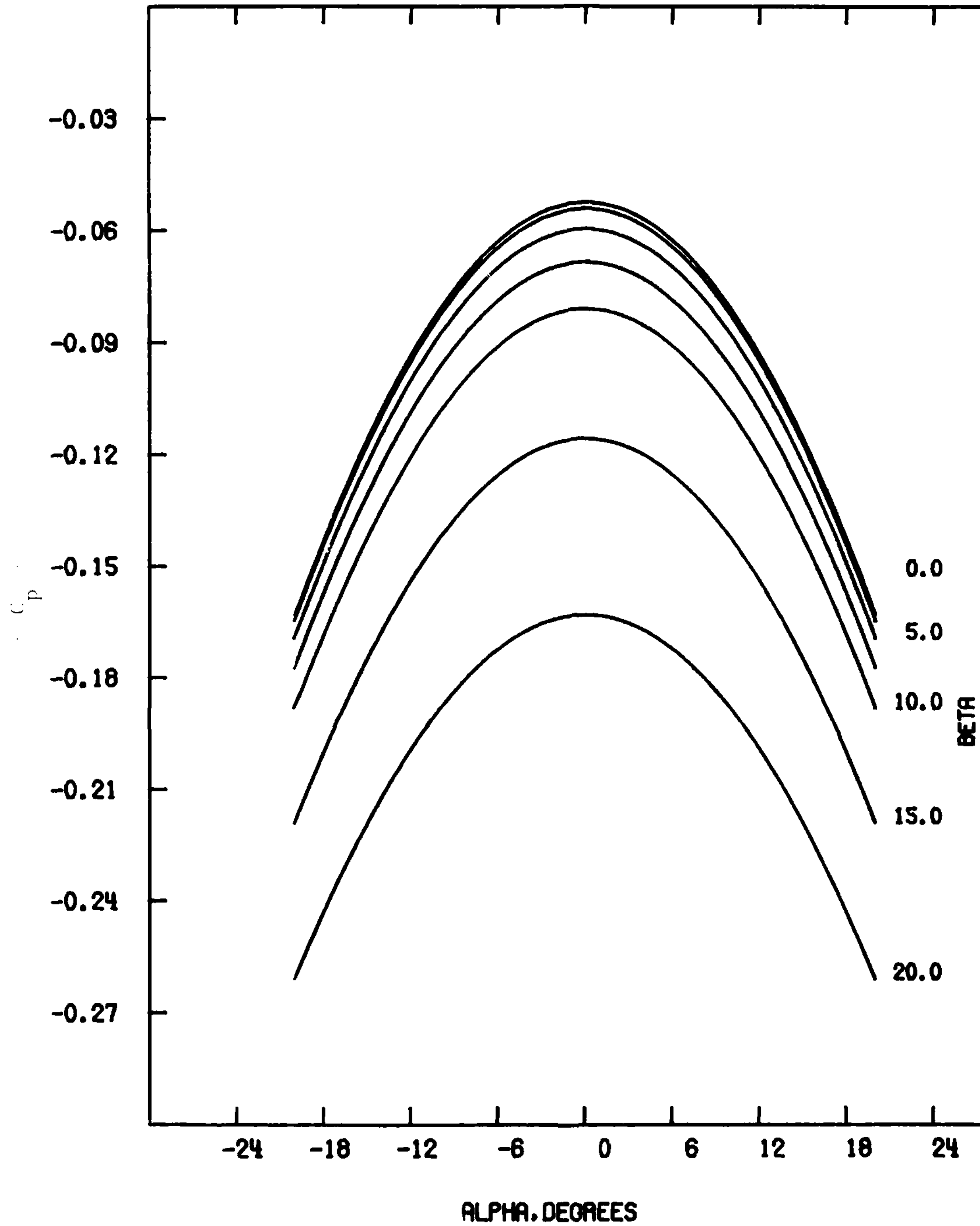

Figure 33. Averaged Pressure Coefficients for a 30° Cone Probe. Side Ports Located at θ_i = 2.5°, 92.5°, 182.5° and 272.5°. z/ℓ = 0.68 and M_∞ = 0.2

APPENDIX A

PROBE CALIBRATION DATA

TABLE

BETA DEG	AVERAGE MACH NUMBER	AVERAGE REYNOLDS NUMBER	AVERAGE TEMPERATURE DEG C
0.0	0.186	10495.	19.1

ALPHA DEG	PS CM H2O	PT CM H2O	P1 CM H2O	P2 CM H2O	P3 CM H2O	P4 CM H2O	P5 CM H2O	DELTA CP (ALPHA)	DELTA CP (BETA)	CP (AVERAGE)	CP (TOTAL)
-20.0	788.968	808.297	807.055	795.959	785.969	787.595	785.525	-0.4327	-0.0230	-0.0107	0.9357
-15.0	788.968	808.279	807.791	794.132	787.730	787.931	787.299	-0.3211	-0.0223	0.0158	0.9747
-10.0	788.968	808.188	808.000	792.485	789.094	788.428	788.611	-0.2111	-0.0252	0.0357	0.9902
-7.5	788.968	808.188	808.048	791.718	789.587	788.737	789.103	-0.1551	-0.0252	0.0426	0.9927
-5.0	788.968	808.197	808.066	790.995	789.975	789.112	789.469	-0.0979	-0.0263	0.0478	0.9932
-2.5	788.968	808.205	808.075	790.676	790.166	789.565	789.674	-0.0578	-0.0256	0.0547	0.9932
0.0	788.968	808.210	808.079	789.879	790.262	790.105	789.770	0.0118	-0.0256	0.0539	0.9932
2.5	788.968	808.201	808.070	789.412	790.184	790.637	789.678	0.0637	-0.0263	0.0525	0.9932
5.0	788.968	808.205	808.031	788.955	789.970	791.256	789.491	0.1196	-0.0249	0.0494	0.9909
7.5	789.313	808.576	808.328	788.955	789.588	792.268	789.539	0.1719	-0.0233	0.0454	0.9871
10.0	789.313	808.572	808.232	788.663	789.531	793.004	789.090	0.2254	-0.0229	0.0394	0.9823
15.0	788.968	808.231	807.556	787.857	787.987	794.154	787.595	0.3269	-0.0204	0.0223	0.9649
20.0	788.968	808.275	806.924	787.443	786.309	795.854	785.961	0.4357	-0.0181	-0.0040	0.9300

BETA DEG	AVERAGE MACH NUMBER	AVERAGE REYNOLDS NUMBER	AVERAGE TEMPERATURE DEG C
2.5	0.186	10628.	16.2

ALPHA DEG	PS CM H2O	PT CM H2O	P1 CM H2O	P2 CM H2O	P3 CM H2O	P4 CM H2O	P5 CM H2O	DELTA CP (ALPHA)	DELTA CP (BETA)	CP (AVERAGE)	CP (TOTAL)
-20.0	788.968	808.161	806.956	795.750	785.505	787.688	786.103	-0.4200	0.0312	-0.0108	0.9272
-15.0	788.968	808.152	807.624	794.055	787.159	787.968	787.715	-0.3173	0.0269	0.0139	0.9725
-10.0	788.968	808.143	807.934	792.374	788.605	788.413	789.095	-0.2066	0.0255	0.0341	0.9891
-7.5	788.968	808.200	808.060	791.641	789.112	788.728	789.588	-0.1515	0.0248	0.0416	0.9927
-5.0	788.968	808.205	808.078	790.981	789.466	789.099	789.911	-0.0978	0.0232	0.0466	0.9934
-2.5	788.968	808.200	808.078	790.346	789.675	789.523	790.090	-0.0429	0.0216	0.0489	0.9936
0.0	788.968	808.205	808.078	789.820	789.745	790.003	790.173	0.0095	0.0222	0.0503	0.9934
2.5	788.968	808.209	808.078	789.352	789.702	790.562	790.095	0.0629	0.0204	0.0499	0.9932
5.0	788.968	808.209	808.043	788.937	789.475	791.195	789.876	0.1173	0.0209	0.0469	0.9914
7.5	788.968	808.196	807.969	788.544	789.121	791.863	789.536	0.1726	0.0216	0.0415	0.9882
10.0	788.968	808.196	807.855	788.247	788.684	792.579	789.095	0.2253	0.0213	0.0355	0.9823
15.0	788.968	808.187	807.436	787.706	787.352	794.261	787.776	0.3411	0.0220	0.0159	0.9609
20.0	788.968	808.183	806.698	787.343	785.671	795.942	786.164	0.4475	0.0257	-0.0098	0.9227

TABLE 1 (Cont'd)

Pressure Coefficients for the Five-Ported, Conical Probe, M_{∞} 0.2

BETA DEG	AVERAGE MACH NUMBER	AVERAGE REYNOLDS NUMBER	AVERAGE TEMPERATURE DEG C
5.0	0.185	10547.	17.5

ALPHA DEG	PS CM H2O	PT CM H2O	P1 CM H2O	P2 CM H2O	P3 CM H2O	P4 CM H2O	P5 CM H2O	DELTA CP (ALPHA)	DELTA CP (BETA)	CP (AVERAGE)	CP (TOTAL)
-20.0	789.313	808.497	807.230	795.998	785.561	787.810	786.954	-0.4268	0.0726	-0.0121	0.9340
-15.0	789.313	808.492	807.925	794.278	787.168	788.085	788.631	-0.3229	0.0763	0.0119	0.9704
-10.0	789.313	808.510	808.278	792.614	788.509	788.544	790.033	-0.2120	0.0794	0.0319	0.9879
-7.5	789.313	808.506	808.340	791.832	789.016	788.898	790.514	-0.1529	0.0780	0.0392	0.9914
-5.0	789.313	808.501	808.361	791.169	789.378	789.265	790.654	-0.0992	0.0769	0.0445	0.9927
-2.5	789.313	808.506	808.366	790.570	789.605	789.684	791.051	-0.0462	0.0753	0.0477	0.9927
0.0	789.313	808.353	808.265	790.033	789.706	790.164	791.081	0.0069	0.0722	0.0490	0.9954
2.5	789.313	808.492	808.348	789.570	789.614	790.701	791.011	0.0590	0.0729	0.0475	0.9925
5.0	789.313	808.471	808.305	789.081	789.396	791.326	790.793	0.1172	0.0729	0.0437	0.9913
7.5	789.313	808.444	808.222	788.797	789.051	792.025	790.439	0.1687	0.0726	0.0400	0.9884
10.0	788.968	808.095	807.768	788.095	788.282	792.387	789.640	0.2242	0.0710	0.0332	0.9829
15.0	788.968	808.108	807.353	787.549	787.025	794.012	788.378	0.3377	0.0707	0.0143	0.9605
20.0	788.968	808.091	806.576	787.046	785.335	795.750	786.640	0.4551	0.0663	-0.0144	0.9208

BETA DEG	AVERAGE MACH NUMBER	AVERAGE REYNOLDS NUMBER	AVERAGE TEMPERATURE DEG C
7.5	0.185	10532.	17.4

ALPHA DEG	PS CM H2O	PT CM H2O	P1 CM H2O	P2 CM H2O	P3 CM H2O	P4 CM H2O	P5 CM H2O	DELTA CP (ALPHA)	DELTA CP (BETA)	CP (AVERAGE)	CP (TOTAL)
-20.0	789.313	808.427	807.034	795.741	785.273	787.129	787.692	-0.4505	0.1266	-0.0185	0.9271
-15.0	789.313	808.410	807.750	793.959	786.806	787.706	789.444	-0.3275	0.1381	0.0087	0.9655
-10.0	789.313	808.414	808.126	792.339	788.068	788.234	790.723	-0.2149	0.1390	0.0277	0.9849
-7.5	789.313	808.410	808.213	791.597	788.561	788.527	791.204	-0.1608	0.1383	0.0345	0.9897
-5.0	789.313	808.410	808.248	790.845	788.933	788.880	791.531	-0.1029	0.1361	0.0385	0.9915
-2.5	788.279	807.375	807.244	789.252	788.126	788.257	790.694	-0.0521	0.1345	0.0421	0.9931
0.0	788.279	807.375	807.244	788.707	788.204	788.750	790.737	0.0023	0.1326	0.0430	0.9931
2.5	788.279	807.375	807.244	788.235	788.117	789.305	790.619	0.0560	0.1310	0.0414	0.9931
5.0	787.934	807.040	806.865	787.541	787.606	789.550	790.096	0.1051	0.1303	0.0400	0.9909
7.5	787.934	807.040	806.791	787.170	787.253	790.262	789.742	0.1618	0.1302	0.0352	0.9865
10.0	787.934	807.048	806.677	786.666	786.855	790.973	789.301	0.2138	0.1279	0.0298	0.9806
15.0	787.934	807.048	806.223	786.213	785.589	792.624	787.969	0.3354	0.1245	0.0086	0.9568
20.0	787.934	807.057	805.467	785.436	784.056	794.371	786.240	0.4672	0.1142	-0.0214	0.9169

TABLE [illegible] (cont'd)

Pressure Coefficients for the Five-Port [illegible] Conical Probe, M [illegible]

BETA DEG	AVERAGE MACH NUMBER	AVERAGE REYNOLDS NUMBER	AVERAGE TEMPERATURE DEG C
10.0	0.186	10479.	19.3

ALPHA DEG	PS CM H2O	PT CM H2O	P1 CM H2O	P2 CM H2O	P3 CM H2O	P4 CM H2O	P5 CM H2O	DELTA CP (ALPHA)	DELTA CP (BETA)	CP (AVERAGE)	CP (TOTAL)
-20.0	788.968	808.146	806.554	795.200	784.675	786.160	787.924	-0.4713	0.1694	-0.0249	0.9169
-15.0	788.965	808.174	807.344	793.256	786.199	786.876	789.937	-0.3322	0.1946	0.0052	0.9568
-10.0	788.966	808.183	807.781	791.841	787.391	787.378	791.261	-0.2323	0.2014	0.0260	0.9791
-7.5	788.966	808.191	807.912	790.846	787.881	787.649	791.754	-0.1663	0.2015	0.0294	0.9855
-5.0	788.968	808.209	807.973	790.147	788.239	787.977	792.060	-0.1128	0.1986	0.0331	0.9877
-2.5	788.968	808.213	808.008	789.527	788.453	788.396	792.243	-0.0588	0.1970	0.0357	0.9893
0.0	788.623	807.873	807.672	788.632	788.213	788.540	791.938	-0.0048	0.1935	0.0368	0.9896
2.5	788.279	807.541	807.323	787.829	787.820	788.750	791.506	0.0478	0.1913	0.0362	0.9887
5.0	788.279	807.546	807.266	787.414	787.580	789.379	791.266	0.1020	0.1913	0.0328	0.9855
7.5	788.279	807.541	807.179	787.056	787.274	790.052	790.908	0.1555	0.1886	0.0282	0.9812
10.0	788.279	807.550	807.039	786.781	786.846	790.820	790.427	0.2096	0.1858	0.0228	0.9735
15.0	788.279	807.555	806.572	786.178	785.637	792.488	789.073	0.3274	0.1763	0.0034	0.9490
20.0	788.279	807.559	805.755	785.165	784.195	794.296	787.239	0.4736	0.1579	-0.0288	0.9065

BETA DEG	AVERAGE MACH NUMBER	AVERAGE REYNOLDS NUMBER	AVERAGE TEMPERATURE DEG C
15.0	0.186	10504.	16.5

ALPHA DEG	PS CM H2O	PT CM H2O	P1 CM H2O	P2 CM H2O	P3 CM H2O	P4 CM H2O	P5 CM H2O	DELTA CP (ALPHA)	DELTA CP (BETA)	CP (AVERAGE)	CP (TOTAL)
-20.0	780.006	795.064	796.896	785.084	775.652	776.326	780.689	-0.4565	0.2642	-0.0301	0.8862
-15.0	780.006	795.038	797.722	783.100	776.834	776.895	782.622	-0.3260	0.3041	-0.0075	0.9308
-10.0	780.006	798.995	798.217	781.436	777.882	777.160	783.926	-0.2252	0.3183	0.0050	0.9590
-7.5	780.006	798.995	798.392	780.667	778.277	777.338	784.369	-0.1753	0.3208	0.0082	0.9677
-5.0	780.006	798.990	798.469	779.980	778.638	777.612	784.669	-0.1247	0.3177	0.0115	0.9725
-2.5	780.006	798.999	798.512	779.376	778.920	777.968	784.821	-0.0741	0.3107	0.0140	0.9744
0.0	780.006	799.086	798.604	778.790	779.020	778.438	784.873	-0.0184	0.3068	0.0143	0.9747
2.5	780.006	799.082	798.565	778.325	778.924	778.955	784.747	0.0330	0.3052	0.0121	0.9729
5.0	780.006	799.086	798.469	777.882	778.612	779.576	784.486	0.0888	0.3079	0.0069	0.9677
7.5	780.006	799.082	798.334	777.606	778.268	780.310	784.126	0.1417	0.3071	0.0038	0.9608
10.0	780.006	799.090	798.169	777.399	777.942	781.006	783.691	0.1890	0.3012	0.0002	0.9517
15.0	780.006	799.108	797.596	776.947	776.878	782.796	782.257	0.3062	0.2816	-0.0150	0.9208
20.0	780.006	799.134	796.876	776.135	775.683	784.677	780.310	0.4466	0.2419	-0.0421	0.8814

TABLE 1 (Cont'd)

Pressure Coefficients for the Five-Ported, Conical Probe, $M_\infty = 0.2$

BETA DEG	AVERAGE MACH NUMBER	AVERAGE REYNOLDS NUMBER	AVERAGE TEMPERATURE DEG C
20.0	0.186	10479.	17.0

ALPHA DEG	PS CM H2O	PT CM H2O	P1 CM H2O	P2 CM H2O	P3 CM H2O	P4 CM H2O	P5 CM H2O	DELTA CP (ALPHA)	DELTA CP (BETA)	CP (AVERAGE)	CP (TOTAL)
-20.0	780.351	799.431	796.311	783.940	775.541	775.593	782.719	-0.4375	0.3762	-0.0473	0.8365
-15.0	780.351	799.413	797.232	781.928	776.536	775.964	784.631	-0.3118	0.4247	-0.0305	0.8856
-10.0	780.351	799.405	797.788	780.155	777.288	776.006	786.021	-0.2178	0.4584	-0.0254	0.9152
-7.5	780.351	799.405	797.975	779.356	777.805	776.032	786.491	-0.1745	0.4559	-0.0226	0.9250
-5.0	780.351	799.252	797.975	778.669	778.474	776.254	786.730	-0.1278	0.4368	-0.0169	0.9324
-2.5	780.696	799.714	798.489	778.380	779.240	776.850	787.235	-0.0804	0.4204	-0.0142	0.9356
0.0	781.040	800.055	798.882	778.177	779.719	777.608	787.593	-0.0259	0.4141	-0.0140	0.9383
2.5	781.730	800.666	799.449	778.419	780.331	778.810	788.130	0.0207	0.4119	-0.0162	0.9358
5.0	782.419	801.394	800.008	778.782	780.585	780.073	788.580	0.0680	0.4213	-0.0218	0.9270
7.5	782.419	801.399	799.826	778.508	779.925	780.781	788.168	0.1197	0.4343	-0.0302	0.9171
10.0	782.419	801.412	799.639	778.356	779.390	781.494	787.655	0.1652	0.4351	-0.0366	0.9067
15.0	782.419	801.507	799.196	778.174	778.565	783.336	786.117	0.2704	0.3956	-0.0456	0.8789
20.0	782.419	801.512	798.209	777.474	777.518	785.382	784.175	0.4142	0.3487	-0.0671	0.8270

TABLE 2

Pressure Coefficients for the Five-Ported, Conical Probe, M_∞ 0.4

BETA DEG	AVERAGE MACH NUMBER	AVERAGE REYNOLDS NUMBER	AVERAGE TEMPERATURE DEG C
0.0	0.402	23798.	15.0

ALPHA DEG	PS CM H2O	PT CM H2O	P1 CM H2O	P2 CM H2O	P3 CM H2O	P4 CM H2O	P5 CM H2O	DELTA CP (ALPHA)	DELTA CP (BETA)	CP (AVERAGE)	CP (TOTAL)
-20.0	784.142	877.056	872.192	816.473	765.822	775.181	763.459	-0.4444	-0.0254	-0.0421	0.9476
-15.0	784.142	876.917	876.431	807.757	775.521	777.639	773.602	-0.3246	-0.0207	-0.0055	0.9948
-10.0	784.142	876.639	876.570	799.740	782.685	780.484	781.202	-0.2082	-0.0182	0.0209	0.9992
-7.5	784.142	876.709	876.709	795.940	785.750	782.129	783.859	-0.1492	-0.0204	0.0300	1.0000
-5.0	784.142	876.639	876.639	792.650	787.716	784.048	785.750	-0.0930	-0.0213	0.0367	1.0000
-2.5	784.142	876.639	876.639	789.701	788.983	786.411	786.837	-0.0356	-0.0232	0.0415	1.0000
0.0	783.453	875.881	875.881	786.346	788.595	788.180	786.403	0.0158	-0.0237	0.0425	1.0000
2.5	783.453	875.881	875.881	783.869	788.397	791.025	786.157	0.0774	-0.0242	0.0423	1.0000
5.0	783.453	875.742	875.742	781.997	787.320	794.220	785.136	0.1324	-0.0237	0.0403	1.0000
7.5	783.108	875.397	875.397	779.781	785.054	797.288	782.987	0.1857	-0.0230	0.0344	1.0000
10.0	784.142	877.022	876.535	779.161	783.651	802.104	781.042	0.2470	-0.0281	0.0253	0.9948
15.0	782.419	875.229	874.708	774.715	775.291	808.113	773.325	0.3599	-0.0212	0.0048	0.9944
20.0	782.419	875.264	869.808	772.436	766.481	816.508	764.401	0.4747	-0.0224	-0.0265	0.9412

BETA DEG	AVERAGE MACH NUMBER	AVERAGE REYNOLDS NUMBER	AVERAGE TEMPERATURE DEG C
2.5	0.403	23898.	14.5

ALPHA DEG	PS CM H2O	PT CM H2O	P1 CM H2O	P2 CM H2O	P3 CM H2O	P4 CM H2O	P5 CM H2O	DELTA CP (ALPHA)	DELTA CP (BETA)	CP (AVERAGE)	CP (TOTAL)
-20.0	782.074	874.641	870.124	814.253	761.485	773.226	764.671	-0.4432	0.0344	-0.0396	0.9512
-15.0	782.074	874.571	874.363	805.594	771.090	775.353	774.776	-0.3269	0.0399	-0.0040	0.9977
-10.0	782.074	874.502	874.293	797.625	778.463	778.066	781.980	-0.2116	0.0380	0.0212	0.9977
-7.5	789.313	881.949	881.949	800.865	788.443	787.214	791.618	-0.1474	0.0364	0.0299	1.0000
-5.0	782.074	874.432	874.328	790.488	783.303	781.583	786.376	-0.0964	0.0333	0.0364	0.9989
-2.5	782.074	874.432	874.432	787.557	784.476	784.003	787.368	-0.0385	0.0313	0.0409	1.0000
0.0	782.074	874.502	874.502	784.816	784.683	785.638	787.737	0.0089	0.0330	0.0394	1.0000
2.5	782.074	874.502	874.502	782.386	784.494	789.287	787.368	0.0747	0.0311	0.0412	1.0000
5.0	782.419	874.847	874.636	780.661	783.503	792.657	786.626	0.1298	0.0295	0.0383	0.9977
7.5	789.313	882.852	882.574	785.408	788.745	803.304	791.676	0.1913	0.0313	0.0318	0.9970
10.0	789.313	883.408	882.852	783.990	786.363	806.915	789.332	0.2436	0.0315	0.0248	0.9941
15.0	789.313	882.157	881.393	781.372	779.178	814.610	782.676	0.3580	0.0301	0.0035	0.9918
20.0	789.313	882.922	877.918	779.141	770.444	823.562	773.374	0.4745	0.0313	-0.0287	0.9465

TABLE 2 (Cont'd)

Pressure Coefficients for the Five-Ported, Conical Probe, M_∞ = 0.4

BETA DEG	AVERAGE MACH NUMBER	AVERAGE REYNOLDS NUMBER	AVERAGE TEMPERATURE DEG C
5.0	0.401	24000.	14.2

ALPHA DEG	PS CM H2O	PT CM H2O	P1 CM H2O	P2 CM H2O	P3 CM H2O	P4 CM H2O	P5 CM H2O	DELTA CP (ALPHA)	DELTA CP (BETA)	CP (AVERAGE)	CP (TOTAL)
-20.0	790.691	883.049	878.880	822.161	768.098	782.987	776.634	-0.4242	0.0924	-0.0349	0.9549
-15.0	790.691	883.049	882.771	813.663	777.476	782.647	786.390	-0.3358	0.0965	-0.0070	0.9970
-10.0	790.691	883.168	882.771	805.439	785.019	785.587	793.716	-0.2146	0.0940	0.0189	0.9955
-7.5	790.691	883.119	883.049	801.780	787.723	787.364	796.174	-0.1560	0.0914	0.0278	0.9992
-5.0	790.691	883.119	883.049	798.594	789.746	789.283	797.781	-0.1007	0.0869	0.0342	0.9992
-2.5	791.381	883.739	883.739	796.268	791.381	792.317	799.492	-0.0428	0.0878	0.0377	1.0000
0.0	791.381	883.739	883.739	793.366	791.929	795.067	799.813	0.0184	0.0854	0.0397	1.0000
2.5	791.381	883.808	883.739	791.362	791.551	797.762	799.359	0.0692	0.0845	0.0392	0.9992
5.0	791.381	883.808	883.739	788.715	790.530	800.995	798.130	0.1329	0.0822	0.0347	0.9992
7.5	791.381	883.947	883.600	786.815	788.828	804.180	796.485	0.1876	0.0827	0.0291	0.9962
10.0	791.381	884.156	883.600	785.000	786.238	808.000	793.479	0.2479	0.0781	0.0194	0.9940
15.0	791.381	884.295	883.669	781.757	778.411	816.148	786.985	0.3701	0.0923	-0.0060	0.9933
20.0	791.381	884.503	879.847	780.037	770.517	824.647	775.962	0.4790	0.0585	-0.0386	0.9500

BETA DEG	AVERAGE MACH NUMBER	AVERAGE REYNOLDS NUMBER	AVERAGE TEMPERATURE DEG C
7.5	0.401	23935.	15.0

ALPHA DEG	PS CM H2O	PT CM H2O	P1 CM H2O	P2 CM H2O	P3 CM H2O	P4 CM H2O	P5 CM H2O	DELTA CP (ALPHA)	DELTA CP (BETA)	CP (AVERAGE)	CP (TOTAL)
-20.0	791.036	883.672	879.502	821.504	766.164	778.454	780.656	-0.4647	0.1564	-0.0469	0.9550
-15.0	791.036	883.672	883.116	812.731	775.608	780.448	790.705	-0.3485	0.1630	-0.0126	0.9940
-10.0	791.036	883.672	883.116	804.157	783.275	783.984	798.192	-0.2178	0.1610	0.0147	0.9940
-7.5	791.036	883.672	883.325	800.631	785.856	785.572	800.480	-0.1626	0.1579	0.0227	0.9962
-5.0	791.036	883.672	883.533	797.143	787.916	787.529	802.153	-0.1038	0.1537	0.0286	0.9985
-2.5	791.036	883.672	883.672	794.061	788.758	789.798	803.042	-0.0460	0.1542	0.0311	1.0000
0.0	791.036	883.672	883.672	791.225	789.259	792.359	803.325	0.0122	0.1518	0.0325	1.0000
2.5	791.036	883.672	883.672	788.985	788.956	795.025	802.854	0.0652	0.1498	0.0315	1.0000
5.0	791.381	884.017	883.906	787.070	788.261	798.773	801.968	0.1263	0.1480	0.0285	0.9977
7.5	791.381	884.017	883.808	785.331	786.465	802.157	800.248	0.1816	0.1488	0.0234	0.9977
10.0	791.381	884.017	883.600	783.676	783.988	805.797	797.790	0.2388	0.1490	0.0155	0.9955
15.0	791.381	884.920	883.530	779.819	777.182	814.125	790.577	0.3668	0.1432	-0.0102	0.9851
20.0	791.381	884.920	879.500	775.835	768.107	823.503	780.538	0.5096	0.1329	-0.0469	0.9421

TABLE 2 (Cont'd)
Pressure Coefficients for the Five-Ported, Conical Probe, $M_\infty = 0.4$

BETA DEG	AVERAGE MACH NUMBER	AVERAGE REYNOLDS NUMBER	AVERAGE TEMPERATURE DEG C
10.0	0.402	24135.	14.1

ALPHA DEG	PS CM H2O	PT CM H2O	P1 CM H2O	P2 CM H2O	P3 CM H2O	P4 CM H2O	P5 CM H2O	DELTA CP (ALPHA)	DELTA CP (BETA)	CP (AVERAGE)	CP (TOTAL)
-20.0	791.381	886.519	879.986	820.960	765.346	773.873	784.489	-0.4949	0.2012	-0.0548	0.9313
-15.0	791.381	885.129	884.086	811.214	774.658	778.477	794.812	-0.3492	0.2150	-0.0170	0.9889
-10.0	791.381	884.607	884.295	802.649	781.994	781.814	802.082	-0.2235	0.2155	0.0081	0.9966
-7.5	791.725	885.056	885.056	795.307	784.957	783.614	804.780	-0.1681	0.2124	0.0154	1.0000
-5.0	792.070	885.610	885.610	796.031	787.239	785.973	806.789	-0.1075	0.2090	0.0207	1.0000
-2.5	792.070	884.776	884.776	793.082	788.071	788.175	807.507	-0.0529	0.2097	0.0231	1.0000
0.0	792.415	885.190	885.190	790.628	789.087	791.072	806.079	0.0048	0.2047	0.0248	1.0000
2.5	792.415	885.329	885.259	788.123	788.709	793.975	807.502	0.0630	0.2023	0.0233	0.9993
5.0	792.415	885.329	885.259	786.024	787.584	797.018	806.377	0.1183	0.2023	0.0198	0.9993
7.5	792.415	885.468	885.468	784.153	785.760	800.715	804.477	0.1780	0.2011	0.0146	1.0000
10.0	792.415	885.468	885.468	782.583	783.415	804.286	802.038	0.2333	0.2001	0.0072	1.0000
15.0	792.415	885.885	884.078	779.015	776.769	812.768	794.684	0.3611	0.1917	-0.0172	0.9807
20.0	792.415	886.441	880.464	773.423	768.347	822.108	784.956	0.5178	0.1766	-0.0554	0.9364

BETA DEG	AVERAGE MACH NUMBER	AVERAGE REYNOLDS NUMBER	AVERAGE TEMPERATURE DEG C
15.0	0.401	23945.	15.0

ALPHA DEG	PS CM H2O	PT CM H2O	P1 CM H2O	P2 CM H2O	P3 CM H2O	P4 CM H2O	P5 CM H2O	DELTA CP (ALPHA)	DELTA CP (BETA)	CP (AVERAGE)	CP (TOTAL)
-20.0	791.725	884.153	874.076	814.669	767.355	768.924	793.843	-0.4949	0.2866	-0.0598	0.8910
-15.0	791.725	883.597	878.072	805.433	773.877	773.594	803.504	-0.3466	0.3225	-0.0286	0.9399
-10.0	791.725	884.431	883.111	796.859	779.559	775.305	810.679	-0.2325	0.3357	-0.0121	0.9858
-7.5	791.725	884.431	883.805	792.954	781.818	776.458	812.995	-0.1779	0.3363	-0.0072	0.9933
-5.0	791.725	884.431	883.805	789.296	783.699	778.141	814.442	-0.1203	0.3316	-0.0036	0.9933
-2.5	791.725	884.431	883.805	786.148	784.872	780.173	815.189	-0.0644	0.3270	-0.0014	0.9933
0.0	792.070	884.845	884.150	783.581	785.850	783.089	815.552	-0.0053	0.3202	-0.0006	0.9925
2.5	792.070	884.915	884.150	781.057	785.235	785.963	814.871	0.0528	0.3192	-0.0031	0.9918
5.0	791.725	884.709	883.805	778.708	783.265	788.937	813.307	0.1100	0.3231	-0.0072	0.9903
7.5	791.725	884.709	883.805	777.007	781.355	792.812	811.228	0.1700	0.3213	-0.0121	0.9903
10.0	791.725	884.848	883.111	775.801	779.549	796.320	808.760	0.2193	0.3137	-0.0171	0.9813
15.0	791.725	884.848	880.157	773.121	773.499	805.234	800.971	0.3448	0.2950	-0.0378	0.9496
20.0	791.725	884.987	874.526	767.005	767.024	814.867	790.969	0.5132	0.2568	-0.0725	0.8879

TABLE 2 (Cont'd)
Pressure Coefficients for the Five-Ported, Conical Probe, M_1 0.4

BETA DEG	AVERAGE MACH NUMBER	AVERAGE REYNOLDS NUMBER	AVERAGE TEMPERATURE DEG C
20.0	0.401	23957.	15.0

ALPHA DEG	PS CM H2O	PT CM H2O	P1 CM H2O	P2 CM H2O	P3 CM H2O	P4 CM H2O	P5 CM H2O	DELTA CP (ALPHA)	DELTA CP (BETA)	CP (AVERAGE)	CP (TOTAL)
-20.0	791.381	884.573	869.979	807.272	764.089	762.558	802.706	-0.4798	0.4144	-0.0775	0.8434
-15.0	791.381	884.364	875.886	797.185	769.392	765.961	812.480	-0.3358	0.4634	-0.0551	0.9088
-10.0	791.381	884.156	878.874	788.195	774.469	766.188	819.287	-0.2372	0.4831	-0.0468	0.9431
-7.5	791.381	884.225	879.917	784.149	777.957	766.887	821.480	-0.1859	0.4688	-0.0405	0.9536
-5.0	791.381	884.156	880.403	780.415	780.963	768.031	822.841	-0.1335	0.4514	-0.0358	0.9596
-2.5	791.381	884.260	880.750	777.201	782.551	769.544	823.399	-0.0824	0.4398	-0.0345	0.9622
0.0	791.381	884.156	880.681	774.270	782.967	771.888	823.333	-0.0257	0.4351	-0.0352	0.9625
2.5	791.381	884.190	880.403	771.850	782.684	774.743	822.577	0.0312	0.4298	-0.0368	0.9592
5.0	791.381	884.190	879.986	769.903	780.698	778.118	821.187	0.0885	0.4363	-0.0421	0.9547
7.5	791.381	884.225	879.222	768.267	776.775	781.956	819.221	0.1474	0.4572	-0.0520	0.9461
10.0	791.381	884.225	878.249	767.502	773.646	785.936	816.498	0.1985	0.4615	-0.0591	0.9356
15.0	791.381	884.503	874.843	766.575	768.825	795.795	808.397	0.3138	0.4249	-0.0696	0.8963
20.0	791.381	884.642	869.006	761.745	762.454	805.750	796.244	0.4718	0.3838	-0.1001	0.8323

TABLE 3

Pressure Coefficients for the Five-Ported, Conical Probe, M = 0.6

BETA DEG	AVERAGE MACH NUMBER	AVERAGE REYNOLDS NUMBER	AVERAGE TEMPERATURE DEG C
0.0	0.580	35971.	15.2

ALPHA DEG	PS CM H2O	PT CM H2O	P1 CM H2O	P2 CM H2O	P3 CM H2O	P4 CM H2O	P5 CM H2O	DELTA CP (ALPHA)	DELTA CP (BETA)	CP (AVERAGE)	CP (TOTAL)
-20.0	786.211	988.022	979.613	853.983	745.989	766.060	738.910	-0.4357	-0.0351	-0.0494	0.9583
-15.0	786.211	988.509	986.007	836.527	767.669	770.786	760.891	-0.3250	-0.0335	-0.0111	0.9876
-10.0	786.211	987.883	987.675	819.172	784.059	777.181	777.804	-0.2082	-0.0310	0.0166	0.9990
-7.5	786.211	987.744	987.744	812.113	789.448	780.077	783.113	-0.1590	-0.0314	0.0247	1.0000
-5.0	786.211	987.814	987.814	804.451	794.194	784.401	787.558	-0.0995	-0.0329	0.0319	1.0000
-2.5	786.211	988.161	988.161	798.015	796.909	788.946	789.750	-0.0449	-0.0355	0.0356	1.0000
0.0	786.211	987.536	987.536	790.957	797.794	794.717	790.715	0.0187	-0.0352	0.0364	1.0000
2.5	785.866	987.261	987.261	784.780	796.605	801.029	789.566	0.0807	-0.0349	0.0354	1.0000
5.0	785.866	987.191	987.191	780.899	794.634	807.626	787.495	0.1328	-0.0355	0.0338	1.0000
7.5	785.866	987.400	987.191	776.675	790.753	815.268	783.453	0.1915	-0.0362	0.0281	0.9990
10.0	785.866	987.469	987.191	773.216	785.504	822.548	778.103	0.2447	-0.0367	0.0197	0.9966
15.0	785.866	987.956	983.647	766.661	770.019	839.984	762.779	0.3618	-0.0358	-0.0047	0.9787
20.0	785.866	986.913	975.864	762.336	750.572	857.500	744.036	0.4733	-0.0325	-0.0361	0.9450

BETA DEG	AVERAGE MACH NUMBER	AVERAGE REYNOLDS NUMBER	AVERAGE TEMPERATURE DEG C
2.5	0.580	35721.	16.4

ALPHA DEG	PS CM H2O	PT CM H2O	P1 CM H2O	P2 CM H2O	P3 CM H2O	P4 CM H2O	P5 CM H2O	DELTA CP (ALPHA)	DELTA CP (BETA)	CP (AVERAGE)	CP (TOTAL)
-20.0	785.866	985.662	977.253	853.598	740.717	765.433	745.403	-0.4413	0.0235	-0.0479	0.9579
-15.0	785.866	987.191	985.454	835.720	762.336	769.818	767.424	-0.3273	0.0253	-0.0101	0.9914
-10.0	785.866	987.261	986.983	818.566	778.646	775.871	783.915	-0.2120	0.0262	0.0168	0.9986
-7.5	786.555	988.436	988.367	811.573	785.047	779.758	790.014	-0.1576	0.0246	0.0250	0.9997
-5.0	786.555	988.506	988.506	804.313	789.431	783.921	793.916	-0.1010	0.0222	0.0314	1.0000
-2.5	786.555	987.950	987.950	797.375	791.804	788.989	796.450	-0.0416	0.0231	0.0352	1.0000
0.0	786.211	987.605	987.605	790.836	792.304	793.913	796.527	0.0153	0.0210	0.0357	1.0000
2.5	786.211	987.397	987.397	785.466	791.701	800.328	795.924	0.0739	0.0210	0.0355	1.0000
5.0	785.866	987.122	987.122	780.476	789.003	807.223	792.945	0.1329	0.0196	0.0325	1.0000
7.5	785.866	986.774	986.496	776.454	785.061	814.664	788.903	0.1902	0.0191	0.0269	0.9986
10.0	785.866	986.705	986.531	773.156	779.893	821.723	783.714	0.2418	0.0190	0.0187	0.9991
15.0	785.521	986.082	982.746	766.778	764.304	839.015	767.703	0.3602	0.0169	-0.0053	0.9834
20.0	785.521	985.943	975.310	762.434	744.697	856.674	746.518	0.4712	0.0191	-0.0369	0.9469

TABLE 3 (Cont'd)

Pressure Coefficients for the Five-Ported, Conical Probe, $M_{,}$ 0.6

BETA DEG	AVERAGE MACH NUMBER	AVERAGE REYNOLDS NUMBER	AVERAGE TEMPERATURE DEG C
5.0	0.580	35699.	16.5

ALPHA DEG	PS CM H2O	PT CM H2O	P1 CM H2O	P2 CM H2O	P3 CM H2O	P4 CM H2O	P5 CM H2O	DELTA CP (ALPHA)	DELTA CP (BETA)	CP (AVERAGE)	CP (TOTAL)
-20.0	785.176	985.598	576.912	851.180	735.564	763.417	753.160	-0.4379	0.0878	-0.0466	0.9567
-15.0	785.176	986.085	582.610	833.201	756.376	766.272	774.397	-0.3331	0.0897	-0.0130	0.9827
-10.0	785.176	986.085	585.737	817.112	772.446	772.446	790.445	-0.2223	0.0896	0.0146	0.9983
-7.5	785.176	986.015	585.946	807.700	778.540	776.428	796.097	-0.1557	0.0874	0.0225	0.9997
-5.0	785.176	986.015	586.015	800.521	782.562	780.591	799.857	-0.0992	0.0861	0.0284	1.0000
-2.5	785.176	986.015	586.015	794.226	784.573	784.975	802.110	-0.0461	0.0873	0.0313	1.0000
0.0	785.176	986.015	586.015	788.032	785.579	790.667	802.834	0.0131	0.0859	0.0329	1.0000
2.5	785.176	986.015	586.015	782.522	785.136	797.384	801.848	0.0740	0.0832	0.0326	1.0000
5.0	785.176	986.363	586.015	777.615	782.844	804.161	799.254	0.1319	0.0816	0.0288	0.9983
7.5	786.555	988.089	587.672	774.690	780.301	812.438	796.530	0.1873	0.0805	0.0220	0.9979
10.0	786.555	988.436	587.602	770.706	774.511	820.442	790.959	0.2464	0.0795	0.0134	0.9959
15.0	786.555	988.645	585.448	763.790	759.889	837.857	775.474	0.3665	0.0771	-0.0114	0.9842
20.0	786.555	988.575	576.866	761.578	739.255	856.962	755.042	0.4722	0.0781	-0.0413	0.9420

BETA DEG	AVERAGE MACH NUMBER	AVERAGE REYNOLDS NUMBER	AVERAGE TEMPERATURE DEG C
7.5	0.580	35797.	16.5

ALPHA DEG	PS CM H2O	PT CM H2O	P1 CM H2O	P2 CM H2O	P3 CM H2O	P4 CM H2O	P5 CM H2O	DELTA CP (ALPHA)	DELTA CP (BETA)	CP (AVERAGE)	CP (TOTAL)
-20.0	786.555	989.131	579.194	850.809	733.624	760.371	761.296	-0.4464	0.1366	-0.0495	0.9509
-15.0	786.555	988.575	985.796	832.649	753.536	763.066	782.533	-0.3444	0.1416	-0.0174	0.9862
-10.0	786.555	988.575	587.880	814.469	770.406	770.688	798.883	-0.2167	0.1410	0.0102	0.9966
-7.5	786.555	988.367	588.089	806.626	776.037	774.308	803.951	-0.1601	0.1383	0.0182	0.9986
-5.0	786.900	988.712	588.573	799.630	780.525	778.655	808.117	-0.1039	0.1367	0.0239	0.9993
-2.5	786.900	988.781	588.781	792.792	782.677	783.582	810.329	-0.0456	0.1370	0.0270	1.0000
0.0	787.245	989.126	589.126	786.883	783.725	789.819	811.216	0.0145	0.1362	0.0281	1.0000
2.5	787.245	989.126	989.126	781.513	783.222	796.174	810.211	0.0726	0.1337	0.0274	1.0000
5.0	787.589	990.096	589.679	777.554	781.194	803.175	806.343	0.1265	0.1341	0.0246	0.9979
7.5	787.589	988.845	588.845	773.351	776.850	810.877	803.115	0.1865	0.1303	0.0172	1.0000
10.0	787.589	988.984	988.915	770.153	771.782	818.218	797.966	0.2367	0.1300	0.0096	0.9997
15.0	787.934	989.396	586.340	762.092	757.104	836.401	762.363	0.3688	0.1254	-0.0171	0.9848
20.0	787.934	989.396	577.445	757.567	736.893	856.290	761.629	0.4900	0.1228	-0.0488	0.9407

TABLE 3 (Cont'd)

Pressure Coefficients for the Five-Ported, Conical Probe, $M_{\infty} = 0.6$

BETA DEG	AVERAGE MACH NUMBER	AVERAGE REYNOLDS NUMBER	AVERAGE TEMPERATURE DEG C
10.0	0.580	35685.	17.0

ALPHA DEG	PS CM H2O	PT CM H2O	P1 CM H2O	P2 CM H2O	P3 CM H2O	P4 CM H2O	P5 CM H2O	DELTA CP (ALPHA)	DELTA CP (BETA)	CP (AVERAGE)	CP (TOTAL)
-20.0	787.245	988.917	977.937	846.933	732.705	751.407	771.076	-0.4737	0.1903	-0.0581	0.9456
-15.0	783.796	985.471	982.552	823.355	746.142	754.836	788.625	-0.3397	0.2017	-0.0248	0.9855
-10.0	787.245	988.917	988.570	811.116	766.832	765.123	807.556	-0.2281	0.2019	0.0020	0.9983
-7.5	787.245	988.917	988.778	802.408	772.785	768.542	813.348	-0.1679	0.2011	0.0100	0.9993
-5.0	787.245	988.917	988.917	794.645	776.586	772.645	816.968	-0.1081	0.2002	0.0150	1.0000
-2.5	787.245	988.917	988.917	787.747	778.758	777.772	818.818	-0.0495	0.1986	0.0175	1.0000
0.0	787.245	988.709	988.709	781.412	779.804	783.745	819.180	0.0116	0.1955	0.0188	1.0000
2.5	787.245	988.709	988.709	776.425	779.160	789.758	818.215	0.0662	0.1939	0.0181	1.0000
5.0	787.245	988.709	986.639	772.162	776.284	796.697	815.862	0.1218	0.1965	0.0149	0.9997
7.5	787.245	988.709	988.500	768.522	772.825	803.876	811.337	0.1755	0.1912	0.0094	0.9990
10.0	787.245	988.639	987.944	765.324	767.516	811.981	805.545	0.2317	0.1888	0.0017	0.9965
15.0	787.245	988.639	982.941	757.016	752.755	830.643	789.457	0.3656	0.1822	-0.0237	0.9717
20.0	787.245	988.639	974.219	745.978	733.710	850.191	768.703	0.5175	0.1738	-0.0626	0.9284

BETA DEG	AVERAGE MACH NUMBER	AVERAGE REYNOLDS NUMBER	AVERAGE TEMPERATURE DEG C
15.0	0.578	36031.	15.7

ALPHA DEG	PS CM H2O	PT CM H2O	P1 CM H2O	P2 CM H2O	P3 CM H2O	P4 CM H2O	P5 CM H2O	DELTA CP (ALPHA)	DELTA CP (BETA)	CP (AVERAGE)	CP (TOTAL)
-20.0	792.759	994.432	975.564	840.663	737.596	738.441	796.480	-0.5069	0.2920	-0.0717	0.9064
-15.0	792.759	995.197	985.185	820.492	752.216	750.266	817.737	-0.3469	0.3237	-0.0375	0.9506
-10.0	792.759	995.127	989.220	801.407	765.188	754.227	832.739	-0.2331	0.3338	-0.0216	0.9708
-7.5	792.759	993.390	990.262	792.961	770.597	756.842	837.606	-0.1800	0.3340	-0.0162	0.9844
-5.0	792.070	994.229	991.866	784.388	774.312	758.948	840.295	-0.1258	0.3264	-0.0128	0.9883
-2.5	792.070	993.743	992.005	777.385	777.570	763.533	841.844	-0.0687	0.3187	-0.0098	0.9914
0.0	792.070	993.812	991.866	771.215	778.696	769.305	842.085	-0.0095	0.3142	-0.0086	0.9904
2.5	792.070	993.882	991.588	765.886	777.309	776.283	841.341	0.0515	0.3173	-0.0092	0.9886
5.0	792.070	993.604	990.755	761.663	773.327	783.986	838.284	0.1108	0.3223	-0.0137	0.9859
7.5	792.070	993.812	989.573	758.003	768.098	792.674	833.257	0.1729	0.3230	-0.0199	0.9790
10.0	792.070	993.743	987.627	755.449	763.453	801.120	827.807	0.2265	0.3191	-0.0254	0.9697
15.0	792.070	993.604	982.276	749.476	750.562	820.828	810.773	0.3540	0.2988	-0.0455	0.9438
20.0	792.070	993.673	972.755	734.635	736.042	840.416	789.777	0.5237	0.2665	-0.0833	0.8962

BETA DEG	AVERAGE MACH NUMBER	AVERAGE REYNOLDS NUMBER	AVERAGE TEMPERATURE DEG C
20.0	0.579	35853.	16.5

[illegible]	[illegible]	P1 CM H2O	P1 CM H2O	P2 CM H2O	P3 CM H2O	P4 CM H2O	P5 CM H2O	DELTA CP (ALPHA)	DELTA CP (BETA)	CP (AVERAGE)	CP (TOTAL)
	[illegible]	993.745	964.625	825.092	730.572	725.343	815.439	-0.4946	0.4208	-0.0890	0.8556
	[illegible]	993.951	975.257	803.171	741.431	734.151	836.112	-0.3419	0.4690	-0.0661	0.9074
	[illegible]	994.021	982.276	783.020	755.469	732.905	850.753	-0.2482	0.4718	-0.0571	0.9418
	[illegible]	993.917	984.222	774.534	764.116	733.810	855.177	-0.2018	0.4511	-0.0503	0.9520
	[illegible]	992.645	983.541	764.183	768.854	735.063	856.631	-0.1439	0.4290	-0.0441	0.9550
	[illegible]	992.714	984.861	756.601	772.126	739.266	858.119	-0.0857	0.4249	-0.0436	0.9612
	790.347	991.880	984.236	750.286	772.770	745.661	857.878	-0.0230	0.4223	-0.0432	0.9621
	790.347	991.776	983.437	745.098	772.147	753.182	856.631	0.0401	0.4194	-0.0426	0.9586
[illegible]	790.347	991.290	982.012	741.619	769.633	761.025	852.931	0.0966	0.4145	-0.0450	0.9538
[illegible]	789.657	990.983	979.724	737.973	758.989	769.547	847.676	0.1568	0.4405	-0.0552	0.9441
[illegible]	789.313	990.846	977.364	736.019	749.896	777.850	842.002	0.2076	0.4570	-0.0639	0.9331
[illegible]	789.313	990.846	970.415	732.963	737.126	796.713	825.472	0.3163	0.4384	-0.0806	0.8986
20.0	789.313	990.916	959.678	722.445	724.456	819.941	803.088	0.4836	0.3900	-0.1083	0.8451

TABLE 4

Pressure Coefficients for the Five-Ported, Conical Probe, $0.12 \leq M_\infty \leq 0.61$

ALPHA DEG 0.0 BETA DEG 0.0

MACH NUMBER	REYNOLDS NUMBER	PS CM H2O	PT CM H2O	TOTAL TEMP (C)	P1 CM H2O	P2 CM H2O	P3 CM H2O	P4 CM H2O	P5 CM H2O	DELTA CP (ALPHA)	DELTA CP (BETA)	CP (AVERAGE)	CP (TOTAL)
0.120	7187.	773.5	781.29	7.0	780.87	773.87	773.81	773.84	773.88	0.0000	-0.0001	0.0490	0.9995
0.129	7759.	773.5	782.56	6.0	782.14	773.91	773.94	773.95	773.82	-0.0001	0.0001	0.0484	0.9995
0.139	8364.	773.5	784.03	6.0	784.03	773.96	774.01	774.02	773.98	-0.0001	0.0000	0.0480	1.0000
0.156	9383.	773.5	786.78	6.0	785.93	773.99	774.04	774.11	774.11	-0.0001	-0.0001	0.0460	0.9989
0.207	12427.	773.5	796.90	6.0	795.21	774.54	774.43	774.37	774.40	0.0002	0.0000	0.0437	0.9979
0.230	13763.	773.5	802.39	7.0	800.49	775.03	774.57	774.32	774.64	0.0009	-0.0001	0.0427	0.9976
0.242	14461.	773.5	805.55	8.0	803.44	775.41	774.71	774.61	774.72	0.0010	-0.0000	0.0460	0.9974
0.252	15139.	773.5	808.29	5.0	805.76	775.60	775.26	774.34	774.47	0.0016	0.0010	0.0443	0.9969
0.275	16558.	773.5	815.26	5.0	812.51	775.74	775.99	774.53	774.29	0.0015	0.0021	0.0423	0.9966
0.305	18375.	773.5	824.96	4.0	821.37	775.74	775.95	775.33	775.23	0.0005	0.0009	0.0433	0.9957
0.344	20713.	773.5	839.30	4.0	835.08	776.30	777.04	776.02	775.19	0.0003	0.0022	0.0430	0.9950
0.366	22052.	773.5	848.37	4.0	844.16	776.16	777.78	776.58	775.03	-0.0005	0.0032	0.0410	0.9950
0.401	24204.	773.5	863.99	3.0	859.98	776.51	777.85	777.64	776.09	-0.0013	0.0020	0.0409	0.9954
0.452	27258.	773.5	889.93	4.0	883.81	778.41	778.20	778.06	778.73	0.0004	-0.0006	0.0441	0.9931
0.472	28500.	773.5	900.90	3.0	893.52	778.62	778.80	778.83	778.10	-0.0002	0.0008	0.0425	0.9918
0.491	29603.	773.5	912.08	4.0	903.43	778.20	779.11	779.81	777.92	-0.0018	0.0013	0.0406	0.9905
0.503	30370.	773.5	919.25	3.0	907.86	778.55	779.39	779.67	778.69	-0.0012	0.0008	0.0416	0.9876
0.518	31304.	773.5	928.96	3.0	917.36	779.53	779.11	780.38	779.39	-0.0009	-0.0003	0.0425	0.9875
0.542	32718.	773.5	944.36	3.0	931.70	782.21	779.53	778.69	780.52	0.0038	-0.0011	0.0427	0.9866
0.564	34119.	773.5	959.76	2.0	946.05	782.21	780.24	778.41	782.49	0.0040	-0.0024	0.0426	0.9857
0.608	36727.	773.5	992.88	3.0	975.58	782.91	783.89	785.16	781.64	-0.0023	0.0023	0.0491	0.9826

REFERENCES

1. Schultz, W. M., et. al., "Several Combination Probes for Surveying Static and Total Pressure and Flow Direction," NACA TN 2830, 1952.

2. Kettle, D. J., "Design and Calibration at Low Speeds of a Static Tube and Pitot-Static Tube with Semi-Ellipsoidal Nose Shapes," J. Roy. Aer. Soc., Vol. 58, 1954, pp. 835-837.

3. Smetena, F. O. and Stuart, J. W. M., "A Study of Angle-of-Attack, Angle-of-Sideslip Pitot-Static Probes," WADC TR 57234, AD118209, 1957.

4. Bryer, D. W., et. al., "Pressure Probes Selected for Three-Dimensional Flow Measurement," Rep. Mem. Aero Res. Coun. London, No. 3037, 1958.

5. Morrison, D. F., et. al., "Hole Size Effect on Hemisphere Pressure Distributions," J. Roy. Aer. Soc., Vol. 71, 1967, pp. 317-319.

6. Wright, M. A., "The Evaluation of a Simplified Form of Presentation for Spherical and Hemispherical Pitometer Calibration Data," J. Sci. Instr. (J. Phys. E), Vol. 3, 1970, pp. 356-362.

7. Schaub, U. W., et. al., "An Investigation of the Three-Dimensional Flow Characteristics of a Non-Nulling Five-Tube Probe," Nat. Res. Council of Canada, Aero Rpt. LR-393, NRC No. 7964, 1964.

8. Dudzinski, J. T. and Krause, L. N., "Flow Direction Measurement with Fixed-Position Probes," NASA TM X-1904, 1969.

9. Beecham, L. J. and Collins, S. J., "Static and Dynamic Response of a Design of a Differential Pressure Yawmeter at Supersonic Speeds," Roy. Aer. Est. Report No. GW19, 1954.

10. Hutton, P. G., "Static Pressure of a Hemispherical-Headed Yawmeter at High Subsonic and Transonic Speeds," Roy. Aer. Est. Tech. Note No. Aero 2525, CP No. 401, 1957.

11. Nowack, C. F. R., "Improved Calibration Method for a Five-Hole Spherical Pitot Probe," J. Sci. Instr (J. Phys. E), Vol. 3, 1970, pp. 21-26.

12. Dau, K., et. al., "The Probes for the Measurement of the Complete Velocity Vector in Subsonic Flow," Aero. J., Vol. 72, 1969, pp. 1066-1068.

13. Spaid, F. W., et. al., "Miniature Probe for Transonic Flow Direction Measurements," AIAA J., Vol. 13, 1975, pp. 253-255.

14. Glawe, G. F., et. al., "A Small Combination Sensing Probe for Measurement of Temperature, Pressure and Flow Direction," NASA TN D-4816, 1968.

15. Treaster, A. L. and Yocum, A. M., "The Calibration and Application of Five-Hole Probes," Penn. State Univ. Applied Research Laboratory Report TM 78-10, 1978.

16. Bryer, D. W. and Pankhurst, D. W., "Pressure Probe Methods for Determining Wind Speed and Flow Direction," Published by Her Majesty's Stationery Office, London, England, 1971.

17. Wuest, W., "Measurement of Flow Speed and Flow Direction by Aerodynamic Probes and Vanes," Paper presented at the 30th Flight Mechanics Panel Meeting in Montreal, Canada, 1967.

18. Hess, J. L. and Smith, A. M. O., "Calculation of Potential Flow about Arbitrary Bodies," Progress in Aeronautical Sciences, Vol. 8, Pergammon Press, 1966.

19. Smith, A. M. O. and Bauer, A. B., "Static-Pressure Probes that are Theoretically Insensitive to Pitch, Yaw and Mach Number, J. Fl. Mech., Vol. 44, 1970, pp. 513-528.

20. Shapiro, A. H., The Dynamics and Thermodynamics of Compressible Fluid Flow, Volume I, The Ronald Press, New York, 1953.

21. Liepmann, H. W. and Roshko, A., Elements of Gas Dynamics, John Wiley & Sons, New York, 1958.

22. Sears, W. R., *General Theory of High Speed Aerodynamics,* Volume VI, Princeton University Press, Princeton, N.J., 1954.

23. Laitone, E. V., "The Subsonic Flow About a Body of Revolution," Quant. of Appl. Math., Vol. 5, 1947, pp. 227-231.

24. Laitone, E. V., "The Linearized Subsonic and Supersonic Flow About Inclined Slender Bodies of Revolution," J. of Aero. Sci., Vol. 14, 1947, pp. 6331-642.

25. Karamcheti, K., Principles of Ideal-Fluid Aerodynamics, John Wiley & Sons, Inc., New York, 1966.

26. Huffman, G. David, "Aerodynamic Analyses for the Compressor Research Facility," AFAPL-TR-79-2021, 1979.

27. DISA Type 55D90 Calibration Equipment Instruction Manual, DISA Information.

28. Garner, H. C., et. al., "Subsonic Wind Tunnel Wall Corrections," AGARDograph 109, October 1966.

29. Page, W. A., "Experimental Study of the Equivalence of Transonic Flow About Slender Cone-Cylinders of Circular and Elliptic Cross-Section," NACA TN 4233, 1958.

30. Livesey, J. L., et. al., "The Static Hole Error Problem," Aircraft Engineering, Vol. 34, 1962, pp. 43-47.

31. Franklin, R. F. and Wallace, J. M., "Absolute Measurement of Static-Hole Error Using Flush Transducers," J. Fl. Mech., Vol. 42, 1970, pp. 33-48.

32. Gorlin, S. M. and Slezinger, I. I., "Wind Tunnels and Their Instrumentation," NASA TTF-346, 1966.

33. Bradshaw, P. and Goodman, D. G., "The Effect of Turbulence on Static-Pressure Tubes," ARC-R/M-3527, Sept. 1966.

☆U.S.Government Printing Office: 1980 — 657-084/184

END

DATE

FILMED

1-81

DTIC